FOREIGN TECHNOLOGY DIVISION

FLIGHT DYNAMICS

by

A. M. Mkhitaryan

DDC

MAY 10 1977

REPORT DOCUMENTATION PAGE		READ INSTRUCTIONS BEFORE COMPLETING FORM
1. REPORT NUMBER FTD-ID(RS)T-1336-76 ✓	2. GOVT ACCESSION NO.	3. RECIPIENT'S CATALOG NUMBER
4. TITLE (and Subtitle) FLIGHT DYNAMICS		5. TYPE OF REPORT & PERIOD COVERED Translation
		6. PERFORMING ORG. REPORT NUMBER
7. AUTHOR(s) A. M. Mkhitaryan		8. CONTRACT OR GRANT NUMBER(s)
9. PERFORMING ORGANIZATION NAME AND ADDRESS Foreign Technology Division Air Force Systems Command U. S. Air Force		10. PROGRAM ELEMENT, PROJECT, TASK AREA & WORK UNIT NUMBERS
11. CONTROLLING OFFICE NAME AND ADDRESS		12. REPORT DATE 1971
		13. NUMBER OF PAGES 1169
14. MONITORING AGENCY NAME & ADDRESS(if different from Controlling Office)		15. SECURITY CLASS. (of this report) UNCLASSIFIED
		15a. DECLASSIFICATION/DOWNGRADING SCHEDULE

16. DISTRIBUTION STATEMENT (of this Report)

Approved for public release; distribution unlimited.

17. DISTRIBUTION STATEMENT (of the abstract entered in Block 20, if different from Report)

18. SUPPLEMENTARY NOTES

19. KEY WORDS (Continue on reverse side if necessary and identify by block number)

20. ABSTRACT (Continue on reverse side if necessary and identify by block number)

01

DD FORM 1 JAN 73 1473   EDITION OF 1 NOV 65 IS OBSOLETE

UNEDITED MACHINE TRANSLATION

FTD-ID(RS)T-1336-76   3 November 1976

FLIGHT DYNAMICS *FTD-76-C-001114*

By: A. M. Mkhitaryan

English pages: 1169

Source: Dinamika Foleta, Izd-vo
"Mashinostroyeniye," Moscow, 1971, PP. 1-368.

Country of origin: USSR
This document is a machine aided translation.
Requester: AC/SI
Approved for public release; distribution unlimited.

PREPARED BY:

TRANSLATION DIVISION
FOREIGN TECHNOLOGY DIVISION
WP-AFB, OHIO.

Page 265.

Chapter ~~&~~ XIV. LONGITUDINAL DISTURBED MOTION.

§ 14.1. Common properties of the longitudinal disturbed motion.

During the low initial disturbances of the kinematic parameters
of the $\Delta V, \Delta \alpha, \Delta \vartheta, \omega_z$ of the longitudinal undisturbed motion, the
longitudinal disturbed motion is described by linear differential
equations (8.9) or (8.13). The coefficients with unknowns in these
equations are the particular derivatives of the projection of the
R_{x1}, R_{y1} of the main vector and M_{z1} of the main moment of the
forces, which act on aircraft.

The methods of the determination of pitching moment of M_{z1} and
its partial derivatives are described in chapter IX. The projections
of the main vector of R_{x1} and R_{y1} on the body axes of coordinates

for a straight flight in vertical plane without bank and slips are
determined by relationships

$$R_{x1} = P_{x1} - X_1 - G \sin \vartheta = P_{x1} - c_{x1} \frac{\rho V^2}{2} S - G \sin \vartheta; \quad (14.1)$$

$$R_{y1} = P_{y1} + Y_1 - G \cos \vartheta = P_{y1} + c_{y1} \frac{\rho V^2}{2} - G \cos \vartheta, \quad (14.2)$$

where X_1 and Y_1 - tangential and normal force; for the low angles of
the attack of $c_{y1} \approx c_y$; $c_{x1} = c_x - \alpha c_y$; P_{y1} — the transverse component of
thrust/rod, caused by the noncoincidence of the velocity vector of
flight with axle/axis $0x_1$ (see § 9.4).

In the given calculations in view of the smallness of the angle
of $\varphi_{\text{ДВ}}$. is set/assumed the $P_x \approx P$.

The particular derivative of R_{x1} in terms of speed will be
determined in the form

$$R_{x1}^{V} = P^{V} - X_{1}^{V} = P^{V} - \frac{1}{a} c_{x1}^{M} \frac{\varrho V^2}{2} S - c_{x1} \varrho V S, \quad (14.3)$$

while the particular derived P^V - according to the altitude-speed engine characteristics. The value of c_{x1}^M is virtually equal to zero with of $M < M_{KP}$, then it it increases and it reaches maximum with Mach number, which precedes the purely supersonic mode/conditions of the flow about the aircraft. Further it decreases and becomes negative.

Page 266.

Assuming that the tangential component of the thrust does not depend on angle of attack, the particular derived R_{x1}^{α} it is possible to write in the form

$$R^a_{x1} = -c^a_{x1} \frac{\varrho V^2}{2} S. \tag{14.4}$$

The value of c^a_{x1} it is located by numerical differentiation of the experimentally obtained dependence of $c_{x1} = \mathcal{F}(\alpha)$.

Since the thrust of engines and drag on pitch angle do not depend,

$$R^{\vartheta}_{x1} = -G \cos \vartheta. \tag{14.5}$$

The partial derivatives of $R^{\delta}_{x1}, R^{\delta}_{x1}, R^{\delta}_{x1}$ are located as increases in the force of periphery during the deflection of controls of unit angle (for example $R^{\delta}_{x1} = -c^{\delta}_{x1} \frac{\varrho V^2}{2} S$). The value of R^{δ}_{x1} is determined from the engine characteristics, which link the angular position of engine-control lever (throttle control) with the engine thrust.

Let us determine now particular derivatives of the value of the projection of the R_y of the main vector on axle/axis Oy_1. If we consider that the value of the projection of thrust on axle/axis Oy_1 does not change during speed change, which sufficiently accurately reflects real state of affairs, then

$$R_{y1}^V = c_{y1}\varrho VS + \frac{1}{a} c_{y1}^M \frac{\varrho V^2}{2} S. \qquad (14.6)$$

Further we find

$$R_{y1}^* = c_{y1}^* \frac{\varrho V^2}{2} S + P_{y1}^*. \qquad (14.7)$$

for an aircraft with TRD according to relationship (9.39) of the $P_{y1}^* = m_s V$, where of the m_B - the flow rate per second of air of engine. Derivative of R_{y1}, in terms of pitch angle is equal to

$$R_{y1}^{\vartheta} = G \sin \vartheta. \tag{14.8}$$

The particular derived $R_{y1}^{\delta_B}$ can be found as follows. The lift coefficient of horizontal tail assembly, referred to wing area, it is possible to write in the form

$$c_{y\,r.o} = c_{y\,r.o}^{a} k_{r.o} A_{r.o} (a + \varphi - \varepsilon_y + n_{\scriptscriptstyle{B}} \delta_{\scriptscriptstyle{B}}) \frac{S_{r.o}}{S}.$$

By differentiating this expression with respect to δ_B, we will obtain

$$c_{y\,r.o}^{\delta_B} = c_{y\,r.o}^{a} k_{r.o} A_{r.o} n_{\scriptscriptstyle{B}} \frac{S_{r.o}}{S}.$$

Page 267.

Now for the partial derivative of $R_y^{\delta B}$ it is possible to write

$$R_y^{\delta_n} = c_{r.o}^{\delta_n} \frac{\varrho V^2}{2} S.$$

If the initial motion bygone establish/installed, then the coefficients with unknowns in equations (8.9) and (8.13) do not depend on time and are constant values.

The solution to the equations of the disturbed motion makes it possible to find the kinematic characteristics α, V, ϑ and ω_z as functions of time. The calculations show that for the real layouts of aircraft the disturbed motion of statically stable aircraft is determined by the character of the basic motion and can consist either of two oscillatory motions or of one oscillatory/vibratory and two aperiodic motions. If the basic motion horizontal, agitated usually is composed of two oscillatory motions; if rectilinear with lift - of two aperiodic and one oscillatory/vibratory motions. The quantitative criteria, which characterize the disturbed motion, are the period of oscillations, the time of damping to half amplitude, the number of oscillation/vibrations down to virtually complete attenuation.

The special feature/peculiarity of the solution to the equations of the longitudinal airplane disturbance entails the fact that among the complex roots of characteristic equation (8.17) it is possible to separate on module/modulus two large and two small roots. It will be below shown that the large complex conjugate roots determine short-period motion, and low - long-period. Long-period (slow) motion is connected in essence with the translation of aircraft in space, and short-period is connected with rotary. The physical nature of the existence of these motions entails the fact that the value and the

direction of the velocity of motion, and also the flight trajectory change considerably slower than the angle of attack of aircraft.

The role of these two motions is different. The long-period motion, which develops slowly in time and space, can be in time noticed and is removed by aircrew, but short-period motion so rapidly which to check and to correct it is extremely difficult.

Analyzing short-period motion, they assume that the flight speed is constant, i.e., long-period motion still not developed. Analyzing long-period motion, they assume that the short-period motion on the strength of its strict course already ended and the angular displacements of aircraft relative to velocity vector are absent $\left(\frac{d^2\beta}{dt^2} = \frac{d\Delta\alpha}{dt} = \Delta\alpha = 0\right)$. These assumptions make it possible substantially to simplify the analysis of airplane disturbance.

Page 268.

§ 14.2. Short-period longitudinal airplane disturbance.

For the simplicity of the analysis of short-period motion, let us consider that the initial state of motion is the straight-and-level flight. Furthermore, let us assume that the control vanes are pressed, the engine power rating constant, and external disturbance/perturbations are absent, i.e., in this case the emergence of the disturbed motion is determined by the initial kinematic disturbance/perturbations $\Delta\alpha$ and $\Delta\vartheta$.

Since in the process of short-period motion the speed does not manage to be changed ($\Delta V = 0$), it is possible to be restricted to the solution to the last/latter two equations of systems (8.13), which taking into account the made assumptions it is possible to write in the form

$$a_{22}^{\cdot}\frac{d\Delta\alpha}{dt} + a_{23}^{\cdot}\frac{d\Delta\vartheta}{dt} + a_{22}\Delta\alpha + a_{23}\Delta\vartheta = 0;$$

$$a_{33}^{\cdot}\frac{d^2\Delta\vartheta}{dt^2} + a_{32}^{\cdot}\frac{d\Delta\alpha}{dt} + a_{33}^{\cdot}\frac{d\Delta\vartheta}{dt} + a_{32}\Delta\alpha = 0.$$

By the term of equation

$$a_{23}\Delta\vartheta = -G\sin\vartheta\Delta\vartheta$$

it is possible to disregard in view of his smallness.

The characteristic equation of the simplified system takes the form

$$\Delta = \begin{vmatrix} a'_{22}p + a_{22} & a'_{23}p \\ a'_{22}p + a_{32} & a'_{33}p^2 + a'_{33}p \end{vmatrix} = 0,$$

or after expansion of a determinant:

$$\Delta = p\left[p^2 a'_{22} a'_{33} + p\left(a_{22} a'_{33} + a_{22} a'_{33} - a'_{32} a'_{23}\right) + a_{22} a'_{33} - a'_{23} a_{32}\right] =$$
$$= a'_{22} a'_{33} p\left(p^2 + 2\xi \Omega_0 p + \Omega_0^2\right), \qquad (14.9)$$

where

$$\Omega_0^2 = \frac{a_{22} a'_{33} - a'_{23} a_{32}}{a'_{22} a'_{33}} ; \qquad (14.10)$$

$$\xi = \frac{a'_{22} a'_{33} + a_{22} a'_{33} - a'_{32} a'_{23}}{2\Omega_0 a'_{22} a'_{33}} . \qquad (14.11)$$

Here Ω_0 is the reference frequency, equal to the oscillation frequency of system in the absence of damping, ξ is a decrement of oscillation/vibrations.

By solving equation (14.9), we will obtain

$$p_{1,2} = \xi \Omega_0 \pm \sqrt{\xi^2 \Omega_0^2 - \Omega_0^2} = \xi \Omega_0 \pm i \Omega_0 \sqrt{1 - \xi^2};$$
$$p_3 = 0.$$

Page 269.

Thus, rapid motion consists of aperiodic, determined by zero
root, and oscillatory motion with the angular frequency of
$v = \Omega_0 \sqrt{1 - \beta^2}.$ In this case an increase in the angle of attack it is
possible to write in the form

$$\Delta a = D_a e^{\zeta t} \sin(\nu t + \varphi) + A_a, \qquad (14.12)$$

where the D_α, A_α and φ are constants, determined by the initial conditions; $\zeta = \xi \Omega_0$ - attenuation factor.

It is not difficult to demonstrate that if the disturbed motion is caused by the initial disturbance of angle of attack, i.e., it is examined after the break-down of perturbing forces, then $A_\alpha = 0$.

Reference frequency can be determined from equation (14.10), by substituting here valuyes in accordance with Table 8.1 and formulas (14.4) - (14.8):

where

$$\Omega_0^2 = \frac{R_y^2 M_z^{\omega_z} + m V M_z^{\alpha}}{m V J_z} = -\frac{R_y^2 b_A}{J_z}\left(m_z^{c_y} + \frac{m_z^{\bar{\omega}_z}}{\mu}\right), \qquad (14.13)$$

$$\bar{\omega}_z = \frac{\omega_z b_A}{V};$$

$$\mu = \frac{2m}{\varrho S b_A}.$$

from expression (14.13) it follows that the reference frequency Ω_0 depends on the longitudinal stability factor of aircraft in terms of the g-force of $m_z^{c_y}$ and coefficient of rotary derivative. With an increase in the longitudinal static stability, increases the frequency of short-period motion.

If aircraft is unstable on the g-force of $(m_z^{c_y} > 0)$, that $\Omega_0^2 < 0$. This means that the oscillatory motion is absent. In this, the instance of the disturbed motion is composed of two aperiodic, one of which in the course of time grow/rises the $(\rho_z > 0)$ exponentially. Thus, the longitudinal short-period motion exists little more than in the presence of the stability of aircraft on g-force.

Let us find the value of attenuation factor ζ:

$$\zeta = -\xi\Omega_0 = -\frac{a_{22}'a_{33}' + a_{22}'a_{33}' - a_{32}'a_{23}'}{2a_{22}'a_{33}'},$$

or, substituting the value of coefficients from Table 8.1:

$$\zeta = \frac{M_z^{m_z} + M_z^{\dot{z}}}{2J_z} - \frac{R_y^a}{2mV}. \qquad (14.14)$$

Page 270.

If attenuation factor $\zeta < 0$, then in the course of time the amplitude of oscillations attenuates, and the short-period disturbed motion is steady. From relationship (14.14) it is evident that the attenuation occurs as a result of damping both rotary (first term in right side) and forward motions.

Damping forward motion is explained by the fact that during a

change of the angle of attack as a result of the

displacement/movement of aircraft in the direction, perpendicular to

speed, appears lift increment of $Y^{\alpha}\Delta\alpha$, directed against this

displacement/movement.

If $\zeta = 0$, then the disturbed motion is harmonic oscillations. If

$\zeta > 0$ (there is no damping), then in the course of time the amplitude

of oscillations increases and, in spite of the presence of stability

on g-force ($\Omega_0^2 > 0$), the short-period motion it becomes unstable.

Consequently, the static stability on g-force is the necessary, but

insufficient stability condition of short-period motion.

During underdamping short-period motion, the crew and the

passengers during prolonged period of time undergo g-forces, which

tires crew and negatively shows up in the health of the passengers.

Therefore it is necessary that the oscillatory motions rapidly would

be discontinued.

To evaluate the quality of short-period motion, are applied

several criteria.

The most widely accepted criterion is the time interval of $t_{0.5}$, during which the amplitude of oscillation it decreases double:

$$De^{\zeta t} = 2De^{\zeta(t+t_{0.5})},$$

whence, logarithmizing, we will obtain

$$t_{0.5} = -\frac{\ln 2}{\zeta} = -\frac{0,693}{\zeta} . \qquad (14.15)$$

The greater the attenuation factor ζ, the lesser the time it will be required to that that amplitude would decrease double.

Logarithmic decrement η is equal to the logarithm of the relation of the amplitudes, measured with time interval, equal to one period of T:

$$n = \ln \frac{De^{\zeta t}}{De^{\zeta(t+T)}} = -\zeta T = -2\pi \frac{\zeta}{\nu}, \qquad (14.16)$$

where the $T = \frac{2\pi}{\nu}$ — the oscillatory period of oscillation.

As the time interval t_3 during which the oscillations virtually were discontinued, it is accepted the time of an amplitude reduction twenty times.
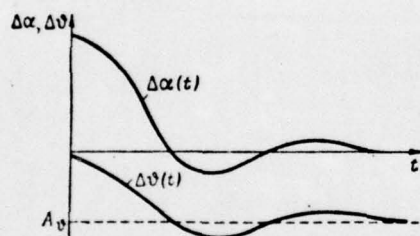
Page 271.

Fig. 14-1. Character of a change of the angle of attack and pitch angle in the process of short-period motion during the initial disturbance/perturbation of angle of attack.

Analogous with formula (14.15) we will obtain

$$t_3 = -\frac{\ln 20}{\zeta}.$$

After dividing t_3 into period of T, We will obtain the number of oscillations n_3 before the complete attenuation:

$$n_3 = \frac{t_3}{\zeta T} = -\frac{\ln 20}{\zeta T} \approx -\frac{3}{\zeta T}. \qquad (14.17)$$

For a passenger aircraft for the target/purposes of the provision for comfort n_3 must be less than three ($n_3 < 3$). This means that in the relation to short-period motion are placed the more stringent requirements, than the condition of its stability.

The changes in the disturbance/perturbations of the angle of attack and pitch angle are determined by expression (14.12), differing only in terms of values constant A, D and φ. For $\Delta\alpha$ the

value of $A_{\alpha} = 0$ while for $\Delta \vartheta$ the value of $A_{2\vartheta} \neq 0$ i.e. after the cessation of short-period motion angle of attack is reduced to original value, and pitch angle turns out to be that which was deflected from original value for the value of $\Delta \vartheta = A_{2\vartheta}$ (Fig. 14.1).

The return of angle of attack to the initial value means the return of angle of attack to the initial value it means return to moment balance, but not to equilibrium of forces, since $\Delta \vartheta \neq 0$. The disequilibrium of forces is the reason for the emergence of long-period motion.

§ 14. 3. Long-period longitudinal airplane disturbance.

The oscillatory period of oscillations in long-period motion approximately to two orders more than the oscillatory period of oscillations in short-period, therefore it is possible to consider that the stable with respect to short-period motion aircraft does not have rapid oscillations, pitching moments are balanced, i.e., changes $\Delta \alpha$ are negligible, $M_z \approx 0$.

Page 272.

In this case the third equation of system (8.13) can be eliminated from examination. Furthermore, during the analysis of long-period motion in the first approximation, it is possible to disregard altitude effect.

The motion of the center of mass, which is obtained during such limitations, for the first time bygone investigated by N. Ye. Joukowski in 1891 was called the name phugoid motion.

At the moment of the phugoid motion, following after short-period motion, the pitch angle differs from pitch angle ϑ_0 the initial motion. If, for example, pitch angle obtained the initial positive increase, then at first aircraft flies with the climb, stalling, and then, since with a decrease in the velocity decreases lift, retards the climb and begins to descend, building up speed. In this motion it passes the initial mode/conditions, losing altitude. In the process of acceleration/dispersal, the lift increases until is discontinued as a result of its increase reduction/descent and will not be initiated the new climb. For the determination of the factors,

which damp this oscillatory motion, we examine the first two equation
of systems (8-13), which under the above-made assumptions take the
following form (the proper motion of aircraft $a_{10} = a_{20} = 0$ is
analyzed):

$$a'_{11} \frac{d\Delta V}{dt} + a_{11}\Delta V + a_{13}\Delta \vartheta = 0,$$

$$a_{21}\Delta V + a'_{23} \frac{d\Delta \vartheta}{dt} + a_{23}\Delta \vartheta = 0.$$

Characteristic equation for this system can be written in the
form of determinant

$$\Delta = \begin{vmatrix} a'_{11}p + a_{11} & a_{13} \\ a_{21} & a'_{23}p + a_{23} \end{vmatrix} = 0,$$

aperture which, we will obtain

$$p^2 + p\left(\frac{a_{23}}{a_{2\dot{3}}} + \frac{a_{11}}{a_{\dot{1}1}}\right) + \frac{a_{11}a_{23} - a_{13}a_{21}}{a_{11}a_{2\dot{3}}} = p^2 - 2\zeta_1 p + \Omega_{01}^2 = 0, \quad (14.18)$$

where ζ_1 - the attenuation factor of long-period motion; Ω_{01} are its reference frequency.

Attenuation factor is equal to:

$$\zeta_1 = -\frac{1}{2}\left(\frac{a_{23}}{a_{2\dot{3}}} + \frac{a_{11}}{a_{\dot{1}1}}\right),$$

or, substituting the value of a_{ij} from Table 8.1:

$$\zeta_1 = \frac{P^V - X_1^V}{2m} + \frac{g \sin \vartheta}{2V}. \qquad (14.19)$$

Page 273.

Passing over to wind coordinate system ($X_1 = X-Y\alpha$) and taking
into account that in the initial flight equilibrium $Y = G \cos \theta$, we
will obtain

$$\zeta = \frac{P^V - X^V}{2m} + \frac{g}{V}\left(\frac{\sin \vartheta}{2} + \alpha \cos \theta\right). \qquad (14.20)$$

By the condition of the attenuation of the amplitude of
oscillations it is $\zeta < 0$. Second term in the right side of expression

(14.20) positively during the climb can become negative during reduction/descent. First term, as a rule, is negative. That means long-period motion stable during reduction/descent can turn out to be unstable during the climb.

If we in the examination of long-period motion introduce less rigid assumptions, after accepting $\frac{d^2\Delta\vartheta}{dt^2} = \frac{d\Delta\alpha}{dt} = 0$, i.e. to disregard only angular acceleration of aircraft and the rate of change in the angle of attack, then in this case it is necessary to consider momental equation. Then the characteristics of long-period motion are depend on derived $m_z^{c_y}$ and $\frac{dm_z}{dc_y}$.

Expression for the reference frequency of long-period motion will take form [1]

$$\Omega_{01} = \frac{g}{V} \sqrt{\frac{2}{m_z^{c_y}} \left(1 + \frac{c_y^M}{2c_y} M\right) \frac{dm_z}{dc_y}} .$$

(14.21).

FOOTNOTE [1] L. G. Totiashvili. Longitudinal stability and the controllability of flight vehicle, RIIGA, Riga, 1963. ENDFOOTNOTE.

Hence it follows that the long-period disturbed motion exists, i.e., $\Omega_{0.1} > 0$, if (with $m_z^{c_y} < 0$) aircraft is stable on the rate of $\left(\frac{dm_z}{dc_y} < 0\right)$.

If aircraft is unstable along the rate of $\left(\frac{dm_z}{dc_y} > 0\right)$, that long-period motion is absent: it falls into two aperiodic motions, of which one it is unstable (Fig. 14.2). For near- and supersonic aircraft this instability, expressed to a great degree for aircraft with thick wing, low or zero sweepbacks and to a slight degree for aircraft with swept or deltas, is observed in certain range of the supercritical Mach numbers.

Density change with height/altitude, not taken into consideration here during analysis, contributes to oscillation damping, since during motion with the climb the lift will decrease not only as a result of deceleration, but also in connection with a decrease in the density.
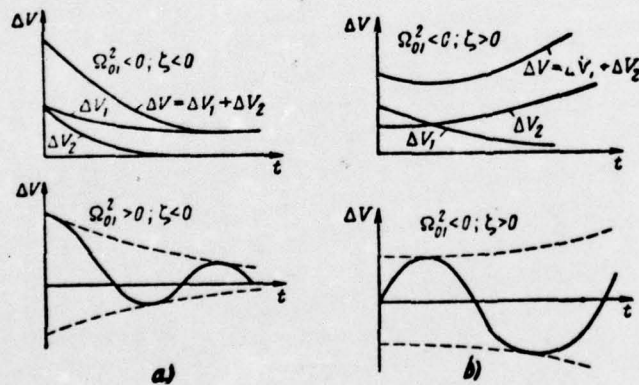
Page 274.

Fig. 14.2. Character of a change in the rate in stable (a) and unstable (b) the disturbed motions.

On the contrary, during a decrease in the height/altitude in the process of oscillatory motion the lift, which hinders this motion, will additionally increase because of an increase in the air density.

§ 14.4. Dynamic longitudinal control characteristics.

Transfer motions.

Any control pressure on aircraft can be considered as the perturbation factor, which causes the appropriate disturbed motion. This motion is accepted to call controlled motion.

A special case of controlled motion is the transfer motion, or transient process is the disturbed motion, caused by step input of the controlling factor. In the process of transfer motion, are reached the new desired values of the parameters of the motions, for obtaining which was undertaken the control pressure.

The function, which describes a change in the parameters of

motion during transient process during the step deflection of control of unit angle, is called of transient function.

In this case of $a_{30} = M_z^{\delta} \Delta \delta_{_B},$ and system (8.13) taking into account the made assumptions will take form

$$a_{22}^{\cdot} \frac{d\Delta \alpha}{dt} + a_{21}^{\cdot} \frac{d\Delta \vartheta}{dt} + a_{22}\Delta \alpha + a_{23}\Delta \vartheta = 0,$$

$$a_{33}^{\cdot} \frac{d^2\Delta \vartheta}{dt^2} + a_{32}^{\cdot} \frac{d\Delta \alpha}{dt} + a_{33}^{\cdot} \frac{d\Delta \vartheta}{dt} + a_{32}\Delta \alpha = a_{30}\Delta \delta_{_B},$$

(14.22)

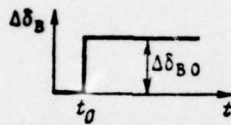where $a_{30} = M_z^{\delta}.$

Page 275.

Fig. 14.3. Diagram of the step deflection of elevator.

The characteristic determinant of heterogeneous linear system (14.22) is determined by the left side of the equations and, which means, is identical with relationship (14.9). The properties of controlled motion in a sufficient measure can be revealed, if is assigned/prescribed the law of the displacement of control. Based on this, we will be restricted to the examination of the transfer motion, caused by the step deflection of elevator. This control assumes to be the instantaneous deflection of control of the angle of $\Delta \delta_{BO}$ and its retention in this position (Fig. 14.3).

In this case the solution of system (14.22) it is possible to write in the form

where

$$\Delta \alpha(t) = \Pi_\alpha(t) \Delta \delta_n, \quad \Delta \vartheta(t) = \Pi_\vartheta(t) \Delta \delta_n,$$

$$\left. \begin{aligned} \Pi_\alpha(t) &= A'_\alpha + D'_\alpha e^{\zeta t} \sin(\nu t + \varphi_\alpha), \\ \Pi_\vartheta(t) &= A_\vartheta + B_\vartheta t + D_\vartheta e^{\zeta t} \sin(\nu t + \varphi_\vartheta) \end{aligned} \right\} \quad (14.23)$$

- transient functions on angle of attack and pitch angle respectively.

Since the characteristic determinants of the transfer motion, caused by the deflection of control, and longitudinal short-period motions (14.9) are identically equal, transfer motion is short-period motion. However, the coefficients of A'_a, D'_a, A_b, B_b, D_b, depending on the initial conditions of the structural-aerodynamic characteristics of aircraft and elevator-effectiveness derivative, differ from the same for the short-period motion, caused by the initial disturbance of angle of attack.

Thus, for instance, in expression (14.12) of $A_\alpha = 0$, a in

(14.23) $A'_\alpha = \frac{a_{3n}}{\Omega_0^2}$. If $\zeta < 0$, i.e., oscillatory motion attenuates,

then with period of time angle of attack reaches the new value, which

differs from the initial by value

$$\Delta\alpha(\infty) = A'_\alpha \Delta\delta_n = \frac{a_{3n}}{\Omega_0^2}\Delta\delta_n. \qquad (14.24)$$

This and be an increase in the angle of attack, for the purpose

of obtaining which was undertaken the control pressure.

Page 276.
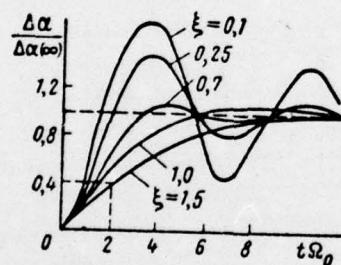
Fig. 14.4. Dependence of transfer motion for different ξ.

From expression for the transient function of pitch angle, it
follows that at the end of transfer motion for a statically stable
aircraft the pitch angle obtains increase, equal to

$$\Delta \vartheta (t_n) = (A_\vartheta + B_\vartheta t_n) \Delta \delta_n, \qquad (14.25)$$

where $t_\varPi$ - the transit time, taken equal to the time of an
amplitude reduction of oscillations twenty times. In the course of
time, an increase in the pitch angle increases proportional to time,
although on angle of attack the aircraft is stabilized. Pitching,
caused component $B_\vartheta t_\text{н} \Delta \delta_\text{в},$ serves as a reason for the development of
long-period transient process. Figure 14.4 shows the character of
transient processes by the angle of attack and pitch at the different
values of the decrement of oscillation.

Analogously are determined the transient functions, also, in the
case of the control displacement of the longitudinal force. During
the deflection of the sector of fuel feed to engine, the transient
process is determined from system (8.13) under the assumption that
$a_{10} = p^{\text{ь}\rho} \Delta \delta_\rho; \quad a_{20} = a_{30} = 0.$

This controlled motion during the step deflection of the sector of fuel feed is continued prolonged period of time, and the pilot has sufficient time for its correction. Therefore in pure/clean form the transfer motion, caused by the step deflection of the sector of fuel feed to engine, does not play so significant role in the evaluation of aircraft handling.

Dynamic characteristics of the longitudinal controlled motion.

By the dynamic characteristics of controlled motion, are understood the criteria, which determine the controlled process, i.e., the indices of the disturbed motion, caused by the control pressure. Since the controlled motion is defined both characteristics of its own airplane disturbance and by the character and the value of the control pressure, the indices of the controllability of motion must include and those, and other characteristics. The structural form of majority of the indices of static controllability can be presented in the following form:

The index of controllability = the value, which characterizes the control pressure / the value, which characterizes the reaction of the motion of the aircraft, caused by this effect.

Page 277.

Such indices include the static handlings examined above (see chapter XII and XIII).

The properties of dynamic aircraft handling can be estimated by its ability rapidly, also, without noticeable oscillations answer the control pressure, i.e., follow a change in the position of controls.

The reaction of aircraft to the control pressure, to the speed of the achievement of the rated value of the parameters of motion, to value of the possible excess/throw/overshoots (overregulation) is characterized by transient functions. Research on transient functions makes it possible to reveal the criteria, which characterize

controlled motion - the quality of transient process.

As it was noted above (see chapter IX), the longitudinal control
pressure on aircraft it is realized by two controls: by an elevator
or by its replacing organ/control and engine-control lever.

The problem of the study of transient process considerably will
be simplified, if we examine separately the motion, caused by the
deflection of elevator, and the motion, caused by the thrust control
or drag. In this case, let us consider that the aircraft does not
undergo the effect of the external perturbation factors.   𝄡 Let us
examine at first the transient process, caused by the deflection of
elevator, after accepting into consideration the following
assumptions:

a) the initial motion - establish/installed and rectilinear;

b) the elevator angle is low (is applicable the principle of
slight disturbances);

c) the control force, caused by the deflection of elevator, considerably less than the aerodynamic lift of aircraft;

d) rate constant ($\Delta V = 0$).

With these assumptions the transfer motion, caused by the deflection of elevator of the angle of $\Delta \delta_B$, can be described by system (8.13), if we into the right side of the momental equation introduce governing torque/moment.

On the well controlled aircraft, it is rapid without oscillations answering the control displacement and force, applied to control levers, the pilots speak: "aircraft follows well the controls" or "walking after steering control (pedals) good". The evaluation of this property can be produced along the delay time of the reaction of aircraft to the control pressure and the absolute value of a change in the parameter of motion.
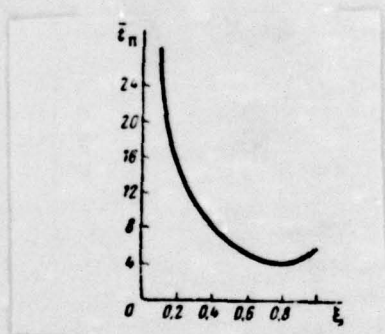
Page 278.

Fig. 14.5. Dependence of the dimensionless time of transfer motion from ξ.

Delay time and the value of the output parameter can be determined,

on the strength of the transfer motion of the aircraft, caused by the

stepped control displacement, or with the aid of the amplitude-phase

characteristics of controlled motion. In the second case the control

displacement is conducted according to harmonic law. Delay is

estimated according to phase displacement between a change in the

parameter of motion in question and a change in the monitored value,

but output value is estimated according to the ratio of their

amplitudes.

Longitudinal control characteristics.

A change in the angle of attack during the deflection of

elevator of $\Delta\delta_B$ is described by expression (14.23). Transit time

shows the delay of the reaction of aircraft to the deflection of

elevator. The time of practical achievement $\Delta\alpha$ (-) with an accuracy

to 5o/o is defined according to equations (14.23) from condition

$$\frac{|\Delta a(t_n)| - |\Delta a(\infty)|}{|\Delta a(\infty)|} = 0,05 = \frac{D_a'}{A_a'} e^{\zeta t_n}.$$

(14.26)

Solving equation (14.26) relative to the transit time of t_n, we obtain

$$t_n = \frac{\ln 20 \frac{D_a'}{A_a'}}{\zeta} = \frac{3 - \ln \sqrt{1 - \zeta^2}}{\zeta \Omega_0}. \quad (14.27)$$

By such form, as one would expect, the transit time completely is determined by its own properties of the short-period disturbed motion.

Let us introduce the concept of dimensionless transit time:

$$\bar{t}_n = t_n \Omega_0.$$

from expression (14.27) it follows that the dimensionless time depends only on the decrement of oscillation ζ. It is necessary to keep in mind that formula (14.27), obtained from equations (14.23), is valid within interval/gap $0 < \zeta < 1$. With $\zeta \geqslant 1$ motion ceases to be oscillatory/vibratory, and solution one should search for in another form. Figure 14.5 gives the dependence of $\bar{t}_\eta (\xi)$, constructed according to formula (14.27), from which it follows that optimum from the viewpoint of a faster achievement of output value one should consider the cases when $0.7 < \zeta < 0.9$.

Page 279.

A decrease in the decrement of oscillation is accompanied by an increase in the excess/throw/overshoot of the parameters of motion (see Fig. 14.4); by excess/throw/overshoot is understood the

difference between the instantaneous value of the parameter of motion and its new potential value of $\delta \alpha_3 = \Delta \alpha$ (t) $\Delta \alpha$ (∞). With considerable excess/throw/overshoot along the angle of attack of oscillation, the motions are perceived in the form of abrupt changes in the acting g-forces, which impedes precise piloting and makes the conditions of comfort worse.

For passenger aircraft the value of $\left| \dfrac{(\delta \alpha_3)_{max}}{\Delta \alpha (\infty)} \right|$ must be not more than 0.15-0.2.

For an aircraft mechanically-controlled, the evaluation of controllability is conducted according to the character of controlled motion, which will depend both on its own properties of airplane disturbance and from the characteristics of the automatic machine of control.

PROBLEMS FOR REPETITION.

1. In what the essence of the simplified examination of the longitudinal disturbed motion?

2. In what the difference between short-period and long-period motions?

3. Which parameters do characterize the oscillatory airplane disturbance?

4. As affects longitudinal stability factor the characteristics of the short-period longitudinal disturbed motion.

5. How does affect static stability level the characteristics of the long-period longitudinal disturbed motion?

Problem.

To determine the characteristics of the short-period and long-period longitudinal disturbed motion (attenuation factor,

oscillation frequency and its period, the decrement of the

attenuation of $t_{0.5}$, the logarithmic decrement of attenuation n, the

time of the complete attenuation t_3), if the characteristic equation

of the longitudinal disturbed motion takes the form

$$p^4 + 6p^3 + 33p^2 + 0.9p + 0.6 = 0.$$

MT/ST-76-1336

Pages 280-299.

CHAPTER XV

LATERAL DISTURBED MOTION.

§ 15.1. Common properties of the lateral disturbed motion.

During the low initial disturbances of the kinematic parameters β, γ, ω_x, ω_y, ψ the lateral disturbed motion is described by

linear differential equations (8.12) or (8.14). Coefficients in these equations depend on the kinematic parameters of the axial motion (ϑ, α, V), which are assumed to be constants and known, from the design characteristics of (J_x, J_y, m) and from the particular force derivative and torque/moments from the kinematic parameters of yawing motion. The particular derivatives of the lateral torque/moments are located as product of the corresponding particular derivatives of moment coefficients to qSl, for example:

$$M_x^\beta = m_x^\beta qSl, \quad M_y^\beta = m_y^\beta qSl,$$
$$M_x^{m_x} = m_x^{m_x} qSl, \ etc.$$

The methods of the determination of the particular derivatives of moment coefficients in $\beta, \omega_x, \omega_y$ and the methods of the determination of perturbing forces and torque/moments, constituting the right sides of the equations and which consist of governing disturbance/perturbations, and the disturbance/perturbations, caused by the effect of medium, are given in chapter X and XI.

The lateral force, i.e., the projection of the main vector $\vec{R}$ on axle/axis Oz_1, is located as projection of aerodynamic force and

gravitational force [1] on axle/axis Oz_1:

$$R_z = G \cos \vartheta \sin \gamma + Z_1,$$

whence with low γ

$$R_z^5 = c_{z_1}^{\vartheta} qS, \quad R_z^T = G \cos \vartheta.$$

FOOTNOTE [1]. The projection of the thrust is small and it can be disregarded. ENDFOOTNOTE.

The structural-aerodynamic characteristics of aircraft are such, that the usually characteristic equation, comprised for the initial system of equations, has two real p_1 and p_2 and two conjugated/combined complex roots of $\mu \pm i\nu$. This means that the lateral disturbed motion consists of two aperiodic motions of the type of Ae^{pt} and one oscillatory motion whose amplitude changes exponentially of the type of $De^{\mu t}$.
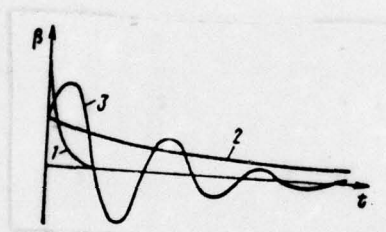
Page 281.

Fig. 15.1. Simplest forms of the lateral disturbed motion: 1. , 2. aperiodic; 3 - oscillatory/vibratory.

Of two real roots p_1 and p_2, as a rule, one in absolute value is considerably more another. If the real roots of characteristic equation and the real part of the complex roots μ are less than zero, the yawing motion of aircraft stable, whereupon stable asymptotically. Typical change in time of one of the parameters of the lateral disturbed motion, which consists of three particular motions, for case $p_1 < 0$, $p_2 < 0$, $\mu < 0$ is given the n of Fig. 15.1.

The motion, which corresponds greater along module/modulus to real root (is curve 1), rapidly attenuates. This motion is accepted to call the motion of roll damping. The smaller for module/modulus real root of characteristic equation corresponds the slowly damped motion; it accepted to call spiral motion. The complex roots of characteristic equation determine the oscillatory motion of aircraft (is curve 3).

In the evaluation of the lateral disturbed motion, the effects of the examined particular motions are not equivalent. At low flight angles of attack, the motion of roll damping, determined in essence by the transverse damping moment, attenuates very rapidly, and in effect it has a weak effect on the development of yawing motion. At wide near-critical angles of attack, when the transverse damping

moment is short and even can become rotating, the motion of roll damping is determining in the development of the lateral disturbed motion.

The spiral motion in many respects is determined by the relationship between the degree of weather cock and lateral stability of aircraft. With low transverse and large weathercock stability the emergent bank is eliminated slowly, and reaction for slip will be considerable, which will lead to the rotation of the nose of aircraft to the side of bank and thereby to a further increase in the roll attitude. This aircraft is spirally unstable, i.e., it has a tendency toward the inlet into spiral motion. However, this motion, while that which was connected with the forward motion of aircraft, is developed very slowly and easily is eliminated.

Page 282.

Therefore the presence of small spiral divergence does not lead to complications in aircraft handling and frequently remains the unnoticed pilot.

The significant effect on the lateral disturbed motion exerts the oscillatory/vibratory phenomenon. Therefore both crew and the passengers estimate the behavior of aircraft in yawing motion as unsatisfactory even in the case of the stability of oscillatory motion, if it attenuates insufficiently rapidly. From foregoing it follows that during the study of the lateral disturbed motion the special attention must be allotted to oscillatory motion. Furthermore, it is necessary to keep in mind that the lateral oscillatory motion, while sufficiently high-frequency (commensurable with the frequency of the longitudinal short-period motion), attenuates more slow than axial motions, which makes it more unpleasant both for the crew and for the passengers.

On stability of motion during the disturbance/perturbation of the initial parameters of yawing motion it is possible to judge by the sign of real roots and the real part of the complex conjugate roots of characteristic equation. Qualitatively yawing motion can be evaluated, by utilizing the stability criteria, examined in chapter VIII. Rausa - Hurwitz' algebraic criterion for polynomial (8.20) is reduced to the execution of inequalities

$$b_1 > 0, \quad b_2 > 0, \quad b_3 > 0, \quad b_4 > 0,$$
$$\mu = b_1 b_2 b_3 - b_3^2 - b_1^2 b_4 > 0,$$

(15.1)

where μ it is called of routh's discriminant.

Since b_{14} is always less than zero, inequality $b_4 > 0$ taking into account (8.21) assumes the form

$$b_{21}b_{33} - b_{23}b_{31} - b_{22}b_{31}b_{43} - b_{21}b_{32}b_{43} < 0. \tag{15.2}$$

After substituting the values of the coefficients of b_{ij} (Table 8.1), we will obtain the following expression for inequality (15.2):

$$\frac{m_x^\beta}{m_\mu^\beta} > \frac{m_x^{\eta}\nu + m_x^{\omega}x \, \mathrm{tg}\,\vartheta\cos\gamma}{m_y^{\eta}\nu + m_y^{\omega}x \, \mathrm{tg}\,\vartheta\cos\gamma}. \tag{15.3}$$

In view of the smallness of the spiral turning up torque/moment
and, therefore, the derivative of $\boxed{m_y^{\bar{\omega}}x}$, inequality (15.3), which
expresses the condition of the spiral stability of aircraft,
approximately can be written thus:

$$\frac{m_x^{\beta}}{m_y^{\beta}} > \frac{m_x^{\bar{\omega}_y}}{n_y^{\bar{\omega}_y}} + \frac{m_x^{\bar{\omega}_x}}{m_y^{\bar{\omega}_y}} \operatorname{tg} \vartheta \cos \gamma, \qquad (15\ 4)$$

whence it follows that on the character of spiral yawing motion the
significant effect exerts the relationships between the static
$\boxed{m_x^{\beta},\ m_y^{\beta}}$ and rotary derivatives of $m_x^{\bar{\omega}}v,\ m_y^{\bar{\omega}}v,\ m_x^{\bar{\omega}}x,$ whereupon with low ϑ
and γ the effect of the last/latter derivative is insignificant.

Page 283.

A sign change of the real part of the complex roots leads to a sign change of routh's discriminant ($\mu < 0$). In this case, the aircraft becomes oscillatory/vibratory unstable.

The analysis of this condition (by analogy with the stability condition of spiral motion) is hinder/hampered as a result of unwieldiness of the obtained expressions. Furthermore, the execution of the stability of the obtained expressions. Furthermore, the execution of the stability of oscillatory motion ($\mu < 0$) do not provide the reference performance of crew. Is necessary fulfilling more stringent requirements for the acceptable conditions of crew activity. The approximate examination and the quantitative indices, which ensure acceptable conditions for a crew, will be presented in the following paragraph.

§   15.2. Rapid yawing motion.

The separation of the longitudinal disturbed motion to rapid and slow made it possible significantly to simplify its investigation, since it came to the analysis of second order equation. Therefore the investigation of the possibility of this separation of yawing motions is of doubtless practical interest. However, the lateral disturbed motion is more complex than longitudinal: here occur the cross couplings between rotary motions with the simultaneous effect on them of forward motion; therefore during the separation of the lateral disturbed motion, is required another approach. Rapid yawing motions it is possible to separate, on the strength of the following special feature/peculiarities of the disturbed motion:

- the at first disturbed motion it is possible to consider rectilinear, i.e., $R_z = 0$, in view of the fact that the spiral motion, connected with the motion of the center of mass, flow/lasts slowly;

- at low angles of attack and, therefore, low pitch angles ϑ the products of $\omega_y \, \mathrm{tg}\, \vartheta, \; \omega_x \alpha$ can be disregarded as small second-order quantities;

- by spiral torque/moments, the especially spiral yawing moment, in the first approximation, can be disregarded in view of their smallness.

When making these assumptions from the equations of lateral disturbed motion (8.14) we obtain the system of equations, which describes the rapid yawing motions of the aircraft:

$$\frac{d\Delta\beta}{dt} - \omega_y = 0, \quad b_{21}\Delta\beta + \frac{d\omega_x}{dt} + b_{22}\omega_x = b_{20},$$
$$b_{31}\Delta\beta + \frac{d\omega_y}{dt} + b_{33}\omega_y = b_{30}, \quad -\omega_x + \frac{d\Delta\gamma}{dt} = 0. \qquad (15.5)$$

Page 284.

We examine this motion under the conditions

$$\Delta\beta(0)=\beta_0; \quad \omega_{x0}=\omega_{y0}=0. \quad \Delta\gamma_0=0;$$
$$b_{20}=b_{30}=0.$$

After eliminating with the aid of the first and third equation of system (15.5) of ω_{y}, we will obtain equation relative to angle β:

$$\frac{d^2\Delta\beta}{dt^2}+b_{33}\frac{d\Delta\beta}{dt}+b_{31}\Delta\beta=0. \qquad (15.6)$$

Its characteristic equation

$$p^2 + b_{33}p + b_{31} = 0.$$

The solution to this equation in $b_{31} > \dfrac{b_{33}^2}{4}$ and $b_{31} > 0$ has two complex conjugate roots:

$$p_{1,2} = -\frac{b_{33}}{2} \pm i \sqrt{b_{31} - \left(\frac{b_{33}}{2}\right)^2},$$

or taking into account the values of b_{3j} (see Table 8.1):

$$p_{1,2} = \frac{M_\mu^{\omega_\mu}}{2J_\mu} \pm i \sqrt{-\frac{M_\mu^\beta}{J_\mu} - \left(\frac{M_\mu^{\omega_\mu}}{2J_\mu}\right)^2}. \tag{15.7}$$

the solution to equation (15.6) it is possible to write in the form

$$\beta = A_3 e^{u_3 t} \cos(\varphi_3 + v_3 t), \tag{15.8}$$

where

$$\mu_\beta = \frac{M_y^{\omega_y}}{2J_y},$$

$$v_\beta = \sqrt{-\frac{M_y^\beta}{J_y} - \left(\frac{M_y^{\omega_y}}{2J_y}\right)^2},$$

(15.9)

A_β and φ_β — integration constant, determined by the initial conditions.

The motion, described by relationship (15.8), is oscillatory motion of yawing with the amplitude of $A_\beta e^{\mu_\beta t}$ and the frequency of v_β.

If aircraft is weather cock stable $(M_y^\beta < 0)$ and possesses the damping properties of $(M_i^{\omega_y} < 0)$, then the oscillatory motion of yawing

rapidly attenuates. The greater the degree of weathercock stability, the greater the oscillation frequency. With an increase in the damping properties, the oscillation/vibrations attenuate faster.

Page 285.

By substituting the value β according to expression (15.8) and b_{2j} according to Table 8.1 in the second equation of system (15.5) and after eliminating from it ω_x with the aid of the fourth equation, we will obtain the lateral equation in the form

$$J_x \frac{d^2\Delta\gamma}{dt^2} - M_x^{\omega}x \frac{d\Delta\gamma}{dt} = - A_\beta e^{\nu_\beta t} \cos(\varphi_\beta + \nu_\beta t).$$

(15. 10)

equation (15.10) heterogeneous. Its characteristic equation has roots

$$p_1 = 0, \qquad p_2 = \frac{M_x^{\bullet}x}{J_x}.$$

The solution to equation (15.10) it is possible to write in the form

$$\Delta \gamma = C_1 + C_2 e^{\frac{M_x^{\omega} x}{J_x} t} + C_3 e^{n \beta t} \cos(\varphi_1 + \nu_\delta t).$$

(15.11)

The constants C_1 and C_2 are located from the initial conditions, but constant C_3 and φ_{τ} - by the substitution of solution (15.11) into equation (15.10). From the analysis of a change in the parameters of

the roll, it follows that it is composed of aperiodic and oscillatory
motions. Aperiodic motion (motion of roll damping) rapidly it
attenuates because of the damping properties of aircraft,
characterized by the condition

$$\underline{M}_{x}^{\omega x} < 0.$$

As criteria, which characterize oscillatory motions, can be
accepted: the time of an amplitude reduction double, the number of
oscillation/vibrations down to the virtually complete attenuation of
motions and the number, which characterizes the relation of the
maximum amplitudes of the angular rates of roll and yawing
(rotation/revolution relative to axle/axes Ox_1 and Oy_1). It is
obvious, the time of an amplitude reduction twice it will be equally

$$t_{0.5} = -\frac{\ln 2}{\mu_\beta} = -\frac{0.693}{\mu_\beta},$$

a the number of oscillation/vibrations before the virtually complete

attenuation of oscillatory motion

$$n_3 \simeq -\frac{3}{\mu_\beta T},$$

where T is an oscillatory period of oscillations.

Page 286.

The relation of the maximum amplitudes of the angular rates of roll and yawing is defined from formulas (15.8) and (15.10) and under the initial conditions $\beta(0) = \beta_0,\ \omega_{x0} = \omega_{y0} = 0$ is approximately equal to:

$$\varkappa = \frac{|\omega_x|_{max}}{|\omega_y|_{max}} = \frac{M_x^\beta J_y}{M_y^\beta J_x} \cdot \frac{1}{\sqrt{1 - \left(\frac{M_x^{\omega_x}}{J_x}\right)^2 \frac{J_y}{M_y^\beta}\left(1 - \frac{M_y^{\omega_y}}{M_x^{\omega_x}} \cdot \frac{J_x}{J_y}\right)}} . \tag{15.12}$$

The practitioner of the operation of aircraft it shows that for
obtaining the acceptable characteristics of rapid yawing motions
necessary satisfaction of condition

$$x < 1 \div 2.$$

as was noted in Chapter X, for an aircraft with swept or delta
wing is characteristic an increase in the degree of lateral stability

with an increase of angle of attack, which leads to an increase in
the $\varkappa$ in flight at high angles of attack. Especially adverse
oscillatory motions can turn out to be for a supersonic aircraft in
flight at high altitudes. In this case as a result of a decrease in
the degree of weathercock stability, directional damping and increase
in the $m_r^?$ (because the flight will occur at high angles of attack)
substantially it will increase $\varkappa.$ An improvement in the
characteristics of oscillatory motion in this case will require the
application/use of automatic devices, which make it possible to raise
directional damping. Such devices find at present wide application.

§ 15.3. Slow yawing motion.

The slow yawing motion in essence is determined by the forward
motion of aircraft. On the strength of the large duration of this
motion, rapid yawing motions manage to completely be discontinued.
Therefore it is possible to approximately consider that the moment of
forces relative to axle/axes Ox_1 and Oy_1 are balanced, but the
angular rate of rotation of velocity vector $\frac{d\beta}{dt} \approx 0.$ When making
these assumptions of equation (8.14) takes the form himself

$$
\left.
\begin{aligned}
b_{11}\Delta\beta + b_{12}\omega_x + b_{13}\omega_y + b_{14}\Delta\gamma &= b_{10}, \\
b_{21}\Delta\beta + b_{22}\omega_x + b_{23}\omega_y &= b_{20}, \\
b_{31}\Delta\beta + b_{32}\omega_x + b_{33}\omega_y &= b_{30}, \\
\frac{d\Delta\gamma}{dt} &\approx \omega_x.
\end{aligned}
\right\}
\qquad (15.13)
$$

In the case of the slow yawing motion, caused by the effect of the momentum/impulse/pulse of cross wind,

$$
b_{10} = b_{20} = b_{30} = 0.
$$

Page 287.   The emergence of slow movement in this case is connected with the presence of the residual attitude of γ_∞ at the torque/moment of the cessation of rapid motions. After eliminating

from the first three equations of system (15.13) of ω_x with the aid
of the fourth, we will obtain

$$
\left.\begin{array}{l}
b_{11}\Delta\beta + (b_{12}p + b_{14})\,\Delta\gamma = b_{12}\gamma_\infty, \\
b_{21}\Delta\beta + b_{22}p\Delta\gamma + b_{23}\omega_y = b_{22}\gamma_\infty, \\
b_{31}\Delta\beta + b_{32}p\Delta\gamma + b_{33}\omega_y = b_{32}\gamma_\infty.
\end{array}\right\}
\tag{15.14}
$$

The characteristic determinant of system (15.14) is equal to

$$
\Delta = \begin{vmatrix}
b_{11} & b_{12}p + b_{14} & 0 \\
b_{21} & b_{22}p & b_{23} \\
b_{31} & b_{32}p & b_{33}
\end{vmatrix} = b_0 p + b_1,
$$

where

$$
\begin{array}{l}
b_0 = b_{11}b_{22}b_{33} + b_{12}b_{23}b_{31} - b_{12}b_{21}b_{33} - b_{11}b_{23}b_{32}, \\
b_1 = b_{14}(b_{23}b_{31} - b_{21}b_{33}).
\end{array}
$$

From equation Δ to zero we find

$$p = -\frac{b_{14}}{b_0}(b_{23}b_{31} - b_{21}b_{33}).$$

Since b_0, as a rule, value positive and if

$$b_{14}(b_{23}b_{31} - b_{21}b_{33}) > 0, \qquad (15.15)$$

that p is value negative, i.e., the corresponding motion will be

stable.

Coefficient b_{14} always less than zero; therefore inequality
(15.15) can be written thus:

$$b_{23}b_{31} - b_{21}b_{33} < 0,$$

that equivalent to inequality (15.4) under the assumption $\vartheta = 0$.
Thus, the slow yawing motion of aircraft, called spiral, is stable,
if

$$\frac{m_x^\beta}{m_y^\beta} > \frac{m_x^{\bar{\omega}_y}}{m_y^{\bar{\omega}_y}}. \qquad (15.16)$$

we examine the process of developing slow yawing motion. At the
torque/moment of the cessation of rapid yawing motions, the aircraft
turns out to be that which was inclined for the angle of γ_∞, as a
result is disturbed the equilibrium of the lateral forces and appears
motion to the side of bank. The developing in this case slip to the

side of the omitted wing will become the reason for the appearance of a static moment of the yawing, which turns the nose of aircraft to the side of the built up wing. The rotation/revolution relative to axle/axis Oy_1 will lead to the appearance of a torque/moment of directional damping, which hinders this motion, and the spiral moment cf roll of $M_x^{\omega_y}\omega_{y_1}$. which attempts to increase bank.

Page 288. If the degree of lateral stability is low, then will develop motion with the building up roll attitude along spiral trajectory. In the case, when aircraft possesses sufficiently large lateral stability, bank will be in the course of time is removed; however, aircraft will make flight with certain yaw angle.

The relationship between the transverse and weathercock stability depends on flight conditions. For an aircraft with sweptback wing, the value of the ratio of lateral stability to weather cock with an increase in the angle of attack increases. Therefore at high angles of attack, as a rule, this aircraft, is spirally stable, and at low angles of attack slow movement either it attenuates very weakly or this motion unstably.

§   15.4. Dynamic characteristics of lateral controllability.

Transient functions of the lateral controlled motion.

During the deflection of the organ/controls of the lateral
control, the pilot absorbs first of all the basic motion, caused by
this action: - bank absorbs during the aileron deflection and yawing
- during the deflection of rudder.

To evaluate the reaction of aircraft to the deflection of the
organ/controls of the lateral control, it suffices to examine
transient process, i.e., the motion, which appears during the step
deflection of ailerons or rudder.

The transfer motion, caused by the deflection of rudder. The
rapid controlled motion, caused by the deflection of rudder, is
described by system (15.5) with

$$\beta_0 = \gamma_0 = \omega_{x0} = \omega_{y0} = 0, \quad b_{20} = \frac{M_x^{\delta_H}}{J_x} \Delta \delta_H = b_{2H} \Delta \delta_H,$$

$$b_{30} = \frac{M_y^{\delta_H}}{J_y} \Delta \delta_H = b_{2H} \Delta \delta_H.$$

then system (15.5) it will be written in the form

$$\left.\begin{aligned} \frac{d\Delta\beta}{dt} &= \omega_y, \\ b_{21}\Delta\beta + \frac{d\omega_x}{dt} + b_{22}\omega_x &= b_{2H}\Delta\delta_H, \\ b_{31}\Delta\beta + \frac{d\omega_y}{dt} + b_{33}\omega_y &= b_{3H}\Delta\delta_H, \\ \frac{d\Delta\gamma}{dt} &= \omega_x. \end{aligned}\right\} \qquad (15.17)$$

After dividing the right and left sides of equations (15.17) to a constant value of the $\Delta\delta_{\text{н}}$, we will obtain the system of equations, in which as independent variables will figure as the transient functions of form

$$\Pi_\beta = \frac{\Delta\beta}{\Delta\delta_{\text{н}}}, \quad \Pi_{\omega_y} = \frac{\omega_y}{\Delta\delta_{\text{н}}}, \quad \Pi_\gamma = \frac{\Delta\gamma}{\Delta\delta_{\text{н}}}, \quad \Pi_{\omega_x} = \frac{\omega_x}{\Delta\delta_{\text{н}}}.$$

from the third and first equations of system (15.17) we will obtain differential equation

$$\frac{d^2\Pi_\beta}{dt^2} + b_{33}\frac{d\Pi_\beta}{dt} + b_{31}\Pi_\beta = b_{3\text{н}},$$

solution of which it can be written in the form

$$\Pi'_\beta(t) = A_\beta + B_\beta e^{\mu_\beta t} \sin(\nu_\beta t + \varphi_\beta).$$

$$(15.18)$$

Here, as this follows from differential equation, $A_\beta = \dfrac{b_{3\text{н}}}{b_{31}}$, and B_β and φ_β - two the arbitrary constants, determined from boundary conditions.

Substituting the initial conditions of $\beta_0 = \omega_{y0} = 0$ in expression (15.18), we will obtain

$$B_\beta = -\frac{b_{3\text{н}}}{b_{31}} \cdot \frac{\sqrt{\nu_\beta^2 + \mu_\beta^2}}{\nu_\beta}, \quad \text{tg}\,\varphi_\beta = -\frac{\nu_3}{\mu_\beta}.$$

If we differentiate from time formula (15.18) and to substitute into the obtained expression the value of the constant of B_β, then we will obtain the following expression for transient function from the angular velocity of the ω_y:

$$\Pi_{\omega_y}(t) = -\frac{l_{3H}}{b_{31}} \frac{\nu_\beta^2 + \mu_\beta^2}{\nu_\beta} e^{\mu_\beta t} \sin \nu_\beta t. \tag{15.19}$$

the transient function on the angular velocity of ω_x with the known dependence of $\Pi_\beta(t)$ is determined from the second equation of system (15.17) and can be represented in the form

$$\Pi_{\omega_x}(t) = A_{\omega_x} + B_{\omega_x} e^{-b_{11}t} + D_{\omega_x} e^{\mu_\beta t} \sin(\nu_\beta t + \varphi_{\omega_x}). \tag{15.20}$$

the integration of dependence (15.20) in time interval 0, t it will make it possible to find transient function from roll attitude:

$$\Pi_\tau(t) = A_\tau + B_\tau t + C_\tau e^{-b_{11}t} + D_\tau e^{\mu_3 t} \sin(v_3 t + \varphi_\tau).$$

(15.21)

the constants of A_{ω_x}, B_{ω_x}, A_τ, B_τ and, etc it is possible to determine from formulas (15.20) and (15.21), on the strength of boundary conditions.

From the analysis of expressions (15.18) - (15.21) it follows:

1. The transient function on slip angle is identical to transient function on angle of attack (14.23) in axial motion. However, the transfer motion of yawing is accompanied by more considerable excess/throw/overshoots on angle (Fig. 15.2).
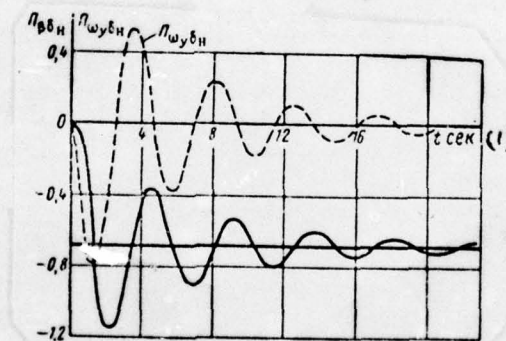
Page 290.

Fig. 15.2. Transient functions on the angle and angular velocity
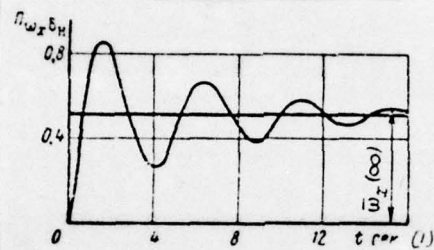
ω_y.
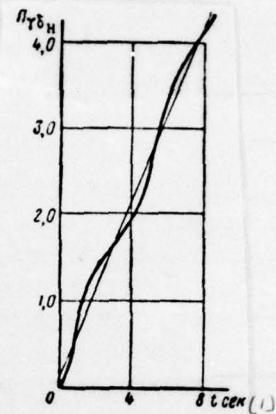

Key: (1). s.

Fig. 15.3.   Fig. 15.4.

Fig. 15.3. Transient function on the angular velocity of ω_x.

Key: (1). s.

Fig. 15.4. Transient function on roll attitude.

Key: (1). s.

2. The motion, caused by the step deflection of rudder, is composed of aperiodic and oscillatory motions. The angular rate of roll in the process of this motion reaches the potential value of $\omega_x(\infty)$ (Fig. 15.3).

3. The taken deflection of rudder leads to a change in the roll attitude in the linear time dependence, on which is placed the oscillatory/vibratory change in the roll attitude, attenuated in the course of time (Fig. 15.4).

The transient functions in the case of the step deflection of ailerons of the angle of $\Delta\delta_\vartheta$ are determined from system of equations (15.5), also, under the initial conditions of $\beta_0 = \omega_{x0} = \omega_{y0} = \gamma_0 = 0$.

Page 291.

In this system as a result of neglect the turning up torque/moment of $(M_y^{\delta_\vartheta})$ one should place $b_{31} = 0$; $b_{20} = b_{23}\Delta\delta_\vartheta = \dfrac{M_x^{\delta_\vartheta}}{J_x}\Delta\delta_\vartheta$. This means that in the initial period during rapid yawing motion there is no motion of yawing, and the roll as it follows now from system (15.5), is

reduced to the following system of equations:

$$
\left.
\begin{array}{l}
\dfrac{d\omega_x}{dt} + b_{22}\omega_x = b_{2\vartheta}\Delta\delta_{\vartheta}, \\[2mm]
\dfrac{d\Delta\gamma}{dt} = \omega_x,
\end{array}
\right\}
\qquad (15.22)
$$

whence we find the transient functions of the roll:

$$
\left.
\begin{array}{l}
\Pi_{\omega_x\delta_\vartheta} = \dfrac{b_{2\vartheta}}{b_{22}}(1 - e^{-b_{22}t}); \\[2mm]
\Pi_{\gamma\delta_\vartheta} = -\dfrac{b_{2\vartheta}}{b_{22}^2}(1 - b_{22}t - e^{-b_{22}t}).
\end{array}
\right\}
\qquad (15.23)
$$

Thus, the step deflection of ailerons produces the aperiodic

rapidly damped roll, in process of which the angular velocity reaches the establish/installed value of $\omega_x(\infty) = \frac{b_{2_9}}{b_{22}}\Delta\delta_9,$ and roll attitude increases proportional to time.

It follows, however, to note that the motion, caused by the step deflection of ailerons, bears more complex character, than this follows from expression (15.22), which describes motion in the initial period of time. Actually, the spiral turning up torque/moment, created by the ailerons of the $M_y^{i_9}\Delta\delta_9,$ directed to the side of wing with the omitted aileron, produces slip for opposite wing and, as a consequence of this, the oscillatory motion of yawing. This same contributes the spiral turning up torque/moment, caused by vertical tail assembly.

CHARACTERISTICS OF LATERAL CONTROLLABILITY.

The dynamic characteristics of the lateral controlled motion reflect the properties of transfer motion, shows the speed of the reaction of aircraft to the governing action.

As it was noted, the motion of yawing, caused by the deflection

of rudder, is analogous with the axial motion, caused by the

deflection of elevator. Therefore this motion also is characterized

by the transit time, determined by formula (14.30), by relative

excess/throw/overshoot on slip angle etc.

Page 292.

However, damping the motion of yawing for contemporary aircraft

is substantially less than damping axial motion. Therefore in the

process of the transfer motion of yawing, are possible considerable

excess/throw/overshoots on slip angle. This especially is noticeable

in flight at high altitudes. In this case, the oscillation/vibrations

of motion are perceived in the form of sharp alternating changes in

the transverse acceleration, which impedes precise piloting, it makes

the conditions of comfort worse on passenger aircraft.

As it is bygone shown above, the deflection of rudder along with

the motion of yawing is accompanied by the roll, which bears also an

oscillatory nature and which delays behind the motion of yawing along

phase to the angle, close to $\pi/2$. Therefore when evaluating the

dynamic characteristics of the lateral controlled motion, it is necessary to consider criterion (see § 15.2)

$$x = \frac{|\omega_x|_{max}}{|\omega_y|_{max}}.$$

In the ideal case neglecting spiral torque/moments the aileron deflection it produces the isolated/insulated roll, which bears aperiodic character.

As the criterion for this motion, can be used values

$$\frac{db_9}{d\omega_x}, \quad \frac{dP_9}{d\omega_x}.$$

In the evaluation of the dynamic properties of the lateral

controlled motion the doubtless interest it represents the analysis

of the amplitude-phase characteristics of the controlled motion, for

obtaining which rudder and aileron they deflect according to harmonic

law. In this case the "walking" of aircraft after controls is

estimated according to phase displacement between the output values

of $(\beta, \gamma, \omega_x, \omega_y)$ and the input effect of $(\delta_\vartheta, \delta_H)$.   The amplitude

ratio of these values characterizes the control effectiveness.

During the execution of the lateral maneuver, as a rule, is

applied the coordinated deflection of the organ/controls of the

lateral control (rudder and ailerons), i.e., the control displacement

it is conducted according to the law, which eliminates the appearance

of a slip angle. Thus, for instance, during the input/introduction of aircraft into bank/turn ailerons are deflected according to the law, necessary for achievement of the preset angle of bank, the control of direction is deflected so that would not appear slip. It is obvious, the law of deflection of rudder it depends on his own properties of aircraft, rudder-effectiveness derivative, pilot's physiological data (determined by the reaction rate of pilot for a change in the slip angle), and also from the law of deflection of ailerons.

Page 293.

If its own disturbed motion attenuates weakly, and the oscillatory period of oscillations is commensurable with the delay time of the reaction of pilot for a change in the slip angle, then the execution of the coordinated motion actually becomes impossible.

PROBLEMS FOR REPETITION.   1. Why is permissible in flying practice small spiral divergence?

2. In what do consist the physical prerequisite/premises of the

separation of yawing motion to rapid and slow?

3. Why for a high-altitude supersonic aircraft it is not always possible to ensure the stability of the yawing motion only by aerodynamic means?

4. In what the sense of the coordinated deflection of the organ/controls of the lateral aircraft control during the execution of the lateral maneuver?

Page 294. Chapter   XVI

SPECIAL FEATURE/~~PECULIARICIES~~ OF ~~the~~ FLIGHT ~~of~~ AIRCRAFT AT HIGH ANGLES OF ATTACK.

§ 16.1. Interaction of the longitudinal and yawing motions of aircraft.

Of real aircraft there does not exist the isolated/insulated
from each other longitudinal and yawing motions. Usually these
motions compose the single disturbed motion; however, the
expansion/decomposition (analysis) of this motion to longitudinal and
lateral (chapter VIII) simplifies the recording of equations and
their solution.

The expansion/decomposition of the motion of aircraft to lateral
and longitudinal is possible only under the completely certain
conditions which are satisfied on the majority of the flight
conditions of contemporary passenger and transport aircraft (subsonic
and transonic layouts). However, in flight at high angles of attack
and in flight at supersonic speeds the longitudinal and yawing
motions are so interconnected that from the separate analysis is
impossible. The factors, responsible for the communication/connection
between the longitudinal and yawing motions, are called usually cross
couplings.

Such factors include cross aerodynamic and inertial couplings,
the elastic deformations of aircraft components etc.

Cross aerodynamic communication/connections are caused by the
dependence of the longitudinal forces and torque/moments on the
kinematic parameters of yawing motion and, in turn, by the dependence
of the lateral forces and torque/moments on the kinematic parameters
of axial motion.

For example with slip aerodynamic lift of aircraft changes not
only as a result of a change in the sweepback of left and right half
wings, but also as a result of a change in the aerodynamic wing-root
interference effect. The delaying wing, as they speak, "is
overshaded" by fuselage, and its lift can noticeably decrease in the
case of low wing monoplane, decreasing the aerodynamic lift of
aircraft as a whole. Furthermore, with slip appears supplementary
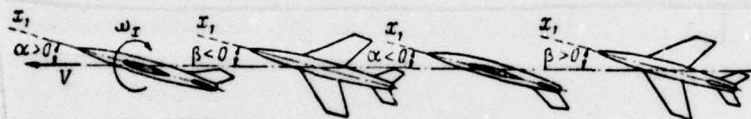lift increment at fuselage.

Page 295.

Fig. 16.1. Change in the angles of attack and slip during the rotation/revolution of aircraft relative to the longitudinal axis.

Since lift increments, which appear with the slip of aircraft, are not applied at the longitudinal focus of aircraft, change in the lift will entail a change in the pitching moment.

Cross aerodynamic communication/connections appear also during the rotation/revolution of aircraft. For example during the rotation/revolution of aircraft relative to axle/axis Ox_1 (Fig. 16.1) angle of attack and slip angle will periodically change. If the rotation/revolution of aircraft is caused by constant rolling moment, then the angular velocity of ω_x will undergo alternations under the action of the rolling moment, which appears with slipping. As a result of a change in the angle of attack and slip angle, will appear stabilized longitudinal and yawing moments, which prevent a change in these angles. Furthermore, the stabilizing moments, creating angular velocities relative to axle/axes Oy_1 and Oz_1, change the position of rotational axis. The greater the longitudinal stability factor on g-force and weather cock static stability, that rotational axis nearer to axle/axis Ox wind coordinate system and further from axle/axis Ox_1 body-fixed system.

Longitudinal-behavior characteristics have an insignificant effect on the lateral forces and torque/moments under cruising

conditions; however, at high angles of attack, are possible different complications. For example if at high angles of attack occurs boundary-layer separation, then the transverse damping moment can substantially decrease and from that which damp be converted into that which rotate.

The emergence of inertia cross connections is caused by inequality to zero of the moments of inertia of aircraft relative to the principal axes of inertia and by the presence of the gyroscopic torque/moments of the rotating parts of the engine.

Gyroscopic torque/moment appears during the rotation/revolution of aircraft relative to any axle/axis, not parallel to the axle/axis of the rotor of engine, and is determined by relationship

$$\vec{M}_{rup} = J_p (\vec{\omega}_p \times \vec{\omega}), \qquad (16.1)$$

where the J_p and $\vec{\omega}_p$ - moment of inertia and the angular rate of rotation of the rotor of the motor respectively; $\vec{\omega}$ are the angular rate of rotation of aircraft.
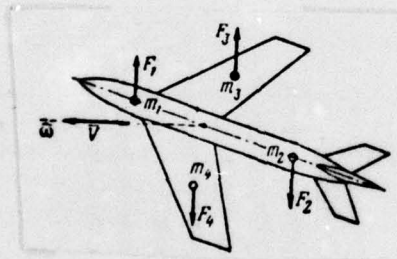
Page 296.

Fig. 16.2. Destabilizing effect of cross inertial moments.

Usually the angle of the engine installation of gggg is small; therefore vector relationship (16.1) in projections on the axis of body coordinate system it is possible to write in the form   .

$$M_{x\,\text{гир}} \approx 0, \quad M_{y\,\text{гир}} \approx -J_p \omega_p \omega_z, \quad M_{z\,\text{гир}} \approx J_p \omega_p \omega_y.$$

From relationship (16.1) it follows that during the rotation/revolution of aircraft around axle/axis Oy_1 appears the pitching moment, and during rotation/revolution in the plane of the symmetry of aircraft, it appears path, i.e., available cross inertial coupling.

Even greater significance for contemporary passenger aircraft has a presence of cross inertial couplings, caused by the weight layout of aircraft (by mass distribution).

Cross inertial moments are considered by those equations of systems (1.19) or (1.23), which describe the rotation/revolution of aircraft, or more precisely - by those terms of these equations which

are equal to the product of angular velocities and a difference in
the moments of the inertia:

$$
\begin{aligned}
M_{x\,\text{ин}} &= (J_z - J_y)\,\omega_z \omega_y, \\
M_{y\,\text{ин}} &= (J_x - J_z)\,\omega_x \omega_z, \\
M_{z\,\text{ин}} &= (J_y - J_x)\,\omega_y \omega_x.
\end{aligned}
\right\}
\qquad (16.2)
$$

    the inertial moments, described by equalities (16.2), always
they are destabilizing. For example if aircraft rotates around the
axle/axis, passing through the center of mass of aircraft and
parallel to velocity vector (Fig. 16.2), then the centrifugal forces,
which appear during rotation/revolution, act in such a way that is
created the torque/moment, which attempts to increase the angle
between the rotational axis and axle/axis Ox_1. Inertial moments
during an increase in the angular rate of rotation can become more
than the aerodynamic righting moments, which will lead to the loss of
stability of aircraft. If inertial moments are more than the
aerodynamic governing torque/moments, which appear during the
deflection of aerodynamic controllers, then aircraft will be
uncontrolled.

For the aircraft of the typical subsonic layouts, for example, of the aircraft of fortieth years, inertia cross torque/moments become dangerous only at the very high angular velocities, virtually not attainable in flight.

Page 297.

However, for the contemporary aircraft, which have a large "mass distribution of" along fuselage, the characteristically significant increase in the inertia cross couplings, caused by the fact that the moments of inertia of J_y and J_z of such aircraft many times are more the moment of inertia of J_x. The relations of the moments of inertia of J_y/J_x and J_z/J_x comprise for subsonic aircraft 2-4, for transonic aircraft 5-8, but for supersonic - 15 and more.

Of the passenger aircraft, which have cruising speeds, which do not exceed the speed of sound, the cross couplings can noticeably affect flight only during the execution of the very energetic

maneuvers, not provided by the rules of flight operations for this class of aircraft. With cross couplings it is necessary to be counted in flight at high angles of attack. The special feature/peculiarities of high-angle-of-attack flight are connected with the fact that the emergence of separation mode/conditions during wing can lead to an abrupt change of the aerodynamic characteristics of aircraft, including its stability characteristics, controllability and damping properties.

§ 16.2. Special feature/peculiarities of aerodynamics of aircraft during high-angle-of-attack flight.

Angles of attack in flight are regulated by the rules of flight operations; therefore the output/yield of aircraft to high angles of attack, close to critical, but the facts more to angles of attack beyond stalling is feasible only as unpremeditated, caused by unforeseen circumstances, by such, as incidence/impingement of aircraft into the ascending gust of air, into wake in front of the flying aircraft, in blast wave, failure of speed indicator, with emergency (for example the failure of engine, the control failure), with intense icing etc. The aerodynamic wing characteristics and aircraft as a whole at high angles of attack sharply differ from

aerodynamic characteristics in operating conditions.

On leaving to high angles of attack on suction side of wing, occurs the boundary-layer separation. Boundary-layer separation appears in that part of the wing on the spread/scope where the lift coefficient of cross section has the greatest value. Of direct/straight and tapered wings with low contraction, the breakaway appears in root cross sections, while of tapered wings with large contraction and of swept it appears in end cross sections [1].

FOOTNOTE [1]. This phenomenon minutely is examined in the course of aerodynamics. ENDFOOTNOTE.

As a result of even small asymmetry in the development of breakaway on sweptback wing, can arise the considerable in value torque/moment, which leads to the bank of aircraft (wing heaviness). An increase in the wing drag in the breakaway zone of boundary layer leads to the appearance of the yawing moment.

Fig. 16.3. Mutual effect of airflow in cross sections with the separation and nonseparated flow of straight wing (a) and swept (b): 1 - the diagram/curve of the distribution of pressure coefficient; 2 - the diagram/curve of rate of flow in spread/scope within the limits of boundary layer.
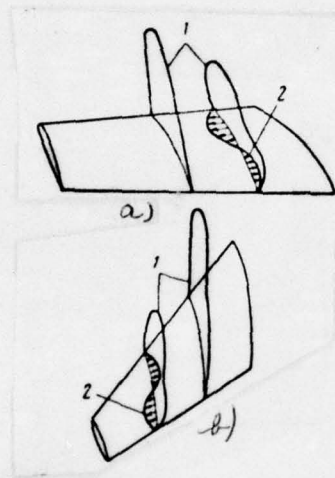
The behavior of aircraft with a further increase in the angle of attack in many respects depends on the speed of the development of flow separation on the wingspan. It can seem that the straight-wing airplane will fall off on a wing more energetic than with swept, because separation the mode/conditions of flow faster is developed on spread/scope of straight wing. This phenomenon can be explained, by analyzing the distribution of pressure coefficient chordwise in different wing sections (Fig. 16.3) and the secondary boundary-layer flow.

In the cross sections of straight wing (Fig. 16.3a) with the developed breakaway the evacuation/rarefaction in nose decreases, while in feed - it increases, which leads to emergence in the nose of the flow of breakaway zone to the zone of nonseparated flow, while in feed it leads to the emergence of reverse flow. This character of the secondary flow accelerates the development of breakaway along the wingspan. Breakaway can achieve even the those cross sections where the lift coefficient is still small. Of sweptback wing the zone of the separation mode/conditions of flow moves towards the incident flow (Fig. 16.3b), which retards the propagation of the breakaway zone of boundary layer. The development of breakaway zone of sweptback wing along spread/scope occurs much more slowly than of straight line.

At high angles of attack, change the longitudinal-behavior characteristics. Boundary-layer separation leads to a decrease in the evacuation/rarefaction in wing leading edge and to an increase in the evacuation/rarefaction in feed. Therefore of straight wing appears the negative pitching moment, under action of which the aircraft attempts to decrease the angle of attack without pilot's interference.

As a result of separation of flow at the ends of sweptback wing, pushed forward back/ago, the lift decreases, while in root cross sections it still continues to grow. This can lead to the center-of-pressure travel forward, and then to the emergence of the pitching torque/moment, which increases angle of attack. The center-of-pressure travel forward can lead to loss of stability on the g-force of aircraft with sweptback wing.

At high angles of attack, appears the prevent/warning agitation of wing whose emergence is explained by the fact that the boundary-layer separation never is stationary.

Page 299. Even with constants the angle of attack, flight speed and
other kinematic characteristics the beginning of breakaway zone
variably oscillates relative to certain mid-position. The lift
coefficient of $c_{y\,тр}$, which corresponds to the beginning of the
agitation of straight wing, is considerably less than $c_{y\,max}$. The
sweptback wing of transonic aircraft possesses more intense
agitation. The more the sweep angle, the lesser the intensity of the
prevent/warning agitation, and the value of $c_{y\,тр}$ approaches $c_{y\,max}$.

The prevent/warning agitation is the source of the timely
information about output/yield to high angles of attack. If during
the wing of aircraft the prevent/warning agitation is absent, then
are applied the special devices, which prevent/warn pilot about
output/yield to high angles of attack.

The appearance of a bank for wing in flight with high angle of
attack by no means not always leads to emergency situation. Of
straight-wing airplane in this case, appears the negative pitching
moment whose action is controlled in the lowering of the "nose" of

aircraft, a decrease in the angle of attack and the transition of aircraft into the mode/conditions of steep descent with an increase in the velocity.

If appears disruption/separation at the ends of the sweptback wing of aircraft, then with bank, for example by the right half wing, and the grow/rising angle of attack under the action of the pitching torque/moment lift will not be parallel to the weight of aircraft - it appears slip for the right half wing. The side component of velocity with slip eliminates disruption/separation. Furthermore, if aircraft did not lose lateral stability, then with slip appears stabilizing moment - bank begins to decrease. In this case now already on left, that is omitted, half wing it can arise the separation of boundary layer. Further all phenomena are repeated.

During the rapid development of disruption/separation at high initial angular rates of rotation aircraft, after losing stability on g-force and falling off on a wing, continues the initial rotation/revolution. The ability of aircraft to enter under specific conditions in the mode/conditions of the stable rotation/revolution of relatively certain axle/axis is connected with the special property of wing, named by autorotation (autogyration).

§16.3. Autorotation of wing at high angles of attack.

Autorotation as property of wing to rotate relative to certain axle/axis during the flow of flow about it at high angle of attack in many respects depends on the coefficients of the normal and tangential components of aerodynamic force, on the angles of attack and slip, on wing planform.

Let us assume that with the angle of attack α to aircraft is interlocked angular velocity ω_x (by the deflection of ailerons or rudder). In this case, as a result of a change in the conditions of flow due to the imposition of rotary motion, will appear the spiral turning up torque/moment, and also, therefore, the angular velocity of ω_y. If ω_x and ω_y they have opposite signs (Fig. 16.4a), then the instantaneous axis, which coincides with the angular velocity of $\omega = \sqrt{\omega_x^2 + \omega_y^2}$, will be turned relative to the longitudinal axis clockwise to the angle $\Delta\varepsilon$, determined from condition

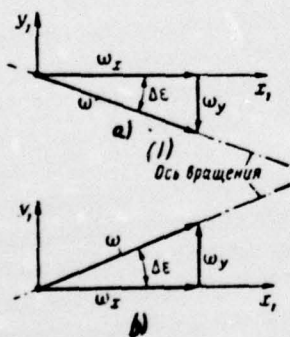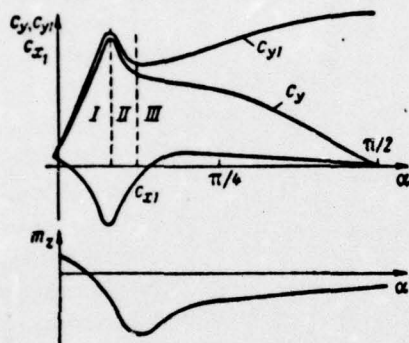$$\text{tg}\,\Delta\varepsilon = \frac{\omega_y}{\omega_x}.$$

Fig. 16.4. Diagram of the rotation/revolution of aircraft with the different (a) and identical (b) signs of the angular velocities of ω_x and ω_y.

Key: (1). Axis of rotation/revolution.

Fig. 16.5. Aerodynamic characteristics of straight wing at high angles of attack.

.   It is obvious, if ω_x and ω_y they have identical signs,

then $\Delta\varepsilon > 0$ and instantaneous axis will be expanded/scanned

counterclockwise (Fig. 16.4b). Depending on the arrangement of

instantaneous axis relative to axle/axis Ox wind coordinate system in

the beginning of rotation/revolution will occur the slip or for the

heaving wing when $\Delta\varepsilon > \alpha$; slip will no with $- \Delta\varepsilon = \alpha$. For a straight

wing at angles of attack below stalling, the rotation/revolution

relative to axle/axis Ox_1 causes the spiral turning up torque/moment,

in sign which coincides with ω_x. In this case the position of

instantaneous axis corresponds to Fig. 16.4b. In angles of attack

beyond stalling the signs of ω_x and ω_y opposite, i.e., the

position of instantaneous axis corresponds to diagram in Fig. 16.4a.

With the noncoincidence of instantaneous axis with ob Ox wind coordinate system depending on the degrees of transverse and weathercock stability appear are the stabilizing (preventing rotation/revolution relative to axle/axis Ox_1) or destabilizing (that facilitate an increase in the rotational speed) static moments of bank and yawings. Besides these torque/moments, appear the torque/moments, caused by the rotation/revolution of aircraft, which are either those which hinder (damping), or rotating.

Fig. 16.6. Diagram for determining the zones of the autorotation:

a — damping; b - autorotation; c - the concealed/latent autorotation.
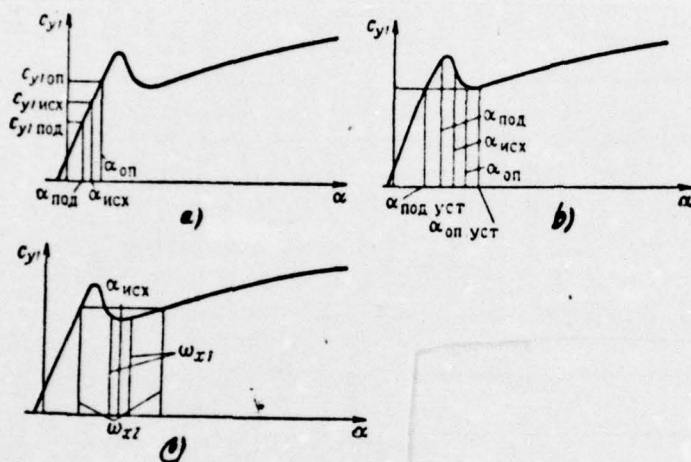
During the agreement of instantaneous axis with axle/axis Ox wind coordinate system the static moments of bank and yawing are absent.

The dependence of the coefficient of the normal force of the straight wing of c_{y1} on angle of attack in body coordinate system (Fig. 16.5) is such, that at angles of attack beyond stalling the value of c_{y1} first decreases (zone II), and then again grow/rises (zone III) is somewhat slower than at angles of attack below stalling (zone I). This character of the dependence of $c_{y1} = f(\alpha)$ leads to the fact that if the aircraft for any reason acquires the angular velocity of ω_x, then depending on the initial angle of attack and value of ω_x to aircraft can act either the damping or rotating rolling moment.

As a result of the rotation/revolution of aircraft around the longitudinal axis, the angle of attack of the being omitted half wing increases, and the angle of attack of the heaving half wing decreases (see §11.3) it is proportional to angular rate of rotation (if ω_x is small). Depending on value and sign of the rolling moment, caused by a change in the angles of attack, it is possible to separate three characteristic cases in the behavior of aircraft, each of which corresponds to the determined range of angles of attack.

1. If aircraft obtained rotation/revolution at angle of attack 0 < α < $\alpha_{\kappa\rho}$ (Fig. 16.6a), then the coefficient of the normal force of the being omitted half wing is higher the coefficient of the normal force of the heaving half wing of $(c_{y1\,оп} > c_{y1\,под})$. In this case appears the damping moment, which impedes rotation/revolution.

Page 302.

2. If angle of attack is such, that the regime point is located on the being omitted segment of a curve of $c_{y1} = f(\alpha)$ (Fig. 16.6b), then even with the very low value of the initial angular rate of rotation of ω_x the coefficient of $c_{y1\,оп}$ is less than $c_{y1\,под}$. In this case appears the directed to the side of rotation/revolution torque/moment, under action of which angular velocity increases until the coefficients of the normal force of the right and left half wings are equaled. In this case the rotation/revolution will be that which was establish/installing, $c_{y1\,оп.\,уст} = c_{y1\,под.\,уст}$, and the angles of attack being omitted $\alpha_{оп.\,уст}$ and heaving the $\alpha_{под.\,уст}$ of half wings will be constant. The angular velocity of the

establish/installed autorotation usually is determined

experimentally. To different angles of attack will correspond the

different angular velocities steady autorotation. The range of angles

of attack with which the least initial rotation/revolution is the

reason for the emergence of the rotating torque/moment, is called the

zone of auto-rotation.

3. If angles of attack correspond to the upward leg of the

dependence of $c_{y1} = f(\alpha)$, then, at first glance, the autorotation of

aircraft it is impossible. However, this is correct only for the low

initial angular velocities of $\omega_x = f(\alpha)$. With an increase in the

rotational speed, the point, which corresponds to the angle of attack

of the heaving half wing, falls on the descending branch and can

arise the situation during which $c_{y1 on} = c_{y1 no\beta}$ (angular velocity

in this case of ω_{x1}). If we now increase the rotational speed,

then with $c_{yon} < c_{yno\beta}$ appears the torque/moment of autorotation. A

further increase in the rotational speed leads to the fact that the

angle of attack of the heaving wing becomes less than critical and

$c_{y1 no\beta}$ begins to rapidly decrease, while $c_{y1 on}$ increases. At

certain new value of the angular velocity of ω_{x2} the coefficients

of the normal force to the left and right of half-wing again are

compared (Fig. 16.6c).

Thus, the range of windmill brake conditions is included between two values of the angular velocity of ω_{x_1} and ω_{x_2}. The range of angles of attack, in which the range of autorotation is limited in value by angular velocity on top and from below, is called the zone of the concealed/latent autorotation. If for each angle of attack of are determined the angular velocities of the establish/installed autorotation, then it is possible to construct the graph/diagram of the dependence of $\omega_x = f(\alpha)$ (Fig. 16.7), called the characteristic of autorotation. By dotted line are shown the mode/conditions of unstable autorotation. Usually of two possible angular velocities in practice, is realized large.

Great effect on the characteristics of autorotation exerts slip. Usually slip for the being omitted half wing is called internal, and on heaving - external. This terminology is explained by the fact that in free-air conditions the aircraft usually is run up/turned to the side of the being omitted half wing which seemingly had been located within the arc of trajectory, described by the center of mass of aircraft. With slip the breakaway zones are displaced to the side of the delaying half wing. For this reason with slip of stable in transverse relation aircraft, is created the supplementary moment of

roll which with external slip increases, and with internal it decreases the angular rate of rotation (Fig. 16.7).
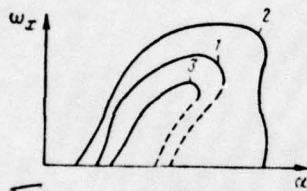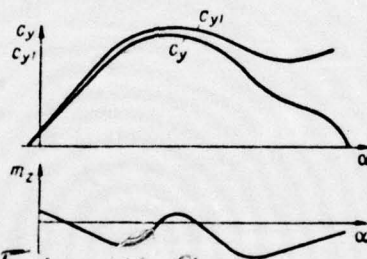
Page 303.

Fig. 16.7.   Fig. 16.8.

Fig. 16.7. The characteristics of the autorotation of the straight wing: 1 - slips no; 2. external slip; 3 - internal slip.

Fig. 16.8. Aerodynamic characteristics of sweptback wing at high angles of attack.

The slip is the powerful means for a change in the characteristics of the autorotation of wing.

Now we will consider the special feature/peculiarity of the autorotation of the sweptback wing, which differs from straight line both by the aerodynamic characteristics and the different yaw effect on these characteristics.

In swept wing dependence curves of $c_{y1} = f(\alpha)$ and $c_y = f(\alpha)$ (Fig. 16.8) are are smoother than of straight line. Maximum in the curve of $c_{y1} = f(\alpha)$ is expressed ill-defined; therefore at the small initial angular velocity of ω_x the difference between the coefficients of the normal force being omitted and heaving of wings is low or virtually even is equal to zero, and the zone of autorotation is comparatively small (Fig. 16.9). Autorotation turns out to be weak, and in certain range of angles of attack beyond stalling, generally it is absent.

With slip the zone of autorotation substantially changes. With the small initial slip of aircraft at different angles of attack, can change both value angular rate of rotation/revolution and its

direction. So complex a character of the behavior of sweptback wing
is explained by the combined effect of the angle of attack and slip
angle on the position of the breakaway zones of boundary layer [1].

FOOTNOTE [1]. M. G. Kotik. The critical behaviors of supersonic
aircraft. M., "machine-building", 1967. ENDFOOTNOTE.

Boundary-layer separation appears during the delaying half wing
(Fig. 16.10), which accelerates rotation/revolution to the side of
this half wing. Then the breakaway appears during the half wing,
pushed forward forward, whereupon the development of breakaway zone
anticipate/leads similar process during the delaying half wing.

Fig. 16.9. The characteristics of the autorotation of the sweptback wing:

1 - slips no; 2. external slip, β = 0.1 ~~is glad~~ *rad;* 3. external slip, β - π/6 ~~is glad.~~ *rad.*

Fig. 16.10. Yaw effect on the position of the breakaway zones of the sweptback wing: I - α = 0.2 ~~is glad;~~ *rad;* II - α = 0.3 ~~is glad;~~ *rad;* III - α = 0.4 ~~is glad;~~ *rad;* IV - α = 0.5 ~~is glad~~ *rad* to V - α = 0.8 rad.
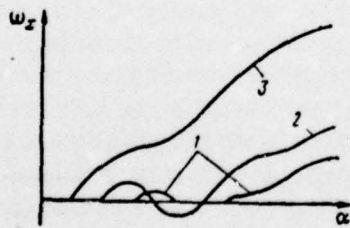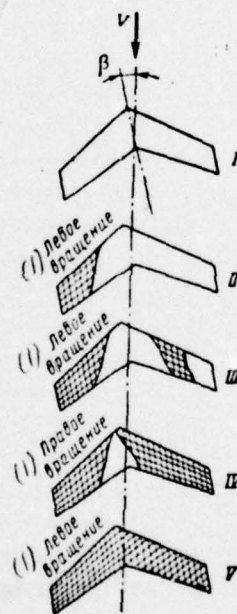
Key: (1) counterclockwise rotation.

Fig. 16.9.

Fig. 16.10.

Rotation/revolution decelerates, ceases and finally when whole pushed forward forward half wing is enveloped by breakaway, and into parts of the delaying half wing, still is retained certain range of nonseparated flow, it begins in the other direction. In Fig. 16.9 contrarotation is reflected by part of the curve 2, arrange/located the below center of abscissas. With a further increase in the angles of attack, the boundary-layer separation seizes entire wing surface; therefore as a result of slip rolling moment is directed to the side of the remaining wing and reduces the initial direction of rotation. At the wide angles (is curved 3 in Fig. 16.9) of the direction of rotation/revolution, it can be constant/invariable.

Thus, the characteristics of the auto-rotation of sweptback wing differ significantly from the characteristics of the autorotation of straight wing and to larger degree depend on the combination of the angles of attack and slip. The autorotation of sweptback wing unlike straight line with slip can be initiated at angle of attack, considerably less critical (with the slip of wing critical angle of attack can decrease by 20-30 o/o from the initial).

The behavior of aircraft at high angles of attack is considerably more complex than the isolated/insulated wing, which is

explained, in the first place, by the mutual effect of aircraft
components; in the second place, fact that during the free flight of
the evolution of aircraft more complex and richer the the transverse
rotation/revolution of wing in the working section of wind tunnel.

Page 305.

§16.4. Corkscrew/spin of aircraft.

The ability of wing to autorotation is the basic reason for the
corkscrew/spin of aircraft. Corkscrew/spin is called the motion of
aircraft along steep spiral, which appears in flight in angles of
attack beyond stalling, which is accompanied by rotation/revolution
around all three axle/axes and by the partial or total loss of
stability. The danger of the incidence/impingement of aircraft into
corkscrew/spin entails the high loss of height/altitude from the
inlet into corkscrew/spin before leaving from it.

Long time the reasons for the inlet of aircraft into
corkscrew/spin remained unknowns; therefore not tales were mastered

and the methods of the removal of aircraft from corkscrew/spin. The
first successful attempt at the intentional inlet into corkscrew/spin
is bygone is undertaken in 1916 by Russian pilot K. K. Artseulov.
However, in view of the complexity of the phenomena, accompany
corkscrew/spin, the flight of Artseulov and attempt at other pilots
could not give the solution to the basic problems, connected with
recovery and its prevention/warning.

Only at the end of 20's the years of Prof. V. S. Pyshnov
demonstrated that the basic reason for corkscrew/spin is the
autogyration of wing. Theoretical analysis in conjunction with the
experimental studies of corkscrew/spin by the test pilots M. M.
Gromov, V. A. Stepanchonk, to V. P. Chkalovs et al. gave possibility
to master the methods of the aircraft control in corkscrew/spin.

The corkscrew/spin of aircraft begins at high angles of attack
with the subsequent stalling of aircraft. Of straight-wings airplane,
the angle of attack with the dumping of α_{cB} differs little from
critical angle of attack, whereupon aircraft usually is dumped to
nose. Aircraft with sweptback wing can fall down for wing even at
angles of attack less than critical, if separation the
mode/conditions of flow is asymmetric, which is possible with slip.

The deflection of ailerons and rudder they can lead to sharp bank and slip. The probability of activation of dumping for aircraft with sweptback wing, assimilated for supersonic aircraft, is more than for the aircraft of old layouts. This is connected with an increase in the virtually minimum speed due to the grown flight altitudes and large specific wing loads. Under these conditions the compressibility of medium exerts a substantial influence on aerodynamic characteristics and with the minimum flight speed of α_{cB} noticeably decreases; therefore flight is made with the angles of attack, close to α_{cB}.

Furthermore, one should consider that for a high-speed aircraft there are limitations on speed, flight mach number, angles of attack, g-force etc. For pilot in flight it is necessary to work large quantity of information which it obtains from instruments - its attention is scattered, the probability of error in the piloting technique increases.

Page 306.

The stalling of aircraft by itself still not means the

unavoidable incidence/impingement of aircraft into corkscrew/spin. If

pilot, energetically deflecting elevator, noses down of aircraft and

thereby will decrease the angle of attack with a simultaneous

increase in the velocity, then aircraft will leave to the

mode/conditions of reduction/descent and to pilot will not difficult

return to horizontal flight conditions.

Aircraft falls into a spin only in those the case, if it was not

impossible to avoid activation of autorotation. During the

rotation/revolution of aircraft, appear the inertial moments. The

inertial moment of pitch leads gradually to an increase in the angle

of attack. In the course of time, can begin the equilibrium of

aerodynamic and inertial moments, aerodynamic and mass forces, which

testifies to the steady-state mode of corkscrew/spin.

In steady spin the aircraft will move over vertical spiral.

Is distinguished stable and unstable corkscrew/spin. For the

unstable corkscrew/spin, observed virtually only in high altitudes,

the characteristically considerable change of the angles of attack,

bank, pitch and slip, and also angular velocities both along the

value and along sign. Aircraft can invert of rotation in
corkscrew/spin, pass from normal corkscrew/spin into inverted (" on
Spin"). The character of oscillations can be that which build up, or
in the form of play.

In the stable corkscrew/spin of direction, the
rotation/revolutions in ω_x and ω_y do not change, although the
values of angular velocities can be variables. When angular rates of
rotation are virtually constants, stable corkscrew/spin can in the
course of time pass into that which was establish/installing.

Upon the inlet of aircraft into corkscrew/spin from level flight
entire process from the inlet of aircraft into corkscrew/spin to
return toward level flight can be divided into a series of the
stages, shown in Fig. 16.11. On transfer section the corkscrew/spin
is usually stable, but being unsteady. At the end of the transfer
section, the spin axis is virtually vertical. The transfer section of
supersonic aircraft turns out to be so extended that the pilot
manages to derive aircraft from corkscrew/spin prior to the beginning
of its vertical section.

Vertical corkscrew/spin is observed in essence of subsonic aircraft, whereupon within the limits of vertical section is feasible steady spin. Since this is the simplest mode/conditions of corkscrew/spin, it possible, although sufficiently approximately, to describe theoretically, which makes it possible to perform highly useful analysis and on its base to manufacture recommendations pilot about recovery. During the analysis of the vertical steady spin, they assume that the engine thrust is equal to zero, the density of air with a change in altitude is constant, and total aerodynamic force R lie/rests at the plane of symmetry.

Fig. 16.11. Stages of accomplishing the corkscrew/spin:

1 - level flight; 2 - transfer section; 3 - vertical corkscrew/spin; 4 - the section of the cessation of autorotation; 5 - dive; 6 - pullout.

Key: (1) the axis of cord (2). trajectories.

Fig. 16.12. the diagram of the forces, which act on aircraft in the vertical steady spin.
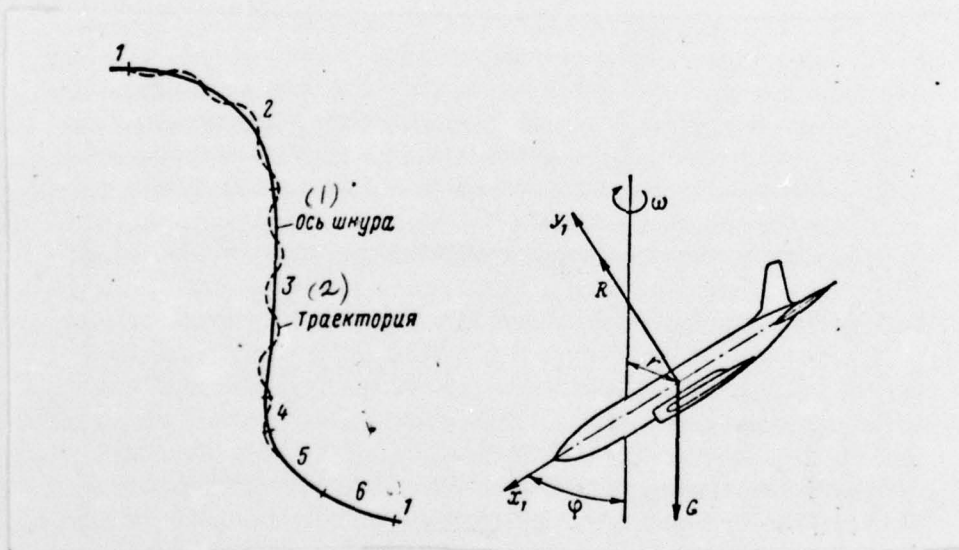

Fig. 16.11.   Fig. 16.12.

After designating the angle between the vertical line and axle/axis OX_1 by ϕ, but the angular rate of rotation of aircraft relative to the vertical axle/axis of through ω (Fig. 16.12), for the projections of angular velocity on coordinate axes we will obtain

$$\left.\begin{array}{l} \omega_y = \omega \sin\varphi, \\ \omega_x = -\omega \cos\varphi, \\ \omega_z = 0. \end{array}\right\} \qquad (16.3)$$

. In vertical corkscrew/spin the trajectory of the motion of the center of mass is close to vertical line, therefore it is possible to rely $\phi \approx \alpha$. The trimmed conditions of aerodynamic and inertial moments taking into account relationships (16.2) can be written in the form

$$M_x = 0, \quad M_y = 0, \quad M_z = (J_y - J_x)\omega_x\omega_y.$$

.   By utilizing for ω_x and ω_y of expression (16.3), we will obtain

$$M_z = (J_x - J_y)\frac{\omega^2}{2}\sin 2\alpha. \tag{16.4}$$

.   In steady spin the longitudinal aerodynamic couple must be equal to the longitudinal inertial moment.

Page 308.

The equations of forces to conveniently write in cylindrical coordinate system:

$$\left.\begin{array}{l} R \sin a = G, \\ R \cos a = m\omega^2 r, \end{array}\right\} \qquad (16.5)$$

where r is a distance of the center of mass of aircraft of spin axis; R - the total aerodynamic force, directed along this axle/axis, since at angles of attack beyond stalling the force of periphery is low.

From the first equation of system (16.5) it is possible to determine g-force in the center of the masses of the aircraft:

$$n = \frac{R}{G} = \frac{1}{\sin a}.$$

.   The greater the angle α, the lesser the g-force.

With $\alpha = 0.6-0.8$ ~~is glad~~ *rad* (spinning dive) $n = 1.5-2$; with $\alpha = 0.8-1$ ~~is glad~~ *rad* (flat corkscrew/spin) $n = 1.15-1.5$; with $\alpha = 1-1.2$ ~~is glad~~ *rad* (vertical corkscrew/spin) $n = 1-1.15$.

After introducing the coefficient of total aerodynamic force, from the first equation of system (16.5) it is possible to find velocity aircraft during motion along trajectory

$$V = \sqrt{\frac{2G}{\rho S c_R \sin u}} = \sqrt{\frac{2Gn}{\rho S c_R}}.$$

. In the first approximation, for angles of attack beyond stalling it is possible to consider that $c_R = c_{y\,max}$. Then, taking into account relationship (3.15), we obtain

$$V = V_{min}\sqrt{n}. \tag{16.6}$$

. That means the more smoothly the corkscrew/spin, the closer the velocity is to minimum. By the term-by-term division of the first

equation of system (16.5) into the second it is possible to determine radius of spin:

$$r = \frac{g}{\omega^2} \text{ctg } \alpha. \tag{16.7}$$

. The time of accomplishing one turn is equal

$$t = \frac{2\pi}{\omega},$$

then the loss of height/altitude for one turn:

$$H = Vt = \frac{2\pi V}{\omega} = \frac{2\pi \sqrt{n}}{\omega} V_{min}. \tag{16.8}$$

.   With ω= 1 rad/s, n = 1 and V_{min} = 60-70 m/s the loss of
height/altitude for turn will be on order 400 m. The value of radius
of spin can be evaluated, after relying $\alpha = \pi/4$; we will obtain $r \approx$
10 m.

Page 309.

By comparing this result with the loss of height/altitude for one
turn, let us arrive at the conclusion that in vertical corkscrew/spin
the aircraft moves over the very extended spiral.

For determining angle of attack α it is possible to use equation (16.4), left side of which is the longitudinal inertial moment.

After dividing both parts of the equation to qSb_A and after introducing dimensionless quantities

$$\bar{\omega} = \frac{\omega l}{2V}; \quad i_z^{'} = \frac{4(J_y - J_x)}{l^2 qSb_A},$$

where the b_A - the chord of wing equivalent, we will obtain equation (16.4) in the form

$$-m_z = i_z^{'}\bar{\omega}^2 \sin 2\alpha. \qquad (16.9)$$

.   Here right side can be named the coefficient of the inertial moment of $m_{z\ \text{ин}}$. The dependences of the values of moment coefficients from the large angle of attack are given in Fig. 16.5 and 16.8.

For determining the coefficient of inertial moment depending on angle of attack it is possible to use characteristic autogyration (see Fig. 16.7), taking into account in this case, that value ω, which enters expression (16.4), is determined with known ω_x and ω_y from condition

$$\omega^2 = \omega_x^2 + \omega_y^2.$$

.   The graph/diagram of the dependence of $m_{z\,\text{ин}} = f(\alpha)$ is shown in Fig. 16.13. In the general case the condition - $m_z = m_{z\,\text{ин}}$ is satisfied at two points, which correspond to the angles of attack α_1 and of α_2 (point K and L). At point K, the moment balance is unstable, since during the probable deviation of angle of attack from α_1 resulting moment will stimulate an increase in this deflection.

In order to derive aircraft from corkscrew/spin, it is necessary to discontinue the autorotation of aircraft, to decrease the angle of

attack and to transfer aircraft to the mode/conditions of the dive from which after an increase in the velocity of flight aircraft can be transferred into horizontal flight condition. However, can arise this situation, when even the complete positive displacement insufficiently in order that the longitudinal aerodynamic couple would exceed in value the longitudinal inertial moment.

Frequently for a recovery, it is necessary to preliminarily create internal slip. In this case as a result of slip, appears the rolling moment, which hinders transverse rotation/revolution, the longitudinal inertial moment decreases (Fig. 16.14) and the energetic deflection of elevator will be sufficiently for the lowering of the nose of aircraft with the subsequent transition to dive.
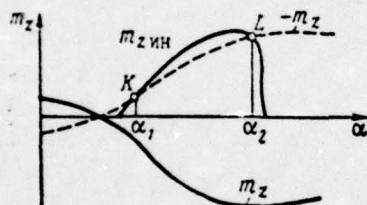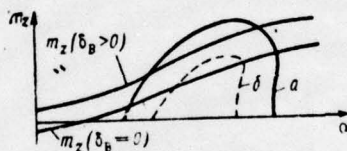
Page 310.

Fig. 16.13.   Fig. 16.14.

Fig. 16.13. Diagram for determining angle of attack in steady spin.

Fig. 16.14. Yaw effect on the conditions of recovery:

a - slips no; b is internal slip.

To stop rotation/revolution by the aileron deflection is usually impossible, and sometimes also dangerously, especially for subsonic aircraft. At high angles of attack, the ailerons are enveloped by the breakaway zone of boundary layer; therefore they are ineffective for the creation of rolling moment and affect the behavior of aircraft in corkscrew/spin in essence because of the fact that the different resistance of left and right half wings during the aileron deflection creates the torque/moment of the M_y, which it can lead to internal or external slip. Most reliably decelerates rotation/revolution by the deflection of rudder "against corkscrew/spin" for the creation of internal slip.

Figure 16.15 shows the recommended into the present time methods of recovery. The first method is applied for a recovery from unstable corkscrew/spin, by the second it is applied from oscillatory/vibratory corkscrew/spin, the third it is applied from stable uniform corkscrew/spin, the fourth - from very stable flat/plane corkscrew/spin. Pilot itself selects the approaching method of recovery depending on the character of corkscrew/spin. The application/use of stronger methods, especially for a supersonic aircraft, can lead to the undesirable phenomena (more nose dive, the transition of left corkscrew/spin to the right, transition of "normal" corkscrew/spin to inverted and, etc).

The behavior of aircraft with the inlet into corkscrew/spin and output/yield from it is studied both in the project stage on models and in flight tests. Best will be the aircraft which more badly falls into a spin and easier it emerges. Are known the aircraft, which the corkscrew/spin emerge "themselves", if all controls are establish/installed into free position. Recently an improvement in the airplane spinning characteristics is made by applying automatic means (for example the automatic machines of damping the angular velocities of ω_x and of ω_y), which make it possible to stabilize aircraft over a wide range of angular velocities.

Page 311.   Fig. 16.15. Scheme of control of aircraft on leaving from corkscrew/spin.

Key: (1). method (2). Corkscrew/spin (3). Spin recovery (4). It began (5). Conclusion (6). It is neutral (7). Ailerons. (8). It is neutral (9). Vol. s (10). On corkscrew/spin (11). Deflection of controls (12). Against corkscrew/spin. On corkscrew/spin.
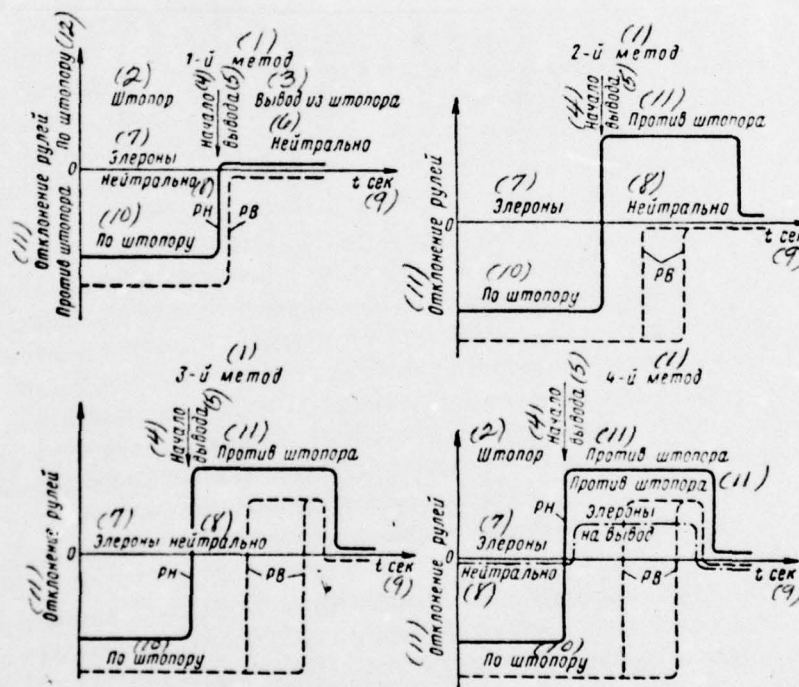
PROBLEMS FOR REPETITION.

1. In which flight conditions of the longitudinal and yawing motion, it is necessary to study together?

2. Which reasons produce an increase in the so-called preventive/warning agitation of aircraft with swept wing? 3. Why in the zone of the concealed/latent autorotation stable will be autorotation with larger lateral velocity? 4. Why elevator can turn out to be ineffective for a recovery from stall?

ZDACA.

Determine is the projection of the cross gyroscopic torque/moment of engine, after using formula (16.1) on the assumption that the angle of φ_{AB} sufficiently large.

Answer/response

$$M_{\text{гир}.x} = J_p \omega_p \omega_z \sin \varphi_{AB},$$
$$M_{\text{гир}.y} = - J_p \omega_p \omega_z \cos \varphi_{AB},$$
$$M_{\text{гир}.z} = J_p \omega_p (\omega_y \cos \varphi - \omega_x \sin \varphi).$$

Page 312.

Chapter XVII.

CONCEPTS ABOUT THE EFFECT OF any ELASTIC _{construction} DEFORMATIONS in CONSTRUCTION ON their STABILITY CHARACTERISTICS AND CONTROLLABILITY.

§ 17.1. Elastic deformations. Wing divergence and tail assembly.

Aircraft possesses great flexibility, which is connected with the requirement for the lightness/ease of construction. Is especially noticeable flexibility for the passenger and other heavy nonmaneuverable aircraft, the safety factor of which is considerably lower than of the maneuverable light aircraft.

Under certain conditions the effect of the elastic deformations of aircraft components on its characteristics is sufficient substantially.

When evaluating many dynamic characteristics of elastic aircraft are used quasi-static deflections, based on the assumption that changes of the aerodynamic loading in the disturbed motion occur so slowly that the construction during entire time of the action perturbed motion is found in static equilibrium. This assumption will not lead to appreciable errors, if the frequencies of the disturbed motion are considerably less than frequencies of the elastic vibrations of construction.

When the difference between these frequencies is low, occurs the considerable mutual effect of elastic displacements and airplane disturbance. In this case problem one should examine taking into account dependence of elastic deformations from time, i.e., with the use of dynamic methods of analysis [1].

FOOTNOTE [1]. 1. Ya. C. Fyn. Introduction to the theory of aeroelasticity, M., IL, 1959. 2. R. L. Bisplingoff, Kh. Ashley, R. L. Khalfmen. / aeroelasticity. M., IL, 1958. ENDFOOTNOTE.

Here will be given only the qualitative analysis of the particular questions of aeroelasticity conformably to the characteristics of stability and controllability of aircraft, based on static method; in this case are made the following assumptions:

a) is valid the strip hypothesis, according to which with the strain of any part of the aircraft the configuration of its cross section does not change;

b) are negligible the strains of aircraft components of the mass forces.

Fig. 17.1. Change in the angle of attack of wing section with twisting strain:

1 - the aerodynamic center line of cross section at subsonic speeds; 2 elastic wing axis; 3 line of cross-sectional foci at supersonic speeds.

Fig. 17.2. Change in the angle of attack of the cross section of sweptback wing with bending.
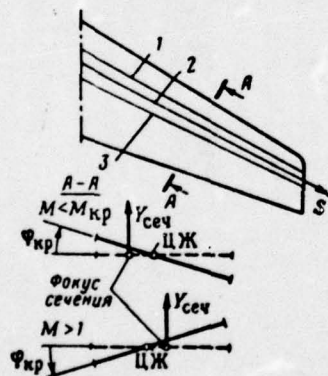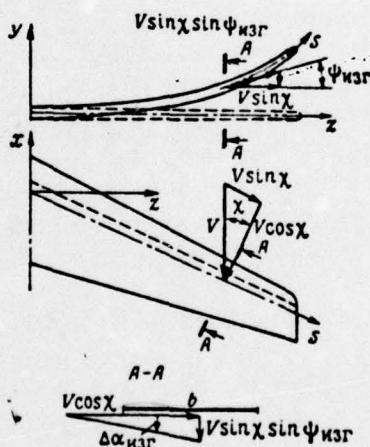

Fig. 17.1.   Fig. 17.2.

Let us examine the effect of strain on the distribution of the local angles of attack of sweptback wing. Straight wing can be considered a special case swept. When making these assumptions wing can be simulated by elastic beam with reinforcing over root cross section. Let us consider that the elastic axle/axis of beam (line of flexural centers) it coincides with the line of the centers of rigidity of cross sections (twist centers of cross sections).

Both the twisting strain and bending strain leads to a change in the local angle of attack of sweptback wing. The increase in the angle of attack, caused by the torsion of $\Delta\alpha_{KP}$, is equal to the angle of torsion (Fig. 17.1), while the increase in the $\Delta\alpha_{И3T}$, caused by bending, it is determined according to Fig. 17.2 by expression

$$\Delta\alpha_{изг} = -\frac{V\sin\chi\sin\psi_{изг}}{V\cos\chi} \approx -\psi_{изг}\,tg\,\chi \approx -\frac{dy}{ds}\,tg\,\chi,$$

where the $\psi_{изг}$ — of dihedral arm sweep in this cross section, caused by bending;

y - the sagging/deflection of elastic axle/axis [1];.

s is a coordinate of cross section throughout elastic axle/axis.

FOOTNOTE [1]. Since to this chapter all phenomena are examined in body coordinate system, index "1" is everywhere lowered. ENDFOOTNOTE.

Thus, the change of the angle of attack in cross section A-A, normal the line of elastic axle/axis, is determined by sum

$$\Delta \alpha_{a\,y} = \Delta \alpha_{\text{кр}} + \Delta \alpha_{\text{изг}} \approx \varphi_{\text{кр}} - \frac{dy}{ds}\,\text{tg}\,\chi. \qquad (17.1)$$

.   A change of the angle of attack in the cross section, parallel

to root chord, we find through formula

$$\Delta \alpha_y \approx \Delta \alpha_{a\,y} \cdot \cos \chi = \varphi_{\kappa p} \cdot \cos \chi - \frac{dy}{ds} \sin \chi. \qquad (17.2)$$

. Specifically, for the straight wing of $\Delta \alpha_y = \varphi_{\kappa p}$.

Let us assume that the average value of a change in the angle of attack, caused by elastic deformations, is equal to an increase in the angle of attack in wing section with the coordinate of $z_{c\rho}$, i.e., the $\Delta \alpha_{y\,cp} = \Delta \alpha_y(z_{cp})$, which is determined by the bending moments and torsion, which act in this cross section, and by value flexural and torsion rigidity.

Let the torsional moment relative to elastic axle/axis in the cross section of $z_{c\rho}$ be equal $M_{z\,\kappa p}$, and the bending moment of $M_{x\,\text{изг}}$. If flight establish/installed and rectangular, then these

torque/moments, while static aerodynamic couples, depend on the angle

of attack of cross section and at low angles of attack can be

expressed by formulas

$$M_{z \, \text{кр}} = M_{z0} + M_{z \, \text{кр}}^{\alpha}(\alpha + \Delta \alpha_y),$$
$$M_{x \, \text{изг}} = M_{x \, \text{изг}}^{\alpha}(\alpha + \Delta \alpha_y).$$

- If the flexural rigidity of the selected cross section and

torsion is characterized by the coefficients of k_E, k_G, then the

equilibrium of aerodynamic and elastic torque/moments in this cross

section is determined by system of equations

$$\left. \begin{array}{l} M_{z0} + M_{z \, \text{кр}}^{\alpha} \alpha + M_{z \, \text{кр}}^{\alpha} \Delta \alpha_y - k_G \varphi_{\text{кр}} = 0, \\ M_{x \, \text{изг}}^{\alpha} \alpha + M_{x \, \text{изг}}^{\alpha} \Delta \alpha_y - k_E \dfrac{dy}{ds} = 0. \end{array} \right\} \qquad (17.3)$$

.   By utilizing equality (17.2) and after solving system (17.3)

relative to $\Delta \alpha_y$, we will obtain

$$\Delta \alpha_y = \frac{k_E (M_{z0} + M_{z\ \kappa p}^\alpha \alpha) \cos \chi - k_G M_{x\ \text{изг}}^\alpha \alpha \sin \chi}{k_G k_E - (k_E M_{z\ \kappa p}^\alpha \cos \chi - k_G M_{x\ \text{изг}}^\alpha \sin \chi)} \quad . \qquad (17.4)$$

.   The aerodynamic couples of $M_{z\ \kappa p}$ and $M_{x\ \text{изг}}$ are proportional

to velocity head; therefore they can be written in the form

$$M_{z\ \kappa p} = M_{z\ \kappa p}^q q; \quad M_{x\ \text{изг}} = M_{x\ \text{изг}}^q q.$$

Page 315.
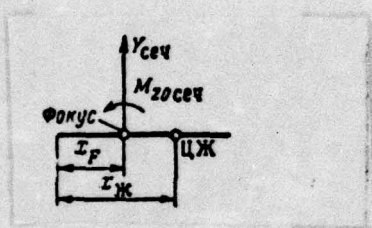
Fig. 17.3. Torque of wing sections.

As it follows from formula (17.4), with an increase in velocity head, the $\Delta\alpha_y$ grow/rises and with certain q it approaches infinity.

The phenomenon with which the equilibrium of the aerodynamic and elastic torque/moments, which act on wing, unstably and any disturbance/perturbation leads to the boundless increase in strains, is called wing divergence, and the corresponding value of velocity head - by critical velocity head.

From formula (17.4) we obtain

$$q_{\text{к.к}} = \frac{k_G k_E}{k_E M_{z\,\text{кр}}^{\alpha q} \cos \chi - k_G M_{x\,\text{изг}}^{\alpha q} \sin \chi} . \quad (17.5)$$

. Derived $M_{z\,\text{кр}}^{zq}$ is equal to

$$M_{z\,\text{кр}}^{zq} = \Delta x_{\text{ж}} c_\nu^z S,$$

where the $\Delta x_{\text{ж}} = x_{\text{ж}} - x_F -$ arm of lift relative to center of rigidity (Fig. 17.3).   ¶ If center of rigidity is arranged after focus (on the contemporary aircraft of $x_{\text{ж}} \approx (0,35 \div 0,4)b$), then torsion produces an increase in the angle of attack and divergence begins when the elastic torque/moment of cross section on the strength of limitedness does not balance aerodynamic. On supersonic velocities, focus, moving back/ago, it can prove to be after center of rigidity. In this case the twisting strain lowers the aerodynamic loading of cross section and divergence there will not be $(q_{\text{д.к}} < 0)$. In the latter case of $q_{\text{д.к}}$, it does not have the physical sense and is the convenient calculated parameter.

It is obvious, expression (17.4) with the aid of formula (17.5) can be written in the form

$$\Delta a_y = \frac{\cos \chi \, \dfrac{M_{z0}}{k_a} + \bar{q}_{\text{л.к}} a}{1 - \bar{q}_{\text{л.к}}}, \qquad (17.6)$$

where

$$\bar{q}_{\text{л.к}} = \frac{q}{q_{\text{л.к}}}.$$

.   The determination of an increase in the angle of attack of horizontal tail assembly somewhat becomes complicated by the dependence of the aerodynamic force of horizontal tail assembly on the strain of wing and fuselage. Under the action of the aerodynamic force of horizontal tail assembly, the fuselage is transformed, which leads to the change in the angle of setting tail assembly. The strain of wing produces change of the rake angle in the range of horizontal tail assembly and, therefore, a change in its true angle of attack.

Page 316.

The increase in the angle of attack of swept horizontal tail

assembly, caused it by elasticity and the elasticity of fuselage, can be determined in the form of sum

$$\Delta\alpha_{y.r.o} = \varphi_{\text{кр.r.o}}\cos\chi_{r.o} - \left(\frac{dy}{ds}\right)_{r.o}\sin\chi_{r.o} + \Delta\varphi_{\phi},\qquad(17.7)$$

where the $\varphi_{\text{кр.r.o}}$ and $\left(\dfrac{dy}{ds}\right)_{r.o}$ — twisting strain and the relative strain of the bending of horizontal tail assembly; $\Delta\varphi_{\phi}$ - the change in the angle of setting horizontal tail assembly, caused by the bending strain of fuselage.

Let $M_{\text{изг.r.o}}$, $M_{\text{кр.r.o}}$ — bending and torsional the moments, which act in the cross section of $z_{\text{ср.r.o}}$; $k_{E\,r.o}$, $k_{G\,r.o}$ are stiffness coefficients of this cross section for bending and torsion, but $k_{E\phi}$— the stiffness coefficient of fuselage to bending.

Then the equilibrium of the elastic and aerodynamic couples, which act on tail assembly, taking into account the elasticity of fuselage is written in the form of system of equations

$$
\left.
\begin{aligned}
M^{e.r.o}_{\text{кр.r.o}}(\alpha_{r.o} + \Delta\alpha_{y.r.o}) - k_{G\,r.o}\varphi_{\text{кр.r.o}} &= 0, \\
M^{e.r.o}_{\text{изг.r.o}}(\alpha_{r.o} + \Delta\alpha_{y.r.o}) - k_{E\,r.o}\left(\frac{dy}{ds}\right)_{r.o} &= 0, \\
\mp Y^{e.r.o}_{r.o}(\alpha_{r.o} + \Delta\alpha_{y.r.o}) - k_{E\,\phi}\Delta\varphi_{\phi} &= 0.
\end{aligned}
\right\}
\qquad (17.8)
$$

Sign "minus" corresponds to the tail assembly, arrange/located in aft fuselage section, positive sign - to canard configuration. Solution of system (17.8) together with equation (17.7) gives the change in the angle of attack of horizontal tail assembly, caused by the elasticity: the

$$
\Delta\alpha_{y.r.o} = \frac{\bar{q}_{\text{л.r.o}}\alpha_{r.o}}{1 - \bar{q}_{\text{л.r.o}}}; \quad \bar{q}_{\text{л.r.o}} = \frac{q_{r.o}}{q_{\text{л.r.o}}}, \qquad (17.9)
$$

where of the $q_{z.r.o}$ — critical velocity head of the divergence of horizontal tail assembly;

$$q_{z.r.o} = \frac{1}{\dfrac{M_{\text{кр.r.o}}^{zq}}{k_{G\,r.o}}\cos\chi_{r.o} - \dfrac{M_{\text{изг}}^{zq}}{k_{E\,r.o}}\sin\chi_{r.o} \pm \dfrac{Y_{r.o}^{zq}}{k_{E\Phi}}} \; .$$

·   If $k_{E\Phi}=\infty$, i.e., fuselage is absolutely rigid, then for a wing with low sweepback or with the low rigidity of the torsion of the tail assembly of $q_{z.r.o}>0.$

With the tail arrangement of tail assembly and elastic fuselage, as a rule, $q_{z.r.o}<0,$ i.e. the divergence of tail assembly is absent. This is connected with the predominant effect of the strain of fuselage, which leads with an increase in velocity head to a decrease in the angle of attack of horizontal tail assembly.

Page 317.

For the aircraft, executed by the diagram of "weft", $q_{\text{д.г.o}} > 0$, with positive $\alpha_{\text{г.o}}$ the strain of fuselage with an increase of q contributes to an increase in the angle of attack of horizontal tail assembly.

§ 17.2. Effect of elastic deformations to the stability characteristics and aircraft handling.

Effect of elasticity on the stability level of aircraft on g-force. The coefficient of the pitching moment of aircraft taking into account the elastic deformations of its parts can be written in the form of sum

$$m_{z\,y} = m_{z0} + [\bar{x}_{\text{т}} - (\bar{x}_F' + \Delta\bar{x}_{F\,y})]\,c_y - A_{\text{г.o}}k_{\text{г.o}}c_{y\,\text{г.o.y}}, \quad (17.10)$$

where the $\Delta \bar{x}_{Fy}$ - displacement of mean aerodynamic center of wing, caused by the redistribution of $c_{y\,ce\,y}$ due to elastic deformations;

$\bar{x}_F'$ are a dimensionless coordinate of the focus of aircraft without horizontal tail assembly.

The increase in the stability level from g-force is determined according to condition (17.10) for formula

$$\Delta m_{z\,y}^{c_y} = m_{z\,y}^{c_y} - m_{z\,\mathbf{x}}^{c_y} = - \Delta \bar{x}_{Fy} - A_{r.o}k_{r.o}\frac{\partial \Delta c_{y\,r.o.y}}{\partial c_y}, \quad (17.11)$$

where the $m_{z\,y}^{c_y}, m_{z\,\mathbf{x}}^{c_y}$ — respectively the degree of stability for

the overload of elastic and absolutely rigid aircraft.

Hence it follows that a change in the degree of stability in overload depends on the displacement of the focus, caused by the elasticity of wing and by the sign of the derivative of $\frac{\partial \Delta c_{y\,r.o.y}}{\partial c_y}$.

For the unswept wing of $\Delta \bar{x}_{Fy} = 0$ and the effect of elasticity on $m_z^{c_y}$ is determined by the sign of $\frac{\partial \Delta c_{y\,r.o.y}}{\partial c_y}$. Disregarding in the first approximation, the effect of zero moment on the strain of aircraft components and counting $c_y \approx c_{y\kappa p}$ (wing), we obtain the following dependence of $\Delta c_{y\,r.o.y}$ on c_y;

$$\Delta c_{y\,r.o.y} = \frac{c_{y\,r.o}^a}{c_y^a}(1 - \epsilon^a)\frac{\bar{q}_{\lambda.r.o} - \bar{q}_{\lambda.\kappa}}{1 - \bar{q}_{\lambda.r.o}} c_y + \frac{c_{y\,r.o}^a \bar{q}_{\lambda.\exists.o}}{1 - \bar{q}_{\lambda.r.o}} \alpha_{0r.o}.$$

Thus:

$$\frac{\partial \Delta c_{y\,r.o.y}}{\partial c_y} = \frac{c_{y\,r.o}^a}{c_y^a}(1 - \epsilon^a)\frac{\bar{q}_{\lambda.r.o} - \bar{q}_{\lambda.\kappa}}{1 - \bar{q}_{\lambda.r.o}}. \qquad (17.12)$$

Page 318.

The displacement of the focus of elastic sweptback wing can be determined approximately by formula 1.

$$\Delta \bar{x}_{F\,y} = \bar{q}_{\text{a.}\text{u}}(\bar{z}_{cp} - \bar{z}_A)\frac{b}{2b_A}\,\text{tg}\,\chi, \qquad (17.13)$$

where the $\bar{z}_{cp}, \bar{z}_A = \dfrac{2z_A}{l}$ are dimensionless coordinates of the selected Wing section and the mean aerodynamic chord.

FOOTNOTE [1]. L. G. Totiashvili. Longitudinal stability and the controllability of flight vehicle. RIIGA, Riga, 1963. ENDFOOTNOTE.

For an aircraft with sweptback by flight surface the picture somewhat becomes complicated in view of a change in the position of the mean aerodynamic center of wing and effect of flexural strains on an increase in the angles of attack of flight surface.

Effect of elasticity on the stability level of aircraft on speed. As the measure of the stability of aircraft for speed serves derivative

$$\left(\frac{dm_z}{dc_y}\right)_{n-1} = m_z^{c_y} + m_z^M \left(\frac{dM}{dc_y}\right)_{n-1}.$$

.   Taking into account (17.10) and disregarding, as this was made
when evaluating $m_{z\,y}^{c_y}$, by the effect of a change in the m_{z0} due to
elastic deformations, after simple conversions we obtain

$$\Delta\left(\frac{dm_z}{dc_y}\right)_y = \left(\frac{dm_z}{dc_y}\right)_y - \left(\frac{dm_z}{dc_y}\right)_{\text{ж}} = \left(\Delta\bar{x}_{F\,y}^{M}\frac{M}{2} - \Delta\bar{x}_{F\,y}\right) +$$

$$+ A_{r.o}k_{r.o}\frac{c_{y\,r.o}^{a}}{c_y^a}(1-\varepsilon_y^a)\frac{(\bar{q}_{\text{х.r.o}} - \bar{q}_{\text{х.к}})\bar{q}_{\text{х.r.o}}}{(1-\bar{q}_{\text{х.r.o}})^2} -$$

$$- A_{r.o}k_{r.o}\frac{c_{y\,r.o}^{a}}{c_y^a}\varepsilon_y^{aM}\frac{M}{2}\frac{\bar{q}_{\text{х.r.o}} - \bar{q}_{\text{х.к}}}{1-\bar{q}_{\text{х.r.o}}}. \qquad (17.14)$$

.   Here $\varepsilon_y^{\alpha M}$ are a derived ε^α on M, which is equal virtually to zero with of $M < M_{KP}$, less than zero with of $M > M_{KP}$. At the supersonic speeds of $\varepsilon_y^{\alpha M}$ it is possible to accept equal to zero. The value of $\Delta \bar{x}_{Fy}^{-M} \frac{M}{2} - \Delta \bar{x}_{Fy}$ becomes zero, if $\Delta \bar{x}_{Fy}$ is determined by formula (17.13).

Based on this, it is possible to consider that the change in the
stability level of aircraft in speed due to the effect of elastic
deformations on all flight speeds, except transonic, in essence is
determined by second term of expression (17.14).

Depending on the design of aircraft (is usual, "weft",
"bobtailed aircraft"), of the form of wing, tail assembly in
plan/layout, the relationship of flexural rigidities and torsion for
a flight surface, the rigidity of fuselage, flight mach number
stability level on speed can either increase $\left[\Delta\left(\frac{dm_z}{dc_y}\right)<0\right]$, or
decrease $\left[\Delta\left(\frac{dm_z}{dc_y}\right)>0\right]$.

Page 319.

For each concrete/specific/actual case the approximate estimate of a
change in the $\frac{dm_z}{dc_y}$ due to the value of the elastic deformations of
construction approximately can be executed according to formula
(17.14).

Effect of elasticity on lateral stability. The bending strain of wing increases of dihedral arm sweep, which contributes to an increase in the m_x^β of elastic aircraft in comparison with rigid. Furthermore, the bending strain of fuselage and the strain of vertical tail assembly under the action of the lateral force are brought depending on the relationship of the rigidities of tail assembly and fuselage to increase or decrease in effective slip angle, which contributes in the first case to an increase, and secondly - to a decrease in the m_x^β.

On aircraft with sweptback wing, the picture becomes complicated as a result of a change in the effective angles of attack of wings with slip. Since during the pushed forward wing the load grow/rises, and effective sweep angle decreases, lateral stability of wing grow/rises both as a result of the change in the $m_{x\psi}^\beta$ and the m_{xl}^β (see Chapter X).

Effect of the elasticity of vertical tail assembly and fuselage on the degree of weathercock stability. The lateral force, which has

effect during slip on vertical tail assembly, causes fuselage bending

and the strain of vertical tail assembly. The increase in the slip

angle, caused by the elasticity of vertical tail assembly and

fuselage, can be determined by formula (17.7) or (17.9). having

preliminarily replaced index "q.o" by "v.o".

Then

$$m_{y\,y}^{3} = m_{y\,\text{ж}}^{\beta} \frac{1}{1 - \bar{q}_{\text{Д.в.о}}} . \qquad (17.15)$$

If $q_{\text{Д.в.о}} < 0$, which is the case for the majority of

aircraft, the degree of feathering stability decreases with the

increase in q. This is especially unpleasant for supersonic aircraft

whose decrease in the m_{y}^{β} with transition to supersonic flight

speeds even without it is the reason of unrest/uneasiness of the

pilots.

Approximate dependence $m_{\nu x}^{\beta} = f(M)$, $m_{\nu y}^{\beta} = f(M)$ are given in Fig. 17.4.

Effect of elasticity on damping characteristics. In chapter XI, is shown that the considerable part of the longitudinal damping moment is determined by horizontal tail assembly.
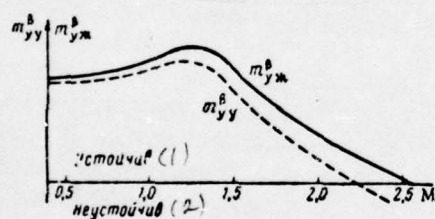
Page 320.

Fig. 17.4. Dependence of $m_{y \divideontimes}^{\beta}$ and m_{yy}^{β} on mach number:

$\divideontimes$ - absolutely rigid aircraft; y - elastic aircraft.

Key: (1). Stable. (2). Is unstable.

Therefore we will be restricted to the examination of the effect of elasticity on this part of the damping moment.

According to equation (17.15):

$$m^{\bar{\omega}_z}_{z\,\text{г.о.у}} = m^{\bar{\omega}_z}_{z\,\text{г.о.ж}}\,\frac{1}{1 - \bar{q}_{\text{л.г.о}}}\,, \qquad (17.16)$$

i.e. if $q_{\text{д.г.о}} > 0$, then the damping moment of horizontal tail assembly ncreases in comparison with the torque/moment of absolutely rigid aircraft. But if $q_{\text{д.г.о}} < 0$, which occurs for aircraft with elastic fuselage and with swept tail assembly, then damping the motion of pitch decreases.

Similarly dependence we will obtain for the damping yawing moment and bank.

Effect of structural elasticity on the control effectiveness. As a result of the center-of-pressure travel of tail assembly with the

deflected control surface of height/altitude (Fig. 17.5) appear the strains, which facilitate a decrease in the governing moment with respect to the center of mass of aircraft. The coefficient of this torque/moment for an elastic aircraft is equal to

$$m_{z\text{у}} = -A_{\text{r.o}}k_{\text{r.o}}c^2_{\text{и r.o}}(n_{\text{н}}\delta_{\text{в}} + \Delta\alpha_{\text{r.o.y}}).$$

.   Then the efficiency ratio of control for an elastic and rigid aircraft is record/written in the form

$$\frac{m^{\delta_{\text{н}}}_{z\text{у}}}{m^{\delta_{\text{н}}}_{z\text{ж}}} = \frac{n_{\text{н}} + \Delta\alpha^{\delta_{\text{н}}}_{\text{r.o.y}}}{n_{\text{в}}}.\qquad (17.17)$$

. At certain value of velocity head of $q_{p.r.o}$, called critical velocity head of the reversal of control, governing torque/moment becomes zero. Obviously $q_{p.r.o}$ can be determined from condition (with $q_{r.o} = q_{p.r.o}$)

$$(n_s \delta_s + \Delta a_{r.o.,y}) = 0. \qquad (17.18)$$
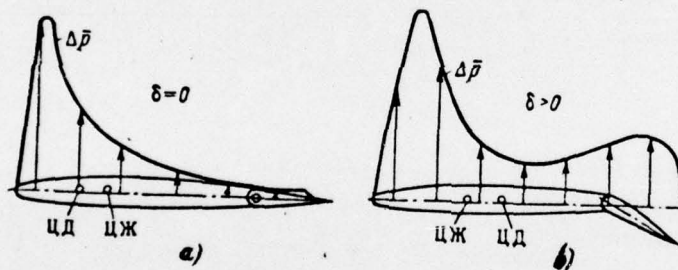
.

Page 321.

Fig. 17.5. Pressure distribution according to the horizontal tail assembly: a — a control in free position; b - angle of deflection is positive.

The joint solution of formulas (17.9) and (17.18) makes it possible to find communication/connection between of $\Delta\alpha_{r.o.y}$ and δ_β in the form

and, therefore, derived $\dfrac{\partial \Delta a_{r.o.y}}{\partial \delta_n}$.

From expressions (17.17), (17.19) we obtain

$$\frac{m_{z\,y}^{\delta_n}}{m_{z\,\varkappa}^{\delta_n}} = \frac{1 - \bar{q}_{p.r.o}}{1 - \bar{q}_{\lambda.r.o}}, \qquad (17.20)$$

where the $\bar{q}_{p.r.o} = \dfrac{q_{r.o}}{q_{p.r.o}}$; $q_{p.r.o}$ — critical velocity head of the reversal of elevator.

Similar dependences occur for the relative rudder-effectiveness

derivative and ailerons.

Figure 17.6 gives the typical for an elastic aircraft dependence of the relative rudder-effectiveness derivative on Mach number at constant flight altitude.
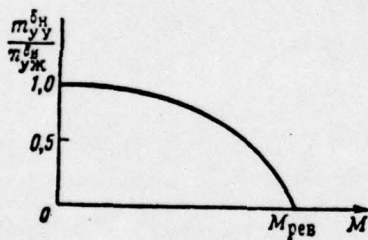
Page 322.

Fig. 17.6. Dependence of the relative rudder-effectiveness derivative on mach number for an elastic aircraft.

In the first approximation, the dynamic stability characteristics and aircraft handling taking into account elastic deformations can be determined by the methods, presented in chapter XIV and XV, with the introduction of corrections for elasticity to the coefficients of a_{ij}, b_{ij} in the theory of quasi-static deflections.

PROBLEMS FOR REPETITION.

1. How elastic bending and wing torque lead to a change in the local angles of attack?

2. As additionally will change the local angle of attack during a rapid change in the angles of curvature and torsion?

3. Explain the physical side of the phenomenon of divergence.

4. Of what consists the special feature/peculiarity of the lateral control of aircraft at the speed, which exceeds the speed of reversal of aileron?

MT/ST-76-1336

Pages 323-345.

Chapter   XVIII

FLIGHT OF AIRCRAFT UNDER SEVERE WEATHER CONDITIONS.

18.1. Gust effect on the flight of aircraft.

The air medium in which flies the aircraft, is found in continuous motion. If this motion little deviates from uniform and rectilinear, then it barely affects the characteristics of flight, changing only the velocity of aircraft earth referenced. Wind effect on fuel consumption per kilometer and on flying range was analyzed in chapter V. The behavior of airplane in flight in the zones of atmospheric turbulence is more complicatedly.

Atmospheric turbulence appears in the area of the high wind velocity gradients and temperature during the interaction of air flow with the surface of the Earth, during convective vertical air circulation as a result of its nonuniform heating on the different sections of the Earth, in the process of cloud formation.

With by periodic the effect of atmospheric turbulence on the flying aircraft the motion of the latter becomes agitated. The effect of perturbing forces causes the vibrations of aircraft and turbulence. The forming under these conditions g-forces lead to the overvoltage of the separate cell/elements of aircraft and the disturbance/breakdown of the comfort of the passengers.

At the torque/moment of the inlet into the descending and
updraft and into the torque/moment of output/yield of them the
aircraft experience/tests jerk/impulses. Fallininto downflow aircraft
seemingly it fails, into that which ascend - seemingly ascends. If in
the process of the disturbed motion airplane leaves to near-critical
angles of attack, then it can fall down for wing with the possible
subsequent inlet into corkscrew/spin.

Since the turbulent phenomena can be described only
statistically, since atmospheric turbulence yet studied sufficiently
fully, the analysis of the behavior of aircraft taking into account
random effects on it from the side of the turbulent atmosphere proves
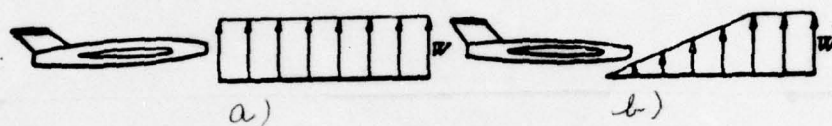to be complex.

Page 324.

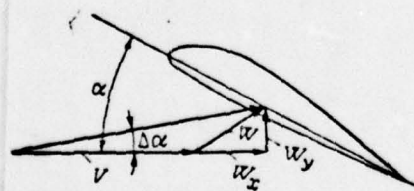Fig. 18.1. Simplest forms of the gust: a) stepped; b) triangular.

Fig. 18.2. Effect of the velocity of gust on angle of attack and the value of airspeed.

Usually is examined effect on the aircraft of the gust, which has the
final extent, a random single strong change in the flight speed in
value. This gust is characterized by extent, the value of the maximum
deviation of flight speed with respect to module/modulus and
direction, and also by the route segment of flight, during which
speed change reaches its maximum (gradient distance). If gradient
distance is equal to zero, then gust is called stepped (Fig. 18.1a).
If the speed of gust changes according to linear law, this gust is
called triangular (Fig. 18.1b). There can be other forms of gusts.

In the general case the velocity vector of gust $\vec{W}$ in wind
coordinate system it is possible to decompose on three components:
$W_x,\ W_y,\ W_z.$ By retaining the diagram of perturbation analysis,
accepted in the preceding/previous chapters, it is possible to
separately examine the effect longitudinal $(W_x,\ W_y)$ and lateral the
(W_z) of gusts.

A change in the aerodynamic lift of aircraft, which flies in
stagnant air at constant velocity, under the action of the
longitudinal gust (Fig. 18.2) it is possible to express by equation

$$\Delta Y = \frac{\partial Y}{\partial \alpha} \Delta \alpha + \frac{\partial Y}{\partial V} \Delta V.$$

Taking into account that

$$Y = c_y^e (\alpha - \alpha_0) \frac{\varrho V^2}{2} S,$$

we will obtain

$$\Delta Y = Y \left(\frac{c_y^e}{c_y} \Delta \alpha + \frac{2 \Delta V}{V} \right). \tag{18.1}$$

since for contemporary high-speed aircraft

$$V \gg W_x; \quad V \gg W_y,$$

that velocity increment of flight polta and angle of attack in the first approximation, it is possible to express as follows:

$$\Delta V \approx W_x; \quad \Delta \alpha \approx \frac{W_y}{V}. \qquad (18.2)$$

Page 325.

Taking into account these values ΔV and $\Delta \alpha$ relationship (18.1) it is possible to rewrite in the form

$$\frac{\Delta Y}{Y} = \frac{c_y^a}{c_y} \frac{W_y}{V} + 2 \frac{W_x}{V}.$$

(18.3)

The first term in the right side of equation (18.3) characterizes the effect of vertical gust (velocity change in the direction) on a change in the lift, and the second - the influence of horizontal gust (velocity change in value).

With a sufficient extent of gust, rapid motion manages to be discontinued to the end of the gust. More complex for an analysis (and dangerous for a flight) is the gust of alternating/variable intensity, especially such, with which the disturbance/perturbation

of angle of attack changes its sign (alternation ascending and
descending gusts).

The greatest danger for aircraft they represent the stepped
vertical gusts of $(W_x=W_z=0)$,   it is explained by two reasons. First,
since the value of the ascending gust can reach to 15-20 m/s, a
change in the angle of attack can be considerable, and with a
decrease in the velocity of flight increases the danger of the
output/yield of aircraft to angles of attack beyond stalling. In the
second place, vertical gust can cause large normal load factors. The
value of normal load factor is determined by the ratio of lift to
weight (2.14), and, thus, with gust

$$n_y + \Delta n_y = \frac{Y + \Delta Y}{G} = n_y + \frac{\Delta Y}{G} .$$

if reference-flight conditions the establish/installed
rectilinear horizontal, then Y = G and

$$\Delta n_y = \frac{c_y^a}{c_y} \frac{W_y}{V} = \frac{1}{2} c_y^a \frac{\rho V W_y}{\frac{G}{S}} . \qquad (18.4)$$

Consequently, the increase in the g-force directly proportional to the flight speed and velocity of vertical gust. The sign of an increase in the g-force is determined by the direction of the velocity of gust ("plus" for that which ascend and "minus" for descending). The increase in the g-force, determined by dependence (18.4), is initial. Its further change will depend on transient-response characteristics.

An increase in the g-force can reach great significance. So, with $c_y^a = 4$, $\rho = 0.5$ kg/m³ (H $\approx$ 8500 m), the flight speed of V = 200 m/s, to the specific wing load p = 3000 N/m² and the speeds of the gust of $W_y = 15$ m/s an increase in the g-force of Δn_y is approximately equal to unity.

Page 326.

Table 18.1.

Интенсивность болтанки (1)	Приращение перегрузки Δn_y (2)	Физиологические ощущения пассажиров (3)
Слабая (4)	0,005—0,2	Неприятные ощущения у отдельных пассажиров (5)
Умеренная (6)	0,2—0,5	Неприятные ощущения у значительной части пассажиров. Затруднительность хождения в салоне (7)
Сильная (8)	0,5—1	Болезненные явления у большинства пассажиров. Возможность травм при хождении по салону (9)
Очень сильная (10)	Больше 1 (11)	Болезненные явления у подавляющего большинства пассажиров. Отделение от кресел и зависание на ремнях (12)

Key: (1). Intensity of turbulence. (2). Increase in the g-force of Δn_y (3). Physiological perceptions of the passengers. (4). Weak. (5). Discomfort in the separate/individual passengers. (6). Moderated. (7). Discomfort of the considerable part of the passengers. Difficulty of walking in salon. (8). Strong. (9). Unhealthy phenomena of the overwhelming majority of the passengers. Isolation/evolution from seats and hovering on belts. (10). Very heavy; (11) Greater than 1; (12). Signs of illness in the overwhelming majority of passengers. Separated from seats and restrained by seat belts.

The permissible overloads are restricted to the ultimates of the structural strength of aircraft and to the conditions of the comfort of the passengers. On the basis of the physiological perceptions of the passengers with g-forces (Table 18.1), as extreme value for passenger aircraft, is taken the value of $\Delta n_y = 0.5$.

Besides vertical gusts, there are horizontal gusts, which lead to a change in the slip angle. Statically stable aircraft reacts to gust by bank to opposite half wing and by turn towards gust. In this case the initial disturbance is characterized by slip angle. Perturbation analysis is made acording to the procedure, given in chapter XV.

18.2. Special feature/peculiarities of the flight of aircraft under the conditions of icing.

Icing affects the flight of aircraft not only as a result of an increase in its flight mass. The ice outgrowths, which are formed on flight surface, change the contours of their airfoil/profile and change the conditions of its flow, which leads to a deterioration in the aerodynamic characteristics, stability characteristics and

controllability and flight fineness ratios. Icing can upset the operation of engines and cause the failure of important controls.

Ice formation on the surface of aircraft, streamlined with air flow, occurs as a result of the presence in the atmosphere of the determined amount of water drops in the liquid state even at minus temperatures. These drops form the clouds, observed at any time of year; during flight of aircraft in clouds at the minus temperature of air, they are crystallized and form a layer of ice on its surface.
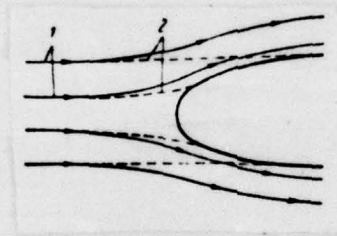
Page 327.

Fig. 18.3. Diagram of the precipitation of drops on the nose of the airfoil/profile: 1 - flow line; 2 - the trajectory of drops.

Icing can occur, also, upon transition of that containing in the atmosphere water pair to ice, passing liquid phase, as a result of the so-called sublimation.

Ice formation usually occurs only on the leading wing edges and tail assembly. This is explained by the fact that the airflow at critical point on leading edge is divided into two parts, which flow around the upper and pressure side of wing (Fig. 18.3), in this case near spout flow lines strongly are bent. The particles of water, which move together with air, do not manage, on the strength of their inertia, to invert of motion following flow lines and, moving over more flat trajectories, they deposit on the spout of airfoil/profile.

If we approximately assume that whole amount of water, which falls on wing, is converted into ice, then the amount of ice, which is formed for time unit per unit of the length of wing (icing intensity I) is determined by formula [1]

$$I = E\omega cV,$$

where E - the complete coefficient of settling; ω are water content of air, or specific humidity (amount water pair in 1 m³ humid air); c is a profile thickness of wing.

FOOTNOTE [1]. O. K. Turnov. Aircraft icing and means for battle with it M, "machine-building", 1965. ENDFOOTNOTE.

The coefficient of settling E in the general case depends on the form of the nose of the airfoil/profile and of the number of $Re_0 = \frac{Vd}{\nu}$, determined according to the size/dimension of drops. The force of inertia are determined by the dimensionless parameter p, which can be calculated according to formula

$$p = k \frac{\varrho_n r 2V}{\mu L} , \qquad\qquad (18.5)$$

where r of the radius of drop; ϱ_b - water density; L - the significant dimension of the streamlined body; μ - the ductility/toughness/viscosity of air; $k = 1 + 0,17 \, Re_0^{2/3}$ - the coefficient, depending on the mode/conditions of the flow of air about the drop.

The physical sense of parameter p, determined by relationship (18.5), lies in the fact that it is proportional to the ratio of force of inertia to the drags of drop.

Page 328.

If value p is close to zero (r — 0), then the drops move together with air. The more parameter p, the more the trajectory of drops they differ from the flow lines of air flow and, therefore, the process of settling drops in the nose of the body more intensive.

as shows theoretical studies [1], the value of the complete coefficient of settling in essence depends on parameter p and is very small from Re_0.

FOOTNOTE [1]. I. P. Mazina. Physical principles of aircraft icing. M, Gidrometeoizdat, 1957. ENDFOOTNOTE.

From the practice of the operation of aircraft, it is known, that the more the flight speed, on the fact at the more low temperature of surrounding air occurs aircraft icing. At supersonic speeds the theoretical heating of the surface of aircraft is so high that, in essence, is observed the only sublimation icing, but drop barely is encountered. The range of the minus temperatures at which occurs the icing, is sufficiently great - from 0°C to -40°C.

Through the data of practice, 80o/o of supercooled clouds they are found in temperature range from 0°C to 10°C. Relative humidity with icing is 80-100o/o, and specific humidity (water content of air) 1 g/kg and more. The water content of the cooled clouds above the territory of the USSR, according to the data of central aerological observatory (TsAO [ЦАО - Central Aerological Observatory]), varies within the limits 0.1 g/m³ - 1.6 g/m³ and depends on the temperature of air. On these GosNII [ГосНИИ - State Scientific Research Institute] GA [ГА,   - Civil Aviation], the greatest probability of icing is observed at height/altitudes ~7000-8000 m (Fig. 18.4).

Depending on flight conditions, can be the various forms of ice formation (Fig. 18.5); however, they all they lead to a decrease in the critical angle of attack and $c_{y max}$.   It can prove to be also that

at constant angle of attack in the process of icing will appear the
developed breakaway zone of boundary layer, which leads to a decrease
in the lift coefficient of wing.

Is especially dangerous the icing of tail assembly. For example
during the wide downwash angles and with considerable deflection of
elevators under the conditions of the pre-landing glide
boundary-layer separation on the lower surface of tail assembly can
lead to boundary-layer separation directly from the spout of tail
assembly, which sharply will lower the effectiveness of the pitch
control of aircraft and can be the reason for the emergence of
emergency situation.

For the protection of aircraft from icing, are applied
mechanical, thermal, physicochemical and the combined methods,
described in special courses.

In all cases the ice formation leads to an increase in the drag
(Fig. 18.6) and, therefore, to an increase in the fuel consumption
per kilometer.

Page 329.
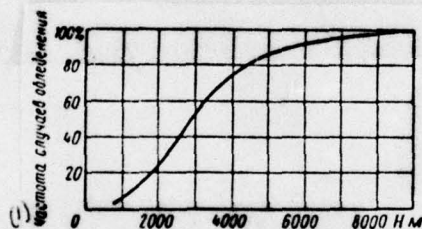
Fig. 18.4. Altitude effect on the probability of aircraft icing (343 cases of icing, according to the data of the experimental flights of aircraft with TRD [ТРД - turbojet engine] and TVD [ТВД - turboprop engine]).

Key: (1). Frequency of the cases of icing.

Fig. 18.5. Form of the ice formation: a) profile; b) U-shaped.

Fig. 18.5.   Fig. 18.6.

Fig. 18.6. Polars of aircraft Il-14 with the different forms of the
icing: 1 - non-icing aircraft; 2 - profile ice 34 mm thickness; 3 -
U-shaped ice 17 mm thickness.

Of aircraft with sweptback wing, predominantly occurs the icing forepart/nose and in the less measure of the rear portion of the wing. The icing of arms it can lead to their intensive vibration.
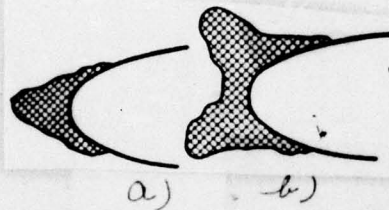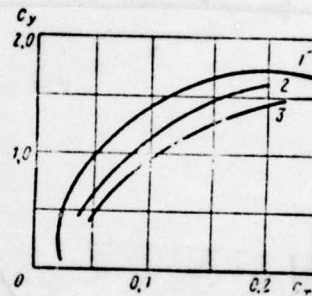
18.3. Flight of aircraft under the conditions of restricted visibility.

The regularity of flights to a considerable degree depends on cloudiness and visibility. Thunderstorms, whirlwinds, the intense residue/settlings, which associate clouds, and also mist/fogs and the duststorms with which is connected the poor visibility, they complicate flight. Under these conditions great assistance exerts the special instruments with which are equipped the aircraft and airports.

The most complex stages of the flight of aircraft are the takeoff and the landing. According to the published in press data ¹, for the 3 of the year of the Second World War USAF [США - United States Air Force] in combat operations lost 70000 aircraft, and as a result of emergencies and catastrophes of approximately 11 000, from which considerable part - during landing.

FOOTNOTE [1]. A. M. Baranov, N. I. Mazurin et al. Aeronautical meteorology. L., Gidrometeoizdat, 1966. ENDFOOTNOTE.

Page 330.

Usually takeoff and landing are conducted visually. However, under severe weather conditions, especially with low clouliness, it is necessary to use special radio equipment.

Have already been develop/processed at present and are experience/tested the systems of automatic landing, which make it possible to make a landing under conditions of the complete absence of visibility for horizontal and for vertical line. It is possible to expect that these systems soon will be equipped all aircraft of average and the long range of flight.

For accomplishing contact landing for each type of airplane, are

necessary the certain conditions of visibility, even if aircraft is
equipped with radio navigation equipment. Its contemporary systems
provide the output/yield of aircraft to takeoff and landing strip
(runways) with some errors by height, horizontal (coincidence of the
projection of the axle/axis of airplane with axle/axis runways) and
speeds.

The correction of these errors is conducted by pilot on visual
orientation. Permissible height of cloudiness on airfield during
landing and the permissible visibility the lower, the more precise
the navigation gear, the lesser the speed of the pre-landing glide
and the more effective the aircraft controls.

For the safety control of landing different aircraft with
different navigation aids, is regulated weather minimum - the minimum
height/altitude of lower cloud base (lower boundary of cloudiness)
and the minimum visibility of reference points. Here the
height/altitude of lower boundary of cloudiness is considered the
greatest height/altitude with which the pilot distinctly sees
landmarks, and by the minimum visibility - the greatest distance
along landing trajectory, with which the pilot can visually
reveal/detect the beginning of takeoff and landing strip.

The international organization of the civil aviation (ICAO) and other special organizations consider necessary the gradual implementation of the means, which ensure landing under conditions of three categories of the growth/build-up of difficulty. The means for first category provide safe landing at the height/altitude of lower boundary of cloudiness 60 m and of the minimum landing visibility 800 m; the means for the second category - at the height/altitude of lower boundary of cloudiness 30 m, of the minimum landing visibility - 400 m. The means for the third category provide for landing at ground level of cloudiness.

Page 331.

Besides examined weather minimum for an aircraft in certain cases, it is necessary to consider weather minimum of airfield, which regulates visibility and the height/altitude of lower boundary of cloudiness depending on the area relief and obstructions on airport approaches.

Questions for repetition

1. How do affect wind gusts the characteristics of the flight of aircraft?

2. Why the icing of tail assembly is especially dangerous under the conditions of the pre-landing glide?

The problem

to determine effective indicator wind gust for an aircraft that *Tus* (134 of the conditions of limitation on dumping, if it is known that the flight was realized at height/altitude H = 11 km at a velocity, corresponding to M = 0.8; the specific wing load was equal to 3500 N/m²; the value of the c_y^α of wing equal to 5.45; the allowed value of the lift coefficient with M = 0.8 equally $c_{y\,доп}=0{,}72.$ effective indicator gust was connected with real indicator gust by the

relationship of $W_{l\infty} = \dfrac{W_l}{K} \approx \dfrac{W_l}{0,9}.$

Answer/response of $W_{l\infty} = 9,9$ m/s.

MT/ST-76-1336

Page 332.

Chapter   XIX

The
DYNAMICS OF ~~the~~ FLIGHT ~~air~~ (HELICOPTER)

The motion of helicopter and the motion of aircraft, can be presented in the form of movable forward motion at the velocity of

the center of mass of helicopter and relative pivoting motion around the center of mass. In accordance with this in the dynamics of the flight of helicopter, are examined trajectory problems and problems on the investigation of the stability characteristics and controllability.

Solution of the trajectory problems of the motion of helicopter makes it possible to determine the forward velocities of level and of vertical flights, acceleration in the different engine power ratings and on the different stages of flight, a change in the flight speed with height/altitude, the ceiling of helicopter etc.

During the study of the possible trajectories of the motion of the helicopter, caused by the acting on it forces, entire mass of helicopter is considered concentrated in its center of mass.

As during the solution of the trajectory problems of aircraft, the kinematic parameters of helicopter are determined with the aid of the equations of motion of a helicopter of type (1.22) in the selected coordinate system.

19.1. Equations of motion. Method of their solution.

During the solution of the trajectory problems of the motion of helicopter, is selected the wind coordinate system (see Chapter I) whose beginning coincides with the center of mass of helicopter, axle/axis OX coincides with the sense of the vector of flight speed, axle/axis Oy lie/rests at the plane of symmetry with positive direction upward, axle/axis Oz forms right-handed coordinate system.

During the motion of helicopter in vertical plane to it, act the following (Fig. 19.1) forces: the thrust of helicopter rotor T, applied to the sleeve of cyclic-pitch control; weight G; the thrust of the tail rotor of T_{xB}, the force of the parasite drag of the $X_{вр}$, caused by the resistance of the cell/elements of helicopter (fuselage, chassis/landing gear, tail boom, etc., with the exception of rotor).

Page 333.

Fig. 19.1. Diagrams of the forces, which act on helicopter.

The system of equations of the unsteady motion of helicopter along curved path takes the form, similar to system (2.10):

$$
\left.
\begin{aligned}
P - X_{\text{вр}} - G \sin\theta &= m\frac{dV}{dt} , \\
Y - G\cos\theta &= mV\frac{d\theta}{dt} , \\
Z_{\text{т}} - T_{\text{хв}} &= 0,
\end{aligned}
\right\}
\tag{19.1}
$$

where P, Y $Z_{\text{т}}$ are projections of the thrust of helicopter rotor respectively on the axis Ox, Oy, Oz.

The case of steady motion along the straight path of equation (19.1) takes the form himself

$$P - X_{\text{вр}} - G\sin\theta = 0, \\ Y - G\cos\theta = 0, \\ Z_{\text{т}} - T_{\text{хв}} = 0.$$ (19.2)

The third equation of system (19.2) written for the helicopter of single-rotor design, at whose reactionary torque of rotor is balanced by torque/moment from the thrust/rod of tail rotor. For helicopters with other methods of the balancing of reactive torque, for example for the helicopters of twin-screw and coaxial diagrams, this equation will take another form, since in these diagrams tail rotor is absent and reactionary torque of rotation/revolution is balanced as a result of the rotation/revolution of screw/propellers to opposite sides.

It is similar to equations for determining the kinematic parameters of aircraft (chapter II, § 2.4) equations (19.2) also are solved by grapho-analytic methods, namely, by the method of the

thrust/rods or by the method of powers.

Page 334.

We convert the first equation of system) 19. 2) to form

$$P = X_{np} + G \sin \theta. \qquad (19.3)$$

The right side of this equation let us name required thrust let us designate its P_n, left - by point of tangency let us designate its P_p. By multiplying both parts of equation (19.3) on V, we will obtain

$$P_p V = (X_{np} + G \sin \theta) V = P_n V = N'_n, \qquad (19.4)$$

where the N'_n - the required power of helicopter; $P_p V = N'_p$ are the

available power of helicopter, expended for the overcoming of the
force of the parasite drag of $X_{вp}$ during the forward motion of
helicopter at speed of V.

Relationship (19.4) for the required power of helicopter
analogous with relationship for the required power of helicopter
analogous with relationship for required power aircraft (2.18), but
in formula (19.4) by required power is considered the only power,
caused by the force of parasite drag, and is not considered the
power, caused by the resisting force of the rotating blade/vanes of
rotor and by the induced velocities, which unavoidably appear during
creation by the rotor of thrust/rod. Taking into account these powers
equation (19.4) will be written in the form

$$N_p = N_n' + N_l + N_{np} = (X_{вp} + G \sin \theta) V + N_l + N_{np} = N_n. \qquad (19.5)$$

where the N_l - the inductive power, caused by inductive losses;
N_{np} - the profile power is, spent on the overcoming of the
resistance of the rotating blade/vanes; N_p - the complete available
power of helicopter (rotor), that includes N_p' and the powers, spent

on profile and inductive losses.

In horizontal flight condition, the flight path angle θ is equal
to zero, and the required power is determined by formula

$$N_n = V X_{np} + N_i + N_{np}.$$

(19.6)

the curve/graphs of change required and the available powers of
helicopter they make it possible to determine the flight
characteristics of helicopter in different mode/conditions.

For determining the flight characteristics of helicopter, let us
use both method of the required and available powers or thrust/rods
and the method of the required and available torque ratios,
constructed in coordinate field $m_{\kappa p} = f(\mu)$. Coefficient μ is equal to
the relation of the velocity component of undisturbed flow,
arrange/located in the plane of the rotation/revolution of rotor, to
the blade tip speed of screw/propeller it is called the
characteristic of the mode/conditions of rotor.

Page 335.

A transition to this method from the method of the required and available powers can be carried out, after expressing required and available powers by the torsional moment in accordance with formulas

$$N_\text{n} = M_\text{кр.п} \omega; \qquad (19.7)$$
$$N_\text{p} = M_\text{кр.p} \omega, \qquad (19.8)$$

where the $M_\text{кр.п}$ and the $M_\text{кр.p}$ are required and had the torsional moments; ω - the angular rate of rotation of screw/propeller.

The torsional moments of $M_\text{кр.п}$ and $M_\text{кр.p}$ can be presented in the form

$$M_{\text{кр.п}} = m_{\text{кр.п}} \sigma \pi R^2 \, \frac{\varrho \, (\omega R)^2}{2} \, R,$$
$$M_{\text{кр.р}} = m_{\text{кр.р}} \sigma \pi R^2 \, \frac{\varrho \, (\omega R)^2}{2} \, R,$$

$$(19.9)$$

where the $m_{\text{кр.п}}$ - the coefficient of the required torsional moment; $m_{\text{кр.р}}$ - the coefficient of the available torsional moment; R - a radius of rotor; σ - solidity/loading factor, equal to the ratio of the total area of the blade/vanes of rotor in plan/layout to the area, swept by rotor.

After the substitution of the values of $M_{\text{кр.п}}$ and $M_{\text{кр.р}}$ in the form (19.7) into formulas (19.9) and (19.8), expressions for torque ratios they are obtained in the following form:

$$m_{\text{кр.п}} = \frac{N_{\text{п}}}{\sigma \pi R^2 \dfrac{\varrho (\omega R)^3}{2}} \;; \tag{19.10}$$

$$m_{\text{кр.р}} = \frac{N_{\text{р}}}{\sigma \pi R^2 \dfrac{\varrho (\omega R)^3}{2}} \;. \tag{19.11}$$

the examined method can be utilized for the calculation of the aerodynamic helicopter characteristics not only single-rotor design, but also other diagrams.

§ 19.2. Required and the available powers of helicopter.

Required power.

Required power during level flight, as noted in the preceding/previous paragraph, it is composed of the powers, spent on the rotation/revolution of rotor and on the overcoming of parasite drag. Let us examine in more detail each of them.

Page 336.

Power, spent on the rotation/revolution of rotor.

This power consists of the inductive power, spent on producing induced velocity, and consequently, propeller thrust, and profile power. According to the theory of ideal screw/propeller [1], inductive power is expressed by relationship

$$N_i = T v_i, \qquad (19.12)$$

where T - rotor thrust; v_i are the induced velocity in the plane of the rotation/revolution of screw/propeller.

FOOTNOTE [1]. A. M. Mkhitaryan. Aerodynamics, chapter ARE XXVI. M, "machine-building". ENDFOOTNOTE.

During the determination of rotor thrust, we utilize a known from the theory of ideal screw/propeller expression

$$T = mv_2, \qquad (19.13)$$

where m - the mass through the screw/propeller of air taking place; v_2 is the induced velocity after screw/propeller, connected with the induced velocity in the plane of rotation/revolution with the relationship of $v_2 = 2v_i$.

While hovering, the forward velocity of helicopter is equal to zero and the mass through the rotor of air taking place depends only on induced velocity, but the thrust/rod of helicopter is equal to its weight. Thus

$$T = \varrho F v_i 2 v_i = 2 \varrho F v_i^2 = G, \qquad (19.14)$$

where $F = \pi R^2$ - the area, swept by rotor (R - a radius of screw/propeller),

whence

$$v_{i\,вис} = \sqrt{\frac{G}{2\varrho F}} \, . \qquad\qquad (19.\,15)$$

After the substitution of the value of $v_{i\,вис}$ into formula (19.12) we obtain

$$N_{i\,вис} = T \sqrt{\frac{T}{2\varrho F}} = G \sqrt{\frac{G}{2\varrho F}} \, . \qquad\qquad (19.\,16)$$

During the forward motion of helicopter (Fig. 19.2) they accept,

that the mass through the screw/propeller of air taking place is determined by the full speed of motion V_1, which is equal to the vector sum forward/progressive by V and of the inductive v_i of speeds.
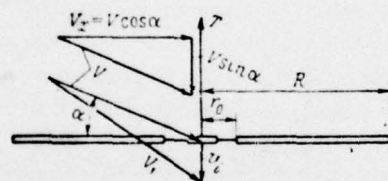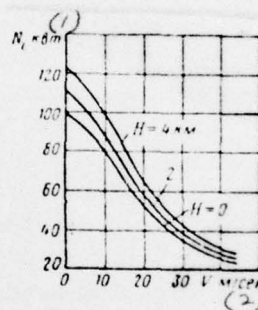
Page 337.

Fig. 19.2.

Fig. 19.3.

Fig. 19.2. Diagram of the inleakage of flow to rotor during the forward motion of helicopter.

Fig. 19.3. Dependence of inductive power on speed and flight altitude.

Key: (1). kW. (2). V, m/s.

In this case of expression for the rotor thrust and induced velocity, takes the form himself

$$T = \varrho F V_1 2 v_i, \\ v_i = \frac{T}{2 \varrho F V_1},$$

(19.17)

where

$$V_1 = \sqrt{(V \sin \alpha + v_i)^2 + (V \cos \alpha)^2}.$$

(19.18)

Substituting the obtained values of induced velocity in formula (19-12) and taking into account that at low angles of attack the rotor thrust is equal to its weight, we will obtain expression for determining the inductive power of helicopter during forward motion in the form

$$N_I = T \frac{T}{2\varrho F V_1} = \frac{G^2}{2\varrho F V_1} \cdot \qquad (19.19)$$

From formula (19.19) it follows that in flight at the determined height/altitude with an increase in forward velocity V inductive power decreases (Fig. 19.3). This is explained by the fact that with $T \approx G$ [see (19.17)] with an increase in velocity V_1 the induced velocity of gggg it decreases and, therefore, decreases inductive power.

tag formulas (19.16) and (19.19) for determining N_i are derived on the basis of the theory of ideal screw/propeller which is constructed under the assumption that the velocity of incident flow and induced velocity in the entire swept area of screw/propeller are identical.

In actuality, the induced velocity along blade/vane is distributed unevenly and has the maximum value with $r/R \approx 0.75$ (here r is a radius of the cross section in question). In connection with this as it will be shown below, inductive power increases.

Page 338.

The indicated nonuniformity of induced-velocity distribution has the greatest values while hovering and decreases with an increase in the forward velocity.

Thus, in real rotor on producing induced velocities is spent large power, than this follows from the theory of ideal screw/propeller, and therefore into formulas (19.16) and (19.19) are introduced the corrections taking into account which the inductive power while hovering and during forward motion is determined from formulas

$$N_I = \xi_V G \sqrt{\frac{G}{2\varrho F}}, \qquad (19.20)$$

$$N_I = \xi_V \frac{G^2}{2\varrho F V_1}, \qquad (19.21)$$

where the ξ_v is correction factor to the nonuniformity of induced

velocities, depending on the ratio of a radius of the nonworking part

of screw/propeller r_0 to its radius R and of the character of

induced-velocity distribution according to a radius of

screw/propeller.

For helicopter screw/propellers while hovering with r_0/R =

0-0.25 correction factors can be taken as 1.2-1.3; with an increase

in forward velocity V, coefficient of ξ_v decreases also with

$V/v_{i\,внс} \geqslant 2$ the coefficient of $\xi_v = 1.$

Besides the nonuniformity of induced velocities the inductive

carrier output screw/propeller, affect the tip losses, caused by the
overflowing of the air through ends and the roots of the blade/vanes
out of high-pressure area hearth by screw/propeller to area of
reduced pressures above the screw/propeller. This overflowing whose
intensity depends on propeller thrust, increases the inductive
carrier output screw/propeller approximately to 3-4o/o.

From formulas (19.20) and (19.21) it follows that with an
increase in altitude of flight the inductive power grow/rises as a
result of a decrease in the air density (see Fig. 19.3).

During the determination of the profile power, spent on the
overcoming of the profile drag of the blade/vanes of helicopter in
different flight conditions, first is examined the profile power of
the blade element of rotor, and then the obtained value of elementary
power is integrated by the area of all propeller blades.

While hovering, the elementary profile power is determined by
the following formula, obtained in the theory of the
isolated/insulated propellor element:

$$dN_{\text{пр}} = dQU = c_{x\,\text{пр}}bdr\,\frac{\varrho\,(\omega r)^2}{2}\,\omega r, \qquad (19.22)$$

where dQ it is determined the force of the profile drag of blade element with a width of dr and by chord b, U it is determined the peripheral speed of cell/element, equal to the product of angular rate of rotation ω to a radius of the chosen cross section, $c_{x\,\text{up}}$ — the coefficient of profile drag of the chosen cell/element.

Page 339.

The profile power of all blade/vanes under the assumptions that the blade/vanes are rectangular and the blade profile drag coefficient in the first approximation, it is determined by its average value of $(c_{x\,\text{пр}} \approx \text{const})$, will be equal to

$$N_{\text{пр}} = k\int\limits_0^R c_{x\,\text{пр}}bdr\,\frac{\varrho\,(\omega r)^3}{2} = kc_{x\,\text{пр}}b\,\frac{\varrho\omega^3}{2}\,\frac{R^4}{4} = \frac{k}{8}\,c_{x\,\text{пр}}bR\varrho\,(\omega R)^3, \qquad (19.23)$$

where k is the amount of blade/vanes; bR - the area of blade/vane in plan/layout.

For trapezoidal in the plan/layout blade the chord and the average value of the coefficient of $c_{x\,np}$ usually are expressed as their values for the cross section, arrange/located at a distance 0.7R from screw axis.

From formula (19.23) it follows that the value of profile power depends on the size/dimensions of blade/vanes, angular velocity of their rotation/revolution and coefficient of profile drag. In turn,, the value of coefficient of profile drag depends on Re number, on the form of airfoil/profile, quality of finish surface and on blade angle of attack. With an increase in the angle of attack, the coefficient of profile drag as for a wing, increases as a result of separation of

flow from the upper surface of blade/vane. The average value of $c_{x\,\text{пр}}$ reflects the value of coefficient of profile drag only in the quite first approximation, since it does not consider the effect of separation of flow from the surface of blade/vane, caused by backflow, and other factors.

Frequently the profile power is expressed as the solidity/loading factor. If expression (19.23) is multiplied and is divided on πR^2, then

$$N_{\text{пр}} = \frac{k}{8} c_{x\,\text{пр}} bR \frac{\pi R^2}{\pi R^2} \varrho (\omega R)^3 = \frac{c_{x\,\text{пр}}}{8} \sigma F \varrho (\omega R)^3. \qquad (19.24)$$

where the $\sigma = \dfrac{kbR}{\pi R^2} = \dfrac{kb}{\pi R}$ - solidity/loading factor; $F = \pi R^2$ - the area, swept spirally.

Under the conditions of forward motion when the constituting forward velocity of V_x is present, (see Fig. 19.2) profile power can be determined by formula

$$N_{\text{пр}} = N_{\text{пр.вис}}(1 + 4{,}65\overline{V}_x^2),$$

(19.25)

where the $N_{\text{пр.вис}}$ - profile power while hovering,

$\overline{V}_x = \dfrac{V_x}{U} = \dfrac{V\cos\alpha}{\omega R} = \mu$ - relative velocity.
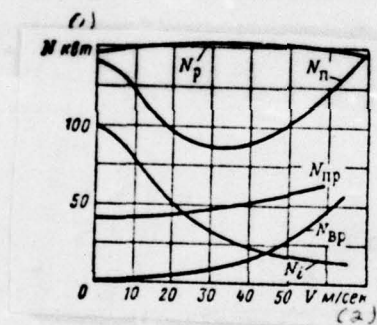
Page 340.

Fig. 19.4. Dependence of N_i, N_{np}, N_{bp}, N_n and N_p on velocity with $H = \text{const}$

Key: (1). kW. (2). V, m/s.

At the low disc incidences $V \cos \alpha \approx V$.

From formula (19.25) it follows that an increase in the forward velocity barely shows up in a change in the profile power. So, if at the maximum speed of the motion of helicopter value $\mu \approx 0.25$, then profile power increases by 28o/o (Fig. 19.4).

Altitude effect on profile power is easy to trace according to formulas (19.23) and (19.24), from which it follows that about other equal conditions not allowing for compressibility the power of N_{np} with height/altitude decreases.

Power, spent on the overcoming of the parasite drag of helicopter.

The harmful power of the N_{np}, required for the overcoming of the resistance of fuselage, chassis/landing gear, the tail boom and other parts of the helicopter (with the exception of rotor) in flight at speed of V, it can be determined by formula

$$N_{np} = X_{np} V.$$
$$(19.26)$$

Substituting the value of $X_{вр}$ from experimental aerodynamics
and converting expression, we obtain

$$N_{вр} = c_{x\,вр}F\,\frac{\varrho V^2}{2}\,V = c_{x\,вр}F\,(R\omega)^3\,\frac{\varrho\overline{V}^3}{2}\,,\qquad (19.27)$$

where $\overline{V} = \dfrac{V}{\omega R}\,.$

Here $c_{xвр}$ are the total coefficient of the parasite drag of
the cell/elements of helicopter pointed out above, determined in
formula $c_{xвр} = \dfrac{\sum c_{xi}S_i}{F}\,,$ where the c_{xi} and S_i are drag

coefficients and the characteristic areas of the cell/elements in question (respectively for a fuselage - the area of maximum cross section, for a tail boom - the moistened surface, etc).

From formula (19.27) it follows that the harmful power is proportional to the cube of the forward velocity of motion (see Fig. 19.4) and that the N_{sp} decreases with an increase in altitude.

Page 341.

The curve/graphs of a change in the required power of helicopter and its constituting [inductive (19.21), profile (19.25) powers and power of parasite drag (19.27)] depending on flight speed are given in Fig. 19.4.

Available power.

By the available power of helicopter rotor, is understood the power, applied to the shaft of rotor from engine plant and expended

on the rotation/revolution of rotor. The available power of the rotor of N_p is less than the effective shaft horsepower of the engine of the N_e:

$$N_p = N_e - (N_\text{в.с} + N_\text{тр} + N_\text{охл} + N_\text{пр} + N_\text{р.в}), \qquad (19.28)$$

where the $N_\text{вс}, N_\text{тр}, N_\text{охл}, N_\text{пр}, N_\text{р.в}$ are the powers, spent respectively on the suction of air, on friction in transmissions, on engine cooling, on different drives and on the rotation/revolution of tail rotor in the helicopters of single-rotor design. All power losses enumerated above can be considered with the aid of the coefficient of the use of a power ξ, then formula (19.28) will take form

$$N_p = N_e \xi. \qquad (19.29)$$

The coefficient of the use of a power of engine it is possible to present in the form of dependence on the coefficient of losses

$$\xi = 1 - \xi_n, \qquad (19.30)$$

where
$$\xi_n = \xi_{\text{вс}} + \xi_{\text{тр}} + \xi_{\text{ох.л}} + \xi_{\text{цр}} + \xi_{\text{р.в}}.$$

The average value of the coefficient of the use of a power equally to $\xi = 0.75 - 0.80$ and, correspondingly, the average value of the coefficient of the losses of $\xi_n = 0.25 \div 0.20.$ Average values of the loss factors the following: $\xi_{\text{вс}} = 0.02$, $\xi_{\text{тр}} = 0.07$, $\xi_{\text{ох.л}} = 0.05$, $\xi_{\text{цр}} = 0.01$, $\xi_{\text{р. в}} = 0.08$. The amount of entering in expression for determining ξ_n coefficients and their values depend on the diagram of helicopter. As an example it is possible to give the values of the loss factors for the helicopter $Mi-6$, for which the

$\xi_{\text{вс}} = 0.021$, $\xi_{\text{тр}} = 0.03$, $\xi_{\text{ох.л}} = 0.02$, $\xi_{\text{цр}} = 0.01$; $\xi_{\text{р.в}}$ depends on flight speed: with $V = 0$ $\xi_{\text{р.в}} = 0.09$, with $V = 270$ km/h and $\xi_{\text{р.в}} = 0.034$, with $V = 320$ km/h of

$\xi_{\text{p. в}} = 0{,}05.$

The value of the engine output of N_e depends on the engine power rating, on height/altitude and flight speed. As during determination effective power the engines, established/installed on aircraft, the power of the N_e of the engines of helicopters is determined from the altitude-speed engine characteristics. The general view of the dependence of available power on flight speed for the fixed height/altitude is shown in Fig. 19.4. Figure 19.5 shows the required and available powers of the flight of helicopter with sea-level engines at different height/altitudes (available powers with an increase in altitude decrease).
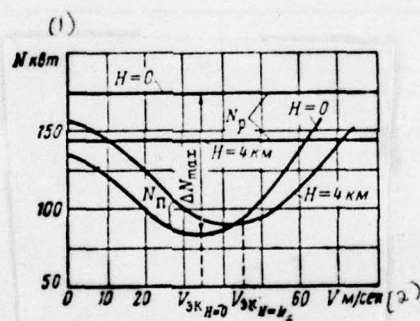
Page 342.

Fig. 19.5. Dependence of the required and available powers on speed for different flight altitudes.

Key: (1). kW. (2). V, m/s.

The obtained above values required and available powers make it possible to examine the basic flight conditions of helicopter and to determine its flight characteristics.

§ 19.3. Helicopter characteristics in the hoverings and vertical climb.

While hovering, the harmful power of helicopter is equal to zero and required power is composed of inductive and profile. By taking into account the value of $N_{i\,вис}$ (19.20) and of $N_{пр.\,вис}$ (19.24), let us write expression for a required power at the height different from zero:

$$N_{п.\,вис\;H} = N_{п.\,вис0} \frac{1}{\sqrt{\Delta}} + \frac{c_{x\,пр}}{8} \sigma F \varrho_0 \Delta (\omega R)^3, \qquad (19.31)$$

where the $N_{i\,вис\,0}$ are inductive power while hovering of the Earth, $\Delta = \dfrac{\varrho_H}{\varrho_0}$.

Since with height/altitude required power increases, and available decreases, there is a ceiling, called the static ceiling of helicopter at which is attained the hovering. At the height/altitude of static ceiling required and the available powers are equal.

The proximity effect of the Earth very strongly shows up in the thrust levels and required power. Near the Earth the induced velocity, created by rotor, decreases as a result of the braking effect of the Earth. A decrease in the induced velocity of $(v_{i2} < v_{i1})$ leads to an increase in the true angles of attack of cross sections (Fig. 19.6). Respectively change the value and the direction of the aerodynamic force R. In summation, near the Earth increases the thrust/rod under almost constant/invariable resisting force to rotation/revolution (constant required power). Therefore, if available power is constant, then with approach/approximation to the earth/ground propeller thrust increases. But if we preserve the thrust/rod of constant, then due to the effect of the Earth decreases required power.
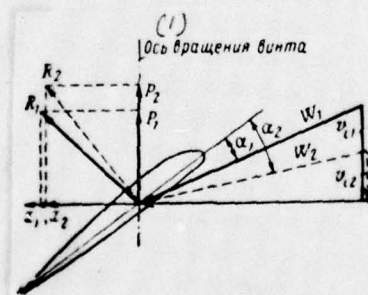
Page 343.

Fig. 19.6. Proximity effect of the Earth on angle of attack and the resultant of blade element (index "2" - taking into account the proximity effect of the Earth).

Key: (1). Propeller axis.

Fig. 19.7. The proximity effect of the Earth on thrust/rod and
carrier output screw/propeller (P and N are a thrust/rod and power
taking into account the proximity effect of the Earth; P_∞ and N_∞
- thrust/rod and power not allowing for the proximity effect of the
Earth; h/R is a relative distance of rotor from the Earth).
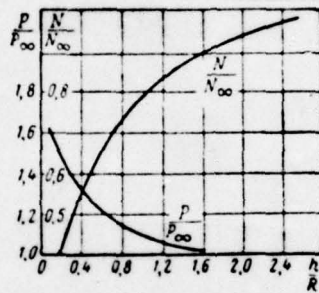
A decrease in the required power with constant propeller thrust occurs as a result of a decrease in the inductive power with a decrease in the induced velocity. The physical picture of the proximity effect of the Earth on the induced velocity of rotor is similar to the effect of the Earth on downwash and respectively - for the inductive reactance of wing. The quantitative results of the effect of the Earth on the characteristics of rotor are given in Fig. 19.7.

The given dependences show a considerable decrease in the required power near the Earth, which makes it possible to accomplish takeoff and hovering of the Earth at less powers. A thrust augmentation of rotor near the Earth substantially gears down of vertical descent under the conditions of autogyration.

Under the conditions of the vertical steady climb, the mass flow per second of the air, which takes place through the rotor, is more than while hovering, since during lift manifests itself the appearance of a speed of external flow. Consequently, in this case for producing the same thrust/rod will be required less induced velocity, than while hovering. As a result of even distribution according to the rotor disk of the speed of external flow, the

nonuniformity of flow after rotor during lift decreases so, that during analysis and performance calculation of helicopter under the conditions of flight it is possible to consider flow after rotor uniform.

The speed of the vertical steady climb of V_y can be determined from equations of motion (19.2).

Page 344.

Since in this case axle/axis Ox coincides with vertical line, the first equation of system (19.2) by analogy with conversion (19.4) it is possible to convert to form

$$N_p = (X_{np} + G)V_y + N_i + N_{np}$$

or

$$N_p = X_{np}V_y + N_i + N_{np} + GV_y = N_n + GV_y, \qquad (19.32)$$

whence

$$V_y = \frac{N_p - N_n}{G}, \qquad (19.33)$$

where the N_p and N_n it coincides the available and required power respectively at the height/altitude in question during the assigned state of motion.

From formula (19.33) it follows that the static ceiling of helicopter can be defined as height/altitude, at which $V_y = 0$.

§ 19.4. Lift of helicopter along inclined trajectory.

During the analysis of the lift of helicopter of inclined trajectory the greatest practical interest they represent such characteristics as the maximum vertical velocity of $V_{y\,max.}$ trajectory speed, by which is reached $V_{y\,max.}$ and the maximum altitude, which can be reached during inclined lift, or the so-called

service ceiling of the helicopter of H_{π}.

the vertical velocity of ggggg V_y the steady climb of the helicopter along inclined trajectory can be determined from transformed equation of motion (19.5)

$$N_p = X_{\bullet p} V + G \sin \theta V + N_i + N_{\pi p},$$ (19.34)

in which

$$V \sin \theta = V_y,$$

a the sum of the remaining terms of the right side of equation (19.34) it is required power in horizontal flight condition (19.6). Hence

$$V_y = \frac{'N_p - N_{\text{и.r.п}}}{G} = \frac{\Delta N}{G}.$$

after determining by the curves of required thrusts and
available powers (Fig. 19.4) excess horsepower ΔN, it is possible to
calculate V_y at the different velocities of flight from trajectory.
It is obvious, the vertical velocity it will be maximum with maximum
ΔN. The maximum margin of power will be at the flight speed, which
corresponds to the minimum required power. This speed is called the
economic speed of $V_{эк}$ by analogy with the economic speed of
aircraft, at which the $N_н$ has the minimum value.

Page 345.
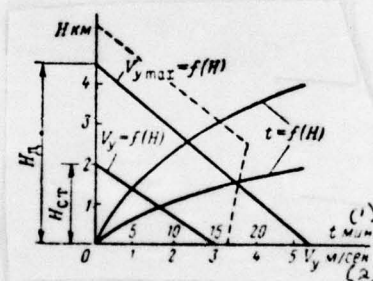
Fig. 19.8. Dependence of $V_y, V_{y\,max}$ and t on flight altitude.

Key: (1). t, min. (2).   m/s.

Thus, the flight of helicopter at the maximum vertical velocity corresponds to flight at economic speed. Let us note that $V_{y\ max}$ during lift in an inclined trajectory is greater than $V_{y\ max}$ during vertical lift (see Fig. 19.8), since in the case of lift along inclined trajectory required power is less and, therefore, more excess horsepower.

With an increase of height/altitude minimum required power increases. A change in the available power in height/altitudes depends on the type of the engine, established/installed on helicopter. So for a helicopter with piston sea-level engine the available power, the margin of power and the vertical velocity of V_y with an increase in altitude decrease.

During the setting up of high-altitude piston engine, the available power increases to the full-throttle height of engine, which leads to an increase in the margin of power and the vertical velocity (Fig. 19.8 - dotted line). After the full-throttle height of engine, the available power falls and this it leads to a decrease in the vertical velocity.

The character of a change in the vertical velocities in

height/altitudes during the setting up of turboprop or turbojet engines also is determined by the character of a change in the available powers in height/altitudes.

On the service ceiling of helicopter, the margin of power and the vertical velocity during lift along inclined trajectory are equal to zero (see Fig. 19.8) and helicopter it can accomplish level flight only at the velocity, equal economic ggggg. With an increase in altitude of flight, the economic speed grow/rises; a change in the $V_{\text{эк}}$ with height/altitude can be calculated by formula

$$V_{\text{эк}} = V_{0\text{эк}} \frac{1}{\sqrt{\Delta}}.$$ (19.36)

At the known values of V_y from height/altitudes it is possible to determine the duration of ascent of helicopter, i.e., to construct to the barogram of lift by the method, presented in chapter IV. LN3 end section.

§ 19.5. The maximum speed of helicopter. Speed range. Limitation of maximum speed.

The mode/conditions of the maximum speed of helicopter in level flight can be obtained in such a case, when engine is in full production, and therefore applied to rotor power (had) has the maximum value. During the steady flight in maximum speed, the available power is equal required and, therefore, the maximum speed can be determined by the point of intersection of the curved required and available powers, constructed for a series of height/altitudes they can have different character depending on the type of the engine, established/installed on helicopter. During the setting up of piston forced-induction engine, the maximum speed increases to the rated altitude of engine, and then it falls (Fig. 19.10), since the power of engine after rated altitude intensively decreases.

If we enter on this same graph the rate of climb of $V_{эк}$ then on service ceiling $V_{max} = V_{эк}$.
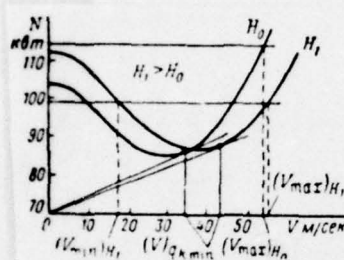
Page 346.

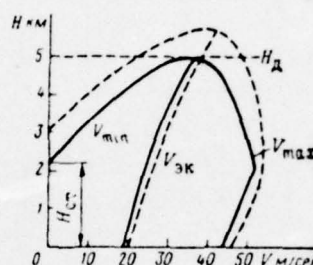Fig. 19.9.   Fig. 19.10

Fig. 19.9. Diagram of the determination of the maximum and minimum speeds of level flight.

Key: (1). kW. (2). m/s.

Fig. 19.10. Speed range on height/altitudes for a helicopter with PD [ПД - instrument panel] (engine high-altitude) and TVD [ТВД -

turboprop engine] (dotted line).

Key: (1). m/s.

In order to determine the speed range of helicopter, it is necessary to reveal a change in the maximum speed of level flight with height/altitude. Since to the height/altitude of static ceiling helicopter has the capability to zoom, its minimum speed to this height/altitude is equal to zero. Higher than static ceiling hovering is impossible, and flight can be realized only in the presence of the horizontal speed which must be more than minimum speed (see Fig. 19.10). With an increase of height/altitude, the V_{min} increases up to the service ceiling where the $V_{min} = V_{max} = V_{эк.}$ Speed range on height/altitudes in the case of setting up on the helicopter of turboprop engine is shown by dotted line in Fig. 19.10.

the maximum speeds, obtained from the condition of using a total power of engine, in the majority of cases cannot be reached in practice, since with an increase in the velocity appears a whole series of the adverse phenomena (flow separation on blade/vane, structural distortion, the appearance of shock waves), for elimination of which it is necessary to restrict maximum speed.
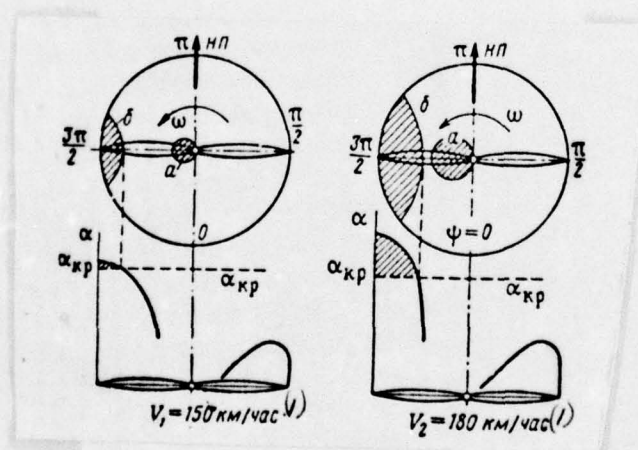
Page 347.

Fig. 19.11. Position of the zone of reverse/inverse flow and zone of disruption/separation.
Key: (1) km/h.

The maximum speed of helicopter is restricted on flow separation on the blade/vane, which goes back/ago, and over the end Mach number on the blade/vane, which goes forward.

Let us examine the limitation of maximum speed on flow separation on the going back/ago blade/vane.

The blade/vane, which goes back/ago, is the blade/vane, peripheral speed which at the point in time in question is directed opposite to flight speed. The blade/vane, which goes forward, is the blade/vane, peripheral speed of which at this torque/moment coincides with direction flight speed. So, at azimuthal angle of $0 < \psi < \pi$ blade/vane goes forward a at angle $\pi < \psi < 2\pi$ blade/vane it goes back/ago (Fig. 19.11). The blade/vane, which goes back/ago, has a zone of the lowered/reduced velocities of airflow. since the blade lift depends on the velocity of airflow, on the blade/vane, which goes forward, it will be more than on the blade/vane, which goes back/ago. In the presence of flapping hinge, the forward going blade/vane, which develops large lift, will wave upward, but the back/ago going blade/vane, which develops less lift, will be omitted. This leads to a decrease in the angles of attack of the cross sections of the forward going blade/vane and to an increase in the

angles of attack of the cross sections of the back/ago going

blade/vane.

As a result of the stroke of the down back/ago going blade/vane

(see Fig. 19.11, V_1 = 150 km/h) on its end part the angles of attack

can become higher than critical, which will lead to flow separation
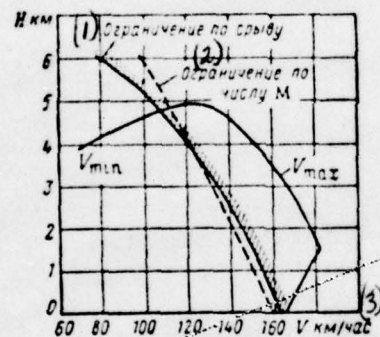
in this area.

Page 348.

Fig. 19.12. Limitations of the maximum speed of helicopter.

Key: (1). Stall limit. (2). Limitation according to mach number. (3). km/h.

The emergence of disruption/separation precisely on the tip part of the blade/vane is explained, in the first place, by the fact that on end cross sections are developed the greatest peripheral speed, which causes a great increase in the angles of attack, and, in the second place, fact that these cross sections have the top speed of lowering, also, because of this the greatest increase in the angles of attack.

With an increase in the velocity of flight, the speed of the stroke of the down back/ago going blade/vane increases. This leads to an even larger increase in the angles of attack and to the expansion of the zone of end breakaway, and also the zone of the reverse/inverse flow about the root part of the blade/vane (see Fig. 19.11, V_2 = 180 km/h).

During the appearance of disruption/separation, sharply grow/rises the resistance of the back/ago going blade/vane and, consequently, also the power, required for its rotation/revolution. Furthermore, appear the vibrations and it deteriorates controllability by helicopter.

Due to the undesirable phenomena enumerated above, which appear as a result of developing disruption/separation on the blade/vane, which goes back/ago, the maximum flight speed it is necessary to restrict (Fig. 19.12).

With an increase of height/altitude for the preservation/retention/maintaining of equality Y = G, it is necessary to increase the angles of attack of the cross sections of blade/vanes, as a result of which with the same flight speed the zones of disruption/separation on the going back/ago blade/vane are expanded. In order not to allow this, it is necessary to decrease the maximum flight speed. Thus, with an increase in altitude the maximum speed, limited by breakaway, decreases.

one of the methods of separation delay is discharging screw/propeller with the aid of the wing of a comparatively small area (for example at Mi-6). With an increase in the trajectory speed, the airfoil lift grow/rises, which makes it possible to decrease the average lift coefficient of screw/propeller and, consequently, also the angles of the cross sections of blade/vane. Application/use of this wing makes it possible to increase maximum speed by 25-30o/o. By the effective means for the tightening of the end

disruption/separation of the back/ago going blade/vane at high speeds
is blade twist. For a decrease in the angles of attack blade tip the
blades twist in such a way that the angles of setting at the end of
the tale are less than of root. Application/use of a twist makes it
possible to raise maximum speed to 8-10o/o.

Page 349.   Let us examine the limitations of maximum speed
according to the end number of M_{κ}. the speed of the end cross
section of the blade/vane, which goes forward, with $\psi = \pi/2$ is equal
to:

$$V_{\kappa} = V_x + R\omega,$$

a end number

$$M_{\kappa} = \frac{V_x + R\omega}{a}.$$

with an increase of velocity the end number of M_κ it can
achieve the critical value at which appear the supersonic zones of
flow, shock waves and wave drag. Furthermore, with a further increase
in the velocity of flight and mach number are possible the flow
separations after shock wave, which leads to an incidence/drop in the
lift effectiveness of screw/propeller. The limitation of maximum
speed according to mach number can be written as

$$V_{orp} \leqslant M_{\kappa.\kappa p} a - R\omega,$$

where the $M_{\kappa.\kappa p}$ - critical mach number of end cross sections. With an

increase of flight altitude, the speed of sound decreases. They

decrease also $M_{\text{к. кр.}}$ since increase the angles of attack as a result

of an increase in the angles of setting. Thus, the rate of limitation

according to mach number decreases (Fig. 19.12).

§19.6. Reduction/descent in the helicopter with engine on.

A reduction/descent in the helicopter power-on is possible both

along vertical and along inclined trajectory.

Since under the conditions of vertical descent the angle of

attack is negative and equal $-\pi/2$, but axle/axis Ox coincides with

vertical line, equations of motion (19.1) for the case of the

establish/installed reduction/descent take the form

$$\left.\begin{array}{r} G - Y - X_{\text{пр}} = 0, \\ P = 0, \\ Z_{\text{т}} - T_{\text{хн}} = 0. \end{array}\right\} \qquad (19.:7)$$

in the first approximation, during vertical descent it is possible to consider that $Y \approx T$, and $X_{вр} \approx 0$. In this case required power as required power while hovering (19.31), it is possible determine by formula

$$N_n \approx N_l + N_{np}.$$

however one should consider the induced velocity of v_i during vertical descent it decreases. This leads to a decrease in the inductive power, and formula (19.12) assumes the form

$$N_l = T(v_l - V_y), \qquad (19.38)$$

where the V_y - the rate of descent in the helicopter.

Page 350.

Fig. 19.13. Formation/education of vortex ring.

Key: (1). Surface of the stagnant flow.

Since required power under the conditions of reduction/descent than less had, the rate of descent is determined by negative margin of power (19.35). The rate of descent in the helicopter with engines on must not exceed 3 m/s. This limitation is connected with the fact that at high rates of descent the rotor can enter into vortex-ring state.

Vortex ring (Fig. 19.13) it is formed as a result of the flowing over of air from the zone of rejection (hearth by screw/propeller) into the zone of draining (above the screw/propeller). During vertical descent the induced velocities in the zone of rejection are braked by counterflow, in consequence of which on certain surface the resultant velocity of flow is equal to zero. The surface of the stagnant flow with an increase in the rate of descent approaches a plane of the rotation/revolution of screw/propeller, thereby contributing to the flowing over of air from the zone of rejection into the zone of draining. In vortex-ring state the power of engine partially is expend/consumed on an increase in the intensity of eddy/vortex and the propeller thrust falls.

External flow in this case attacks not to screw/propeller, but to eddy/vortex it flows about the it as body. During the flow about

the eddy/vortex at its upper part, appear the breakaway zones, which

leads to the strong agitation of helicopter and to the loss of its

controllability. To avoid these unpleasant phenomena, the rates of

vertical descent are restricted; is restricted also the use of

mode/conditions of vertical descent.

The basic form of a reduction/descent in the helicopter while

the motor is running is the reduction/descent along inclined

trajectory ($|\theta| < \pi/2$). As in the mode/conditions of lift, in

helicopter in the mode/conditions of a reduction/descent in the act

the thrust of screw/propeller t, weight G the force of the parasite

drag of $X_{вp}$ (Fig. 19.14). In this case of equation of motion, take

the form

$$
\left.
\begin{aligned}
G \sin \theta - P - X_{вp} &= 0, \\
Y - C \cos \theta &= 0, \\
Z_{т} - T_{x_{н}} &= 0,
\end{aligned}
\right\} \qquad (19.39)
$$

where P, Y, $Z_{т}$ - the projections of thrust t on the axis of wind

coordinate system.

Figure 19.14 shows a reduction/descent in the helicopter with the negative angle of attack. The component of propeller thrust to axle/axis Ox is decelerating force.
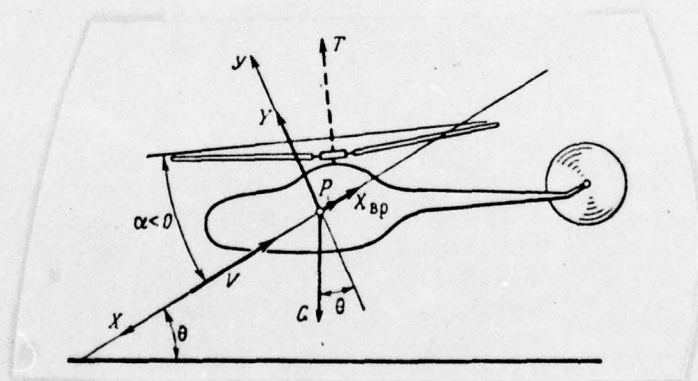
Page 351.

Fig. 19.14. Diagram of the forces, acting on a helicopter during reduction/descent.

With the slope/inclination of the plane of the rotation/revolution of screw/propeller forward the angle of attack can be positive and then the projection of thrust/rod P it will become motive-power. Most frequently during reduction/descent angle of attack is close to zero or has small negative value.

The basic parameters, which characterize a reduction/descent in the helicopter, are the rate of V_{CH} and the angle of descent θ. The qualitative and quantitative analysis of V_{CH} and angle θ can be carried out both through equations (19.39) and through the graphic dependence of the available and required powers (Fig. 19.15a) under the conditions of reduction/descent. The available power under the conditions of reduction/descent is determined from formula (19.29) and depends on the engine power rating. The required power during reduction/descent, on the strength of first equation (19.39), taking into account profile and inductive powers (19.5) is determined by formula

or

$$N_\text{n} = N_t + N_\text{np} + X_\text{np}V - VG\sin\theta$$
$$N_\text{u} = N_\text{n.r.n} - VG\sin\theta. \qquad (19.40)$$

from formula (19.40) follows that the required power under the conditions of reduction/descent is less than the required power under the conditions of level flight to value VG sine θ. With an increase in the flight path angle, the value of required power is reduced. If by the chart of a change in the required power it decreases. If on the graph of the change of required power we enter change had the power, then on the points of their intersection (point 1, 2, 3, 4 in Fig. 1.15a) it is possible to determine the rate of steady-state reduction/descent at the fixed flight path angle, and these data make it possible to construct the characteristic of reduction/descent (Fig. 19.15b). Such characteristics usually are constructed for the different blade angles of rotor.

Fig. 19.15. Available and required power during reduction/descent
(a). Characteristic of reduction/descent (b).

Fig. 19.16. Flow about the blade element during autorotation.

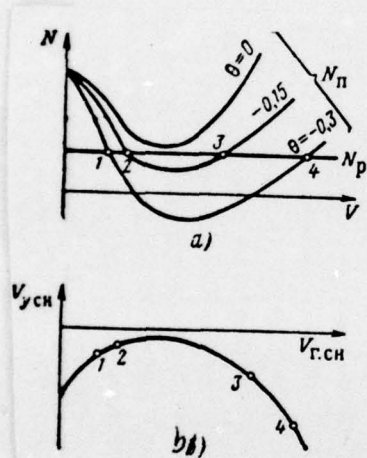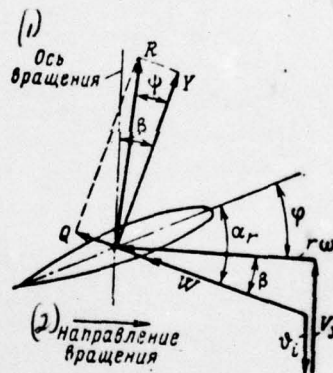Key: (1). Rotational axis. (2). Direction of rotation.

Fig 19.15.   Fig. 19.16.

Both under the conditions of vertical descent and under the conditions of reduction/descent along inclined trajectory for the horizontal and vertical components of rate of descent there are limitations, which have as a goal to avoid the transition of rotor to vortex-ring state.

19.7. a reduction/descent in the helicopter under the conditions of autorotation.

The work of the rotor of helicopter under the conditions of autorotation is characteristic fact that the blade/vanes rotate because of the energy of the incident flow, creating in this case thrust/rod without supply of power from engine. This property of rotor makes it possible for helicopters to accomplish safe landing with the failure of engine, with a breakage in the tail rotor, its transmission or the main shaft of screw/propeller. For the determination of conditions under which is possible the autorotation of rotor, let us examine the cell/element of its blade/vane during a vertical descent in the helicopter (Fig. 19.16). The rate of flow W is equal to vector sum circular/neighboring $r\omega$, vertical V_y and inductive the v_i of rates.

During the flow the blade element of airflow about at an angle the attack of α_r with a velocity of W appears resultant force R whose projections on the axis of the velocity coordinate system are equal to the lift force of Y relative to screw axis is equal to the angle of indraft of jet β; the angle between resulting R and lift Y the we designate through ψ.

Page 353.

The values of angles β and x depend on the angle of attack of blade element, the equal to the sum of angles of setting of blade/vane ϕ and of inflow β, i.e., $\alpha_r = \beta + \phi$.

If $\beta > \psi$, then resulting R has this slope/inclination as this shown in Fig. 19.16, and its projection R sine (β is ψ) on the plane of rotation/revolution causes the rotary acceleration of blade/vane (at the plane of rotation/revolution lie/rests peripheral speed $r\omega$). If $\beta < \psi$, then force R is deflected from screw axis to left side and its projection R sine (β is ψ) causes braking screw/propeller. With

equality β and ψ the angular rate of rotation of blade/vane will be constant. Thus, the values of angles β and   determine the mode/conditions of the rotation/revolution of propeller blades.

Angle ψ, as this follows from figure 19.16, is equal $\psi = \text{arctg} \dfrac{Q}{Y} = \text{arctg} \dfrac{c_x}{c_y}$ and depends on the angle of attack of blade element. With an increase in the angle of attack up to $\alpha_{\text{наив}}$ angle ψ decreases; with a further increase in the α_r angle increases as a result of an intense increase in the c_x (Fig. 19.17). The angle β also is determined by the angle of α_r in accordance with the expression of $\beta = \alpha_r - \varphi$.

compare a change in angles of ψ and β θ in dependence on α_r. The graph of the change of angle β on α_r takes the form of straight line, directed to the axle/axis of α_r at an angle, equal to $\pi/4$ rad. Ugol $\beta = 0$, when the $\alpha_r = \varphi$, i.e., the zero value of angle β is determined by point on the axis of the α_r, in which $\alpha_r = \varphi$. With an increase in the angle of the setting of blade/vane, straight line $\beta = \alpha_r - \varphi$ is shift/sheared to the right from the origin of coordinates (see $\varphi = \varphi_2$).

By comparing a change in the $\psi = f(\alpha_r)$ and $\beta = f_i(\alpha_r)$, we come to the conclusion that in certain range of the angles of attack of the α_r, which correspond to points a and b, and at preset angle $\phi = \phi_1$ the angle β is greater than angle of and, therefore, projection R sine (β is ψ) it contributes to the rotation/revolution of propeller blade. The noted range of mode/conditions is called the mode of autorotation, or of the autogyration of rotor, and the diagram, presented in Fig. 19.17, it is called the diagram of autorotation. The angles of attack of α_{ra} and α_{rb}, which correspond to points a and b, are characterized by the establish/installed autorotation - stable at point a and unstable at point b. Let us explain this.

At the angle of attack, greater than α_{ra}, the angular rate of rotation of blade/vane increases, which, in turn, leads to an increase in the induced velocity of v_i, with an increase in the induced velocity (see Fig. 19.16) angle β it decreases and, therefore, they decrease projection by resulting R sine (β is ψ) and the rate of autorotation. With an angle of attack less than α_{ra}, decrease angular velocity of rotation of blade and, therefore, induced velocity the v_i. With a decrease in the v_i increase the vertical velocity of V_y and the angle β, which leads to an increase in the angular rate of rotation of blade/vanes and return to the

mode/conditions of the establish/installed autorotation, which

corresponds to point a.

Page 354.

Fig. 19.17. Diagram of autorotation.

Key: (1) Area of the being accelerated autorotation.

By similar considerations it is possible to show that at point b the establish/installed autorotation is unstable.

From the given in Fig. 19.17 diagram of autorotation, it follows also that if the blade angle increases, then the range of autorotation decreases and with $\varphi = \varphi_{max}$ the autorotation is possible only at one unique value β (point c).

Thus, at the low values of the blade angle of the screw/propeller of characteristic autorotations will be most favorable: therefore upon transition from power-on flight to windmill brake conditions necessary to decrease the blade angles of screw/propeller.

One should consider that the given analysis is bygone is given for the chosen blade element. But if we examine the relationship between angles β and gggg for the cross sections, arrange/located at different distances from screw axis, then at the definite rates of descent in the cross section, arrange/located nearer to root part and having less peripheral speed, will have wide angles β, than end cross sections. It can happen so that for more close to the screw axis of

the cross sections of $\beta > \psi$, and for end $\beta < \psi$ and then about the autogyration of rotor it is possible to speak only when the torque of blade/vane will be more than moment of resistance.

For determining the rate of descent in the helicopter from vertical line, it is convenient to consider autorotation of the rotor as disk, which creates resistance. During the establish/installed reduction/descent the resistance of screw/propeller is equal to the weight of helicopter. The resisting force of screw/propeller can be presented as

$$X = c_x \frac{\varrho V_y^2}{2} F = G,$$

whence the rate of vertical descent

$$V_y = \sqrt{\frac{2G}{\varrho F c_x}}, \qquad (19.41)$$

where the c_x - the drag coefficient of the screw/propeller which, according to the experimental data, on the average is equal to 1.3.

The rate of V_y of the Earth is equal to

$$V_{y0} \approx 1.1\sqrt{p}, \qquad (19.42)$$

where p = G/F - specific load on screw/propeller.

Page 355.

Formula (19.42) does not consider the effect of the Earth on the characteristics of screw/propeller.

For a decrease in the V_N during landing it is possible to use the so-called detriment/blasting of helicopter, which entails a sharp increase in the blade angle of screw/propeller during approach/approximation for the earth/ground, which makes it possible to short-term increase thrust/rod and for its count to considerably decrease the rate of descent.

During the application/use of this procedure, it is necessary most accurate possible to calculate torque/moment and duration of detriment/blasting, since with prolonged detriment/blasting along a reduction/descent in the vertical velocity decreases number of revolutions in connection with the increasing resistance of blade/vanes, but due to this falls thrust/rod and again increases rate of descent.

Vertical rate of descent can be decreased also by transition from vertical descent to reduction/descent in inclined trajectory under the conditions of autorotation the physical flow pattern of blade/vane more complex than during vertical descent. Is explained this by the change of the rate of the flow about the blade/vane in its different azimuthal positions and by the presence of the stroke of blade/vanes, what during vertical descent no. However, the qualitative side of the examined autorotation under the conditions of vertical descent remains. The minimum vertical rate of descent in flight along inclined trajectory usually is considerably lower than the vertical velocity during vertical descent. The minimum vertical rate of descent is possible in flight cf helicopter at economic speed. This is explained by the fact that under these conditions the required power for a flight with the free-running speed of $V = V_{эк}$ has the minimum value (Fig. 19.5). For accomplishing landing "like and aircraft" at helicopter must be the running landing gear in order that it could after touchdown complete range/path on the earth/ground.

19.8. Distance and the duration of flight of helicopter.

Hourly fuel consumption for the helicopter of $q_{ч}$ can be

expressed through the specific fuel consumption of fuel by the engine of c_e and the power of the engine of the N_e:

$$q_u = c_e N_e.$$

during the steady flight

$$N_p = N_n = \xi N_e,$$

where ξ is expressed the coefficient of power losses.

Then

$$q_u = \frac{c_e N_p}{\xi} = \frac{c_e N_n}{\xi}. \qquad (19.43)$$

Page 356.

The fuel consumption per kilometer for a helicopter

$$q_{\text{к}} = \frac{q_{\text{ч}}}{V} = \frac{c_e N_{\text{п}}}{\xi V} . \qquad (19.44)$$

from known $q_{\text{ч}}, q_{\text{к}}$ and $G_{\text{т}}$ is defined duration of flight in the

hours:

$$t = \frac{G_T}{q_4}$$

and its distance the km:

$$L = \frac{G_T}{q_K}.$$

as it follows from expression (19.43), the hourly consumption of fuel/propellant depends on $c_e, N_п$ and ξ. If we in the first approximation, consider c_e and ξ constants, then the hour of the consumption of fuel/propellant will be proportional to required power

and the character of its change depending on speed it will be the same, as and N_n; in these conditions the minimum value of the hourly consumption of the fuel/propellant of $q_{\text{ч}}$ corresponds $V_{\text{эк}}$ (Fig. 19.5).

The expenditure/consumption per kilometer under these conditions has the minimum value at the speed by which $\left(\dfrac{N_n}{V}\right)_{\text{min}}$. Graphically this mode/conditions is determined by the point of contact of the tangency of straight line, carried out from the origin of coordinates, from curved required power, i.e., for achievement of the maximum range of flight, speed must be higher than economic (Fig. 19.9).

If on helicopter is established/installed sea-level engine, then with an increase in altitude the specific consumption of the fuel/propellant of c_e and the minimal required power of $N_{n\,\text{min}}$ increase. As a result with an increase of height/altitude, increases the minimum hourly consumption of fuel/propellant.

An increase in the fuel consumption per kilometer with an increase of the height/altitude less is intense, than of hourly

consumption, since with an increase in the c_e with an increase of
height/altitude the relationship of the $\left(\dfrac{N_n}{V}\right)_{min}$ of somewhat
decreases (Fig. 19.9). Thus, for a helicopter with low-level piston
engine the distance and duration of flight will be maximum of the
Earth.

During setting up on the helicopter of forced-induction engine
of $\left(\dfrac{N_n}{V}\right)_{min}$ and the c_e decrease to rated altitude and the
consumption per kilometer on to rated altitude somewhat less than of
the Earth.

In the case of the setting up of turboprop engine, the distance
and the duration of flight with an increase in the altitude
grow/rise.

Page 357.
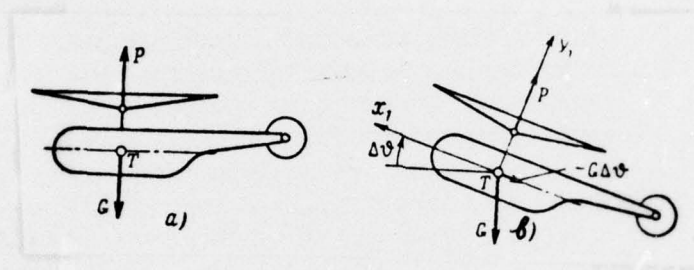
Fig. 19.18. Motion of the tulip of rotor during a change in the angle of the slope of the fuselage: a) starting position; b) the position through the small time interval.

Fig. 19.19. Effect of the slope/inclination of shaft on the position of the plane of the rotation/revolution of rotor.

Key: (1). Blade/vanes are located in the plane, normal to the plane of the rotation of shaft. (2). Blade/vanes are located in the plane

of the rotation of shaft. (3). The starting position of shaft. (4).
Position of shaft after deflection on $\Delta\vartheta$.

19.9. Concept about stability and controllability of helicopter.

We will be restricted to the examination of stability and controllability of single-rotor helicopter with hinge fitting blade/vanes.

Stability of helicopter while hovering. The stability of the position of equilibrium of helicopter while hovering is determined by forces and the torque/moments, created by rotor during the action on it of disturbance/perturbations. If under the influence of disturbance/perturbations the fuselage of helicopter and together with it the shaft of rotor they turned themselves to angle $\Delta \vartheta = \Delta \alpha$ (Fig. 19.18), and blade/vane at this moment was located in the plane of the slope/inclination of shaft, i.e., it coincided with the fore-and-aft plane of helicopter, equilibrium of forces, acting on blade/vane, it is not disturbed. This is explained by the fact that the axle/axis of the flapping hinge, which links blade/vane with shaft, did not change its position. However, during the rotation of blade/vane along azimuth through angle $+\pi/2$, fulcrum will be sloped

to the angle of $+\Delta\alpha$, if the blade/vane advances, and to angle $-\Delta\alpha$, if the blade/vane moves back/ago (Fig. 19.19).
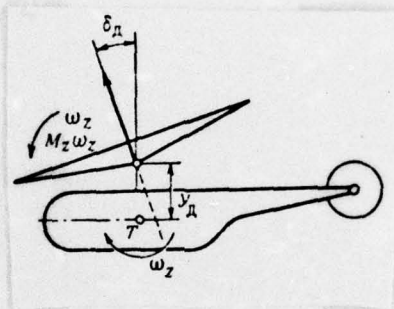
Page 358.

Fig. 19.20. Diagram for determining the damping moment, which appears with pitching.

The emergent cyclic increase in the lift force of the blade of ΔY_{M} will lead to flapping and the slope/inclination of the tulip of rotor back/ago. This deflection of tulip will occur until the plane of the rotation/revolution of blade/vanes becomes normal to shaft.

Since on the initial position of equilibrium the thrust line passed through the center of mass of helicopter, also in new position it will pass through this center. Since other parts of the helicopter of aerodynamic forces are not created, during a change in the angle of attack while hovering equilibrium of pitching moments is not disturbed, i.e.,

$$M_z^a = \frac{\partial M_z}{\partial a} = 0,$$

which means the static neutrality of helicopter on angle of attack.

However, in this case turns out to be that which was disturbed the equilibrium of forces of thrust/rod and weight, as a result of which appears the forward motion of helicopter back/ago. Forward speed changes the speed of the flow about forward going and back/ago going the blade/vanes, which leads to flapping blade/vanes and the deflection of the tulip of rotor forward. The thrust line now passes after the center of mass, creating negative pitching moment, i.e., the torque/moment, which attempts to return helicopter to starting position on angle of attack. Consequently, the behavior of helicopter during a change in the angle of attack is analogous with the behavior of aircraft with bank.

Thus it is possible to be convinced of the neutrality of helicopter along bank. The position of the center of mass of helicopter does not affect its angle of attack stability. However, it exerts a substantial influence on balance. Based on this for a helicopter with tail rotor desirable that the center of mass would be arrange/located about the axle/axis of rotor.

Damping the longitudinal (transverse) rotation/revolution of helicopter. Above it was noted that during the instantaneous deflection of shaft of certain angle the disk of rotor follows after

it with certain delay, determined by the moments of inertia of blade/
vanes. That means during the rotation/revolution of helicopter with
angular velocity ω_z , the rotor disk will be delayed by an angle of
$\delta_{\mathit{\Pi}}$ (Fig. 19.20), depending on ω_z (this will be seen during hel-
copter rotation relative to the longitudinal axis at the angular
velocity of ω_x).

Page 359.

If we designate the angular rate of rotation of the rotor of
ω_H and to equate torque/moments from the centrifugal and
aerodynamic forces of the relatively flapping hinge of blade/vane,
then we will obtain dependence

$$\frac{\delta_1}{\omega_z} = \frac{8}{\gamma \omega_H} ,$$

where the $\dfrac{1}{\gamma} = \dfrac{c_y^a b_{0.70} R^4}{2 J_{r.\text{ш}}}$ - the characteristic of the mass
distribution of blade/vane; $J_{r.\text{ш}}$ - the moment of the mass inertia of
blade/vane relative to the axle/axis of flapping hinge.

FOOTNOTE [1]. To A. Gesso, G. Meyers. Aerodynamics of helicopter. M., Oborongiz, 1954. ENDFOOTNOTE.

Then according to Fig. 19.20 damping moments is equal to

$$M_z = M_z^{\omega_z} \omega_z = - P y_{_\text{A}} \delta_{_\text{A}} = - P y_{_\text{A}} \frac{\delta}{\gamma \omega_{_\text{H}}} \omega_z. \qquad (19.45)$$

similar dependence it occurs for the torque/moment of roll damping

$$M_x \approx - P y_{_\text{A}} \frac{\delta}{\gamma \omega_{_\text{H}}} \omega_x. \qquad (19.46)$$

from formulas (19.45), (19.46) it follows that pitch damping and bank is more of helicopter with the low angular rate of rotation of the rotor of ω_H and relatively larger blade-mass factor $1/\gamma$. For the target/purpose of an increase $1/\gamma$ on some helicopters, are applied the gyroscopic stabilizing rods.

Characteristics of the longitudinal disturbed motion while hovering. The approximate equations of the disturbed motion in the initial state of equilibrium while hovering in the connected with helicopter coordinate system can be written in the form

$$-G\Delta\vartheta \approx m\,\frac{d\Delta V}{dt}\,,$$
$$M_z^V\Delta V + M_z^{m_z}\,\frac{d\Delta\vartheta}{dt} = J_z\,\frac{d^2\Delta\vartheta}{dt^2}\,. \qquad\qquad (19.47)$$

by the equation of normal forces in this case it is possible to
disregard.

The characteristic determinant of system (19.47) takes the form

$$\Delta = p^3 - \frac{M_z^{m_z}}{J_z}\,p^2 + g\,\frac{M_z^V}{J_z}\,, \qquad\qquad (19.48)$$

where p - roots the of characteristic equation.

By equating Δ to zero and by analyzing the roots of
characteristic equation (see Chapter XIV), we come to the conclusion
that the disturbed motion is composed of oscillatory and aperiodic
motions. On the basis of the criterion for Rauss-Gurvits (see Chapter
VIII) we are convinced that the oscillatory motion is unstable.

Page 360.

the oscillatory period of oscillations can be determined in the

first approximation, if we accept the $J_z = 0$:

$$T_0 = \frac{2\pi}{\Omega_0} \approx \frac{2\pi}{\sqrt{g}} \sqrt{ - \frac{M_z^{\omega_z}}{M_z^V}}, \qquad (19.49)$$

where Ω_0 is circular oscillation frequency.

Stability of the rectilinear steady-state motion of helicopter. Static angle of attack stability. If in the forward motion of helicopter at rate V angle of attack of fuselage increased on $\Delta\alpha$, then appear the longitudinal static moments, caused by rotor, fuselage and stabilizer (in the case of the presence of the same). The torque/moments, created by rotor and fuselage, are destabilizing. The pitching moment of fuselage is analogous to the pitching moment of fuselage for an aircraft.

With an increase in the angle of attack, change the lifts,

created forward going and back/ago going by blade/vanes. These
changes in the are proportional to the rate of the motion of
blade/vane. Actually, blade lift is proportional to angle of attack
and to the square of the rate of the motion of the blade/vane
relative to air W, which with low α is approximately equal to
component in the plane of the rotation/revolution of the
screw/propeller of $(W \approx W_x)$.   A change in blade angle of attack is
equal of the $\frac{\Delta \dot{W}_y}{W_x}$, where the ΔW_y - increase normal to the plane of
rotation/revolution of the velocity component of blade/vane. It is
obvious, lift increment of the blade/vane of $\Delta Y_{\pi} \sim \Delta \alpha W_x^2$ or
$\Delta Y_{\pi} \sim \Delta W_y W_x$.   Since ΔW_y constant, but W_x on the going forward
blade/vane are more than on back/ago going, also an increase in the
ΔY_{π} on it will be more, which will cause flapping blade/vanes, which
leads to the slope/inclination of the tulip of rotor back/ago (Fig.
19.21). The thrust line of $P + P^z \Delta \alpha$ will pass before the center of
mass and, consequently, will create the pitching destabilizing
torque/moment. It is analogous, if $\Delta \alpha < 0$, then also $M_{z_{HB}} < 0$.

Thus, $M^z_{z_{HH}} > 0$,   i.e., rotor in forward motion contributes to
the instability of helicopter on angle of attack.

It is obvious, the M^z_r of helicopter it will be composed of

values

$$M_z^\alpha = M_{z\,\text{нв}}^\alpha + M_{z\,\phi}^\alpha + M_{z\,\text{ст}}^\alpha$$

where the $M_{z\,\text{нв}}^\alpha$, $M_{z\,\phi}^\alpha$, $M_{z\,\text{ст}}^\alpha$ are derivatives on angle of attack from the moments of rotor, fuselage and stabilizer respectively.

In the absence of stabilizer, the helicopter is unstable on angle of attack.
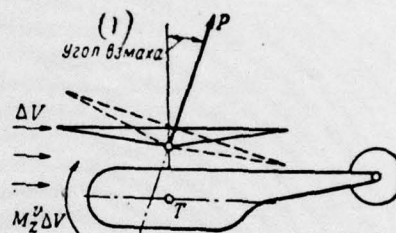
Page 361.
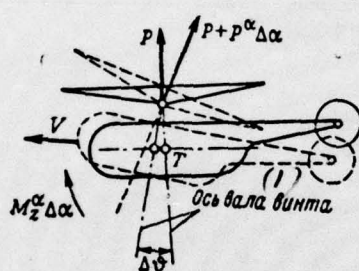

Fig . 19.21.   *Fig . 19.22.*

Fig. 19.21. the emergence of torque/moment during a change of the angle of attack in flight (dotted line - the position of helicopter after a change in the angle of attack).

Key: (1). Axle/axis of propeller shaft.

Fig. 19.22. Emergence of torque/moment during a change in the flight

speed of helicopter.

Key: (1). Flapping angle.

Stability of helicopter on speed. As it was noted above, an increase in the velocity of flight (with constant α) it leads to the deflection of rotor back/ago (Fig. 19.22), as a result of which appears the pitching torque/moment, which facilitates the flight path curvature of upward motion and, therefore, to the restoration/reduction of the initial velocity of upward motion and, therefore, to the restoration/reduction of the initial velocity of motion. This same contributes the torque/moment, created by fuselage; on stabilizer appears the destabilizing torque/moment. As a whole the derived M_z^V of helicopter is positive, which indicates the presence of speed stability.

Longitudinal disturbed motion of helicopter. The disturbed motion, caused by pitching, approximately can be described by the system of the linearized equations, written in the velocity system of the coordinates:

$$\left. \begin{aligned} m\,\frac{d\Delta V}{dt} &= -G\Delta\theta, \\ mV\,\frac{d\Delta\theta}{dt} &= P^a\Delta\alpha, \\ J_z\,\frac{d^2\Delta\theta}{dt^2} &= M_z^a\Delta\alpha + M_z^V\Delta V + M_z^{\omega_z}\frac{d\Delta\theta}{dt} \,. \end{aligned} \right\} \qquad (19.50)$$

during the compilation of equations it is accepted that the principal axis of inertia coincides with axle/axis 0x the cattle coordinate system and that the J_z in the process of the disturbed movement remains constant. Characteristic determinant of system (19.50) takes the form

$$\Delta = \frac{P^z}{mV} \, p^3 - \left(\frac{P^z}{mV} \, \frac{M_z^{\omega z}}{J_z} + \frac{M_z^a}{J_z} \right) p^2 + \frac{g P^z}{mV} \, \frac{M_z^V}{J_z} \, , \quad (19.51)$$

where the P^α - derivative in terms of the angle of attack of rotor thrust.

Page 362.

As in the case of hovering, the longitudinal disturbed motion is composed of aperiodic and oscillatory motions. The latter is unstable. Approximately angular oscillation frequency it is possible to find from expression (19-51), by disregarding the moment of inertia of the helicopter of the J_z:

$$Q_V = \sqrt{-\dfrac{gM_z^V}{M_z^{\omega_z} + \dfrac{M_z^\alpha}{P^2}mV}},$$

whence the period of oscillations

$$T_V = 2\pi\sqrt{\dfrac{-M_z^{\omega_z} - mV\dfrac{M_z^\alpha}{P^2}}{gM_z^V}}. \tag{19.52}$$

considering $V = 0$, from relationship (19.52) it is possible to determine the oscillatory period of oscillations while hovering (19.49).

To a reduction/descent in the degree of the oscillatory instability contribute an increase in the damping and a decrease in the stability level in velocity. Since the period of the vibrations of helicopter is sufficiently great (15-20 s), is oscillatory instability, if the gradient of the increase of amplitude is small, does not cause considerable difficulties in control. The account of

the torque/moment of J_z will lead to an increase in the period of the vibrations of helicopter.

PROBLEMS FOR REPETITION.

1. Which methods are utilized during the flight performance test of helicopter?

2. How does affect the proximity of the Earth inductive power?

3. Why the service ceiling of helicopter is greater than static?

4. How is caused the limitation of the vertical rate of descent in the helicopter power-on?

5. To which angles of setting (low or large) to favorably establish/install the blade/vanes of rotor with descent under the conditions of autorotation. Why?

6. By which indices is characterized the mode/conditions of the maximum flying distance of helicopter.

PROBLEM.

To determine, to what is equal the projection of the Z_T of rotor thrust on the axle/axis of the O_z of helicopter Mi-6 under the following conditions: in level flight the shaft horsepower of rotor is equal to $N = 4500$ kW, and the revolutions of screw/propeller are equal to $n = 116$ r/min; arm from the center of mass of helicopter to the axle/axis of the tail rotor of $L_{T.B.} = 23$ m.

Answer/response: 16000 n.

Page 363.

Literature

1. Александров В. Л. Воздушные винты. М., Оборонгиз, 1951.

2. Байдаков В. Б., Иванов-Эмин Л. Н. Аэромеханика летательных аппаратов. М., «Машиностроение», 1965.

3. Бараков А. М., Мазурин Н. И. и др. Авиационная метеорология. Л., Гидрометеоиздат, 1966.

4. Бухгольц Н. Н. Основной курс теоретической механики, ч. I и II. М., «Наука», 1969.

5. Ветчинкин В. П. Динамика самолета. М., Госмаштехиздат, 1933.

6. Гессоу А., Майерс Г. Аэродинамика вертолета. М., Оборонгиз, 1954.

7. Горбатенко С. А., Макашов Э. М., Полушкин Ю. Ф., Шефтель Л. В., Механика полета. М., «Машиностроение», 1969.

8. Горощенко Б. Г. Динамика полета самолета. М., Оборонгиз, 1954.

9. Демидович Б. П., Марон И. А. Основы вычислительной математики. М., «Наука», 1970.

10. Егер С. М. Проектирование пассажирских реактивных самолетов. М., «Машиностроение», 1964.

11. Калачев Г. С. Показатели маневренности, управляемости и устойчивости. М., Оборонгиз, 1953.

12. Котик М. Г. Критические режимы сверхзвукового самолета. М., «Машиностроение», 1967.

13. Лебедев А. А., Стражева И. В., Сахаров Г. И. Аэромеханика самолета. М., Оборонгиз, 1955.

14. Лебедев А. А., Чернобровкин Л. С. Динамика полета. М., Оборонгиз, 1962.

15. Мазин И. П. Физические основы обледенения самолетов. М., Гидрометеоиздат, 1957.

16. Мельников А. П. Аэродинамика больших скоростей. М., Воениздат, 1961.

17. Миеле Анджело. Механика полета. Теория траекторий полета, т. I. М., «Наука». 1965

18. Миль М. Л., Некрасов А. А., Браверман А. С., Гродко Л. Н., Лейканд М. А. Вертолеты. Расчет и проектирование, кн. I. М., «Машиностроение», 1966.

19. Мхитарян А. М. Аэродинамика. М., «Машиностроение», 1970.

20. Остославский И. В. Аэродинамика самолета. М., Оборонгиз, 1957.

21. Остославский И. В. Стражева И. В. Динамика полета. Траектории летательных аппаратов. М., «Машиностроение», 1969.

22. Остославский И. В., Стражева И. В. Динамика полета. Устойчивость и управляемость летательных аппаратов. М., «Машиностроение», 1965.

23. Прицкер Д. М., Турьян В. А. Аэромеханика. М., Оборонгиз, 1960.

24. Смирнов В. И. Курс высшей математики. М., ГТТЛ, 1957.

25. Современная математика для инженеров. Под ред. Э. Ф. Беккенбаха. М., ИЛ, 1958.

26. Солодовников В. В. Техническая кибернетика, кн. 2. М., «Машиностроение», 1967.

27. Трунов О. К. Обледенение самолетов и средства борьбы с ним. М., «Машиностроение», 1965.

28. Фабрикант Н. Я. Аэродинамика. М., «Наука», 1964.

Noted Misprints

(1) Стр.	(2) Строка	(3) Напечатано	(4) Должно быть
43	(5) 10 сверху	(6) ракет	(7) растет
66	(5) 21 сверху	$M_{\text{пр}} = \sqrt{\dfrac{T_{\text{пр}} - T}{r\dfrac{k-1}{2} - T}} = \sqrt{\dfrac{T_{\text{пр}} - T}{0,2r - T}}$	$M_{\text{пр}} = \sqrt{\dfrac{T_{\text{пр}} - T}{r\dfrac{k-1}{2}T}} = \sqrt{\dfrac{T_{\text{пр}} - T}{0,2rT}}$
125	(8) 1 снизу	$+ \dfrac{10\varrho}{G/S} \Big)\Big];$	$+ \dfrac{10\varrho g}{G/S} \Big)\Big];$
126	(5) 1 сверху	$+ \dfrac{15\varrho}{G/S} \Big) +$	$+ \dfrac{15\varrho g}{G/S} \Big) +$
180	(8) 3 снизу	$\overset{\bullet}{m}_{zp} = 0,05 \dfrac{x_{pi}D^2}{Sb_A} c_y$	$\overset{\bullet}{m}_{zp} = 0,05i \dfrac{x_p D^2}{Sb_A} c_y$
194	(5) 4 сверху	$+ c_{\text{зм.г}}^{\beta} k_{S\text{м.г}} \big]^{\beta}$	$+ c_{\text{зм.г}}^{3} K_{S\text{м.г}} \big] \beta$

Key: (1) Page; (2) Line; (3) Printed; (4) Should be; (5) from above;
(6) of rockets; (7) increases; (8) from below.